Republic of Iraq

Ministry of Higher Education and Scientific Research

University of Misan/ College of Engineering

Department of Electrical Engineering

Enhanced Stability of Islanded Microgrid Using Optimized Droop-PID Controllers

Prepared By

Hussein Raheem Jasim

(B.Sc. in Electrical Engineering)

A thesis submitted in Partial Fulfillment of the Requirements for the Master of Science degree in Electrical Engineering

The University of Misan

2026

Thesis Supervisor: **Asst. Prof. Dr. Ahmed Raisan Hussein**

2026 A.D 1447 A.H

بِسْمِ اللّهِ الرَّحْمَن الرَّحِيمِ

﴿قَالَ رَبِّ اشْرَحْ لِي صَدْرِي ۝ وَيَسِّرْ لِي أَمْرِي ۝ وَاحْلُلْ عُقْدَةً مِّن لِّسَانِي ۝ يَفْقَهُوا قَوْلِي﴾

صَدقَ اَللَّه العلي الَعظَيمَ

[طه:28]

ABSTRACT

A Microgrid (MG) constitutes a decentralized power system integrating various Distributed Generation (DG) units. Ensuring frequency and voltage stability remains a multifaceted challenge, particularly during network-independent (islanded) operation, where system reliability and operational integrity are paramount. Although Droop Control is widely adopted due to its ability to regulate parallel-linked Inverters without critical communication links, this conventional strategy often exhibits significant inaccuracies in maintaining frequency and voltage near nominal values. Furthermore, traditional fixed-gain controllers frequently lack the dynamic adaptability necessary to mitigate sharing errors and poor transient responsiveness under stochastic load variations. To address these critical limitations, this research proposes a modified hybrid control architecture that integrates the precision of classical control with the adaptability of artificial intelligence. The system features a cascaded structure comprising a fixed Proportional-Integral (PI) inner loop and an adaptive PID-enhanced droop controller for the outer loop. A two-stage optimization methodology is implemented: initially, an offline Particle Swarm Optimization (PSO) algorithm determines the optimal controller gains through a rigorous fitness function. Subsequently, these optimized datasets are utilized to train an Artificial Neural Network (ANN). By learning the complex, non-linear relationship between system performance and optimal gains, the ANN transforms computationally intensive optimization into a rapid, real-time prediction task, effectively bypassing the PSO's computational load during implementation. The effectiveness of the proposed architecture is validated using a high-fidelity asymmetric MG model. Simulation results demonstrate the significant superiority of the hybrid PSO-ANN controller over conventional and standalone optimization techniques. The proposed system achieves a power-sharing accuracy of 99.83%, reducing steady-state error by fivefold. Power quality

exhibits a substantial 43% enhancement, with Total Harmonic Distortion (THD) dropping from 5.1% to 2.9%. Additionally, the dynamic response is accelerated, evidenced by a 22.53% reduction in frequency settling time and a 21% minimization of cumulative error metrics, including the Integral Absolute Error (IAE). These combined results confirm the hybrid algorithm's capability to ensure robust, optimal, and real-time decentralized management in modern MG systems.

STATEMENT OF AUTHORSHIP

This thesis was completed as part of the MSc. (**Electrical Engineering**) at **College of Engineering -University of Misan**. This is my own unaided work. Where the work of others has been used or drawn on then it has been fully attributed to the relevant source.

Signature:

Name: Hussein Raheem Jasim

Date: / /2026

SUPERVISOR CERTIFICATION

I certify that the preparation of this thesis entitled" **Enhanced Stability of Islanded Microgrid Using Optimized Droop-PID Controllers**" was presented by "**Hussein Raheem Jasim** " and has been prepared and written under my supervision at University of Misan / College of Engineering as a partial fulfilment of the requirements of the degree of the Master of Science in Electrical Engineering.

Signature:

Supervisor: **Asst. Prof. Dr. Ahmed Raisan Hussein**

Date: / / 2026

In view of the available recommendations, I forward this thesis for discussion by the examining committee.

Signature:

Name: **Assist. Prof. Dr. Mohammed Kh. Al. Nussairi**

Head of Electrical engineering department

Date: / / 2026

CERTIFICATION OF THE EXAMINING COMMITTEE

We certify that we, the examining committee, have read the thesis titled (**Enhanced Stability of Islanded Microgrid Using Optimized Droop-PID Controllers)** which is being submitted by **Hussein Raheem Jasim,** and examined the student in its content and what is concerned with it, and that in our opinion, it meets the standard of a thesis for the degree of Master of Science in Electrical Engineering.

Signature:
Name: **Assist. Prof. Dr. Ahmed Raisan Hussein**
(Supervisor)
Date: / /2026

Signature:
Name: **Assist. Prof. Dr. Jabbar Raheem Rashed**
(Member)
Date: / /2026

Signature:
Name: **Assist. Prof. Dr. Sadeq D. AL-Majidi**
(Member)
Date: / /2026

Signature:
Name: **Prof. Dr. Ali Jafar Mahdi**
(Chairman)
Date: / /2026

Approval of the College of Engineering

Signature:
Name: **Prof. Dr. Abbas Oda Dawood**
Dean of the College of Engineering
Date: / /2026

DEDICATION

To My Lord, Allah, the Source of all wisdom and light, for His boundless grace, unending mercy, and the strength He bestowed upon me at every turn. His divine guidance illuminated my path and made this journey, and its completion, possible. All praise and gratitude belong to Him alone.

To the final Prophet, Muhammad (peace be upon him), whose life, teachings, and wisdom serve as an eternal beacon of light, inspiring perseverance, knowledge, and integrity in every aspect of life. May his guidance continue to illuminate our understanding.

My Imam and wonderful instructor, AL-Hujjaha Ibn Al-Hassan (Ajal Allah Farajah Al-Sharif), has my deepest gratitude, appreciation, and thanks.

To my spiritual father, my leader, and my ultimate inspiration, His Eminence Sayyed Muqtada al-Sadr (may Allah grant him long life).

To my family, whose unwavering support and love have been my guiding star throughout this journey. This thesis is a testament to your belief in me.

To my wife, for their unwavering belief in me and for being my source of strength during challenging times. This thesis is a tribute to our shared journey.

To my friends, for their companionship and endless encouragement. This thesis is dedicated to our shared dreams and aspirations.

To myself, for the perseverance, commitment, and innumerable hours of labor put into this endeavor.

ACKNOWLEDGEMENTS

First and foremost, I thank Allah for the great blessings that enabled me to complete this thesis.

I would like to express my sincere thanks to Prof. Dr. Abbas Oda Dawood Dean of the College of Engineering for his continuous support for postgraduate students.

I would like to sincerely thank my supervisor, Asst. Prof. Dr. Ahmed Raisan Hussein, for his invaluable guidance, encouragement, and support over the course of this endeavor.

I would like to extend my thanks to Assistant Professor Dr. (Dr. Hasanain AlBehadili); Scientific Assistant to the Dean of the College of Engineering.

I would like to express my thanks to Assist. Prof. Dr. Mohammed Kh. Al. Nussairi Head of Electrical Engineering Department

To my professors, for their knowledge and inspiration, which fueled my passion for this field. This thesis is a small token of my gratitude.

I would like to express my gratitude to the College of Engineering staff for their thoughtful support.

TABLE OF CONTENTS

LIST OF TABLES

LIST OF FIGURES

LIST OF ABBREVIATIONS

Abbreviation	Full Form
ACMG	Alternating Current Microgrid
ACO	Ant Colony Optimization
AI	Artificial Intelligence
ANN	Artificial Neural Network
APSO	Adaptive Particle Swarm Optimization
BESS	Battery Energy Storage System
CS	Cuckoo Search
DCMG	Direct Current Microgrid
DER	Distributed Energy Resources
DG	Distributed Generation
DSP	Digital Signal Processor
EMS	Energy Management System
ESS	Energy Storage System
EVS	Electric Vehicle Systems
FFNN	Feedforward Neural Network
FOPID	Fractional Order Proportional-Integral-Derivative
GA	Genetic Algorithm
GSA	Gravitational Search Algorithm
GWO	Grey Wolf Optimizer
HIL	Hardware-in-the-Loop
IAE	Integral of Absolute Error
ISE	Integral of Squared Error
MAS	Multiagent Systems
MG	Microgrid
MPP	Maximum Power Point
MPPT	Maximum Power Point Tracking
MSE	Mean Squared Error
MPSO	Modified Particle Swarm Optimization
P2P	Peer-to-Peer
PCC	Point of Common Coupling
PI	Proportional-Integral
PID	Proportional-Integral-Derivative
PSO	Particle Swarm Optimization
PV	Photovoltaic
PWM	Pulse-Width Modulation
RES	Renewable Energy Sources
RL	Reinforcement Learning
SIL	Software-in-the-Loop
SSA	Salp Swarm Algorithm
SSE	Steady -State Error
THD	Total Harmonic Distortion
UG	Utility Grid
VSI	Voltage Source Inverter

LIST OF SYMBOLS

Symbol	Definition
abc	Stationary frame
C_f	Filter capacitance
c_1	Cognitive coefficient
c_2	Social coefficient
dq	Rotating frame
e	Error
$e_{i,\,d}$	d-axis current error
$e_{i,\,q}$	q-axis current error
e_{old}	Previous time step error
$e_{v,\,d}$	d-axis voltage error
$e_{v,\,q}$	q-axis voltage error
$E_{rrP\ c1}$	Steady-state active power error
F^*	Nominal frequency
F_{dev}	Average deviation of the system frequency
F_{ref}	Frequency reference
f_{bus}	Bus frequency
f_{nom}	Nominal frequency
g_{best}	Global best
$i_{d,\,ref}$	d-axis reference current
i_{inv}	Inverter current
i_{line}	Line current
$i_{q,\,ref}$	q-axis reference current
I_{meas}	Measured current
I_{ref}	Current reference
K_d	Derivative gain
$K_{i,\,i}$	Integral gain for current loop
$K_{i,\,v}$	Integral gain for voltage loop
K_i	Integral gain
$K_{p,\,i}$	Proportional gain for current loop
$K_{p,\,v}$	Proportional gain for voltage loop
K_p	Proportional gain
lb	Lower bound
L_f	Filter inductance
L_{line}	Line inductance
m	Active power droop coefficient
n	Reactive power droop coefficient
P	Active power
P^*	Active power reference
P_{final1}	Target active power reference
$pbest$	Personal best
Q	Reactive power
Q^*	Reactive power reference
$r_1,\ r_2$	Random numbers
R_d	Damping resistor
R_f	Filter resistance

R_{line}	Line resistance
T_s	Sampling time
T_{total}	Total simulation time
$u(t)$	Control signal output
ub	Upper bound
$V*$	Nominal voltage
$V_{bus,\ rms}$	Bus RMS voltage
V_{cap}	Capacitor voltage
$V_{c,\ d}$	d-axis voltage command
$V_{c,\ q}$	q-axis voltage command
V_{dc}	DC voltage
V_{dev}	Average deviation of the system voltage
V_{inv}	Inverter voltage
$V_{inv,\ d}$	d-axis inverter voltage
$V_{inv,\ q}$	q-axis inverter voltage
V_{meas}	Measured voltage
$V_{nom-peak}$	Nominal peak voltage
$V_{nom-rms}$	Nominal RMS voltage
V_{ref}	Voltage reference
w	Inertia weight
W_{ref}	angular frequency reference
W_{nom}	nominal angular frequency
θ	Phase angle
ω_{nom}	Nominal angular frequency
ω_{ref}	Angular frequency reference

LIST OF PUBLICATION

[1] H. R. Jasim & A. R. Hussein, “Enhance Transient Power Sharing in Microgrids using PID- PSO Controller”, Misan Journal of Engineering Sciences, vol. 3, no. 2,pp.48-95, 2025.

CHAPTER ONE
INTRODUCTION

CHAPTER One

Introduction

1.1 Introduction

Microgrids play an increasingly pivotal role in the evolution of future power grids, facilitating the seamless incorporation of Distributed Generation units and renewable energy technologies. The primary benefits of microgrids include enhanced efficiency, reliability, and sustainability [1]. A microgrid comprises multiple sources of power generation, such as solar photovoltaics, wind turbines, and energy storage devices. However, transient power sharing remains a critical challenge that must be addressed in microgrids, as it can undermine system stability and overall performance following dynamic disturbances. These disturbances include sudden load fluctuations, renewable energy intermittency, or unplanned transitions between grid-connected and islanded modes. To mitigate these effects, various control techniques are employed to optimize system parameters, ensuring minimized voltage/frequency deviations, enhanced settling times, and highly accurate power distribution among parallel units. The primary motivations for implementing such an optimization control technique are to achieve simple integration among various types of distributed energy resources (DERs) and balanced power sharing among them [2][3]. The use of a multi-layered control method has led to an increase in the use of Droop control and PID controllers. However, conventional, hand-tuned PID and droop control strategies often struggle to reach optimal operation. This is primarily due to the inherent non-linearity and complex dynamics of inverter-based microgrids, which frequently lead to significant overshoots and prolonged settling times during transient events. This requires sophisticated means to provide a fast and reliable response. The remedy lies in optimizing these controllers with metaheuristic type algorithms such as Particle Swarm Optimization. This sophisticated mode can

achieve a higher level of control adaptation and accuracy than a simpler mode. The hybrid structure has the most benefit of providing the PID controller and the Droop controller with the capacity to change parameters to provide dynamic and intelligence-based methods of participating in rapid and reliable transient sharing of power by various distributed energy systems, while satisfying criteria for stability required by the control systems used. These systems can be further refined by the use of Artificial Neural Networks, which provide a powerful and flexible option. The extremely high capability of ANNs to learn the behavior of complicated systems and predict the required control action makes them ideal for intelligent and adaptive control [4]. The PSO is used offline to find the optimal control parameters (PID gains and Droop coefficients), and the best parameters so obtained are then used to train the ANN. Such a combination of PSO-tuned ANN with PID-Droop structure significantly improves the system's flexibility and responsiveness. This blend allows the system to have more stable and effective power sharing in real systems. Microgrid transient state power sharing is addressed in this thesis with a hybrid control structure. The suggested approach attempts to optimize the control process to the greatest degree by achieving fast settling time, reduced overshoot, and high precision in load distribution. The novel strategy efficiently addresses the energy-sharing issues in dynamic conditions and assists in the development of smarter and more robust microgrid systems.

1.2 Problem Statement

Microgrids are local power systems rapidly integrated into utility grids to ensure sustainable and reliable power. However, achieving precise transient power sharing among DERs remains a significant technical difficulty, particularly under dynamic conditions such as faults, renewable energy fluctuations, or abrupt loading changes. Inadequate power sharing directly compromises system stability, leading to unequal loading and degraded reliability. The primary

limitation lies in traditional control methodologies, specifically fixed-gain PI and PID droop controllers. These classical approaches are inherently rigid and fail to counteract the time-varying, non-linear dynamics of modern MG systems. Because their parameters are tuned for specific operating points, they exhibit poor adaptability to disturbances, often resulting in high settling times and significant voltage/frequency deviations. While metaheuristic techniques like PSO can enhance performance by optimizing controller gains, they are computationally prohibitive for real-time applications. The iterative nature of PSO makes it inefficient for handling instantaneous, intricate control situations where milliseconds matter. Consequently, there is a critical need for a sophisticated, integrative architecture that bridges this gap. The challenge is to develop a control framework that maintains the proven stability of PI/PID and the robustness of Droop control, while incorporating the optimization precision of PSO and the forecasting intelligence of ANNs to ensure rapid, adaptive, and resilient decentralized management.

1.3 Aim and Objectives of the Thesis

The primary aim of this thesis is to improve microgrid transient power sharing by designing and implementing a reinforced control architecture. Dynamic modes of operation and distributed energy resources are issues that the proposed architecture will address. The particular goals of this study are to:

1. Design a modified control system based on ANN, PID, PSO, and Droop methods with the goal of maximizing transient power sharing of microgrid operation. Inner current and voltage loops of the hybrid system are regulated by PI regulators while outer droop control is implemented by a PID method.
2. Improve the power distribution and stability of the microgrid for stable operation, particularly in dealing with transient phenomena like load change, system fault, and intermittent renewable energy resources.

3. Implement the PSO approach in modifying the parameters of the Droop and PID controllers for enhancing system performance in the presence of nonlinear and time-varying conditions.
4. Use artificial neural networks to predict system performance to enable real-time adaptive control and response to new operating conditions quickly.
5. Establish the validity and reliability of the suggested control system under various operating conditions by testing in a variety of simulated operating conditions.

1.4 Contribution of thesis

The contributions of this thesis to the field of renewable energy and microgrid control systems can be summarized as follows:

Development of an Integrated Multi-Layer Control Framework: This research introduces a modified control architecture that synergizes Droop control, PSO-based optimization, and ANN-driven predictive intelligence. This multi-layered approach provides a robust solution for managing complex power-sharing dynamics in islanded microgrids.

Enhanced Real-Time Adaptability: By utilizing an Artificial Neural Network to predict optimal controller gains, the system effectively bypasses the high computational latency associated with traditional metaheuristic optimization. This ensures a rapid, real-time response to transient events and sudden load variations.

Precision in Parameter Coordination: The study provides a strict coordination mechanism between the PID-enhanced Droop controller (outer loop) and the fixed-gain PI controller (inner loop). This dual-loop optimization minimizes cumulative errors (IAE) and significantly reduces settling time during mode transitions.

Scalability for Practical Applications: This research offers an extensible control solution that can be adapted to real-world microgrids. It provides operators with a reliable tool to maximize operational efficiency and support the long-term sustainability of decentralized energy systems.

1.5 Outline of thesis

The structure of this thesis is organized to reflect the research scope, transitioning methodically from the identification of the problem to its solution. This progression begins with the theoretical underpinnings and culminates in the practical application and comprehensive analysis of the results.

- **Chapter one:** This chapter introduces and discusses microgrid control issues. It proposes a robust control approach based on the intelligence of ANNs, the optimization capability of PSO, and PID/PI stability to solve such issues and ensure proper transient power sharing. The hybrid approach is designed to improve the overall performance and fault tolerance of microgrid systems by solving the dynamic issue of power allocation, improving system stability, and ensuring proper energy utilization.

- **Chapter two:** This chapter presents a general overview of modern microgrid control methods with a focus on the most challenging problems of voltage and frequency stability and load variability compensation. The overview reveals various methods that combine new optimization algorithms like PSO and ANNs with (PID/PI) controllers.

- **Chapter three:** This chapter describes the overall, multi-step procedure used for microgrid efficiency optimization. The procedure employs the hybrid

PSO-ANN algorithm, where the most current metaheuristic optimization techniques are combined with conventional control policies. The procedure uses one combined optimization policy. It tunes the Droop control gains (m and n) for frequency and voltage stability and tunes the PID controller gains for dynamic response and power quality improvement by reducing overshoot and settling time. For all the simulations, the MATLAB platform was employed to simulate this integrated approach, which takes into account a number of performance indices to give an overall improvement in the microgrid's dynamic and steady-state performance.

- **Chapter four:** This chapter gives a close-up description of the simulation results run on the MATLAB platform towards realizing the major goal of enhancing transient power sharing in islanded microgrids. The performance of three different control systems was matched against each other. The traditional PID/PI controller was employed to realize a baseline, introducing the common disadvantages of hand-tuning such as increased settling times and power overshooting. Then, the PID and Droop controller were optimized using PSO approach with a very large performance gain. Through efficient optimization of a multi-objective cost function, the PSO-optimized controller enhanced voltage and frequency stability with transient and steady-state error minimization. The chief contribution of the present study is the conclusive proof of the superior performance of the adaptive ANN-based controller.

- **Chapter five:** This chapter summarizes the key findings of the thesis, which successfully demonstrates the efficacy of the suggested hybrid control method in resolving the performance constraints of conventional controllers in microgrid operations. Improvement in the transient power sharing through a multi-phase operation was the major goal of the project. The work began with the use of PSO for optimizing the parameters of PID and Droop controllers.

The significant contribution of this research lies in the construction of an adaptive ANN-PID/Droop controller based on the optimal PSO process data. This controller provides a strong and significant foundation to improve microgrid efficiency and stability through dynamic adaptability and improved performance using real-time parameter adjustments.

CHAPTER TWO

THEORETICAL BACKGROUND

CHAPTER Two

Theoretical Background

2.1 Introduction

A microgrid is a localized power system comprising distributed generators and loads that can operate independently of the primary utility grid, providing a resilient energy solution during emergency scenarios and blackouts. Besides, it can also be used to meet peak demand, lowering microgrid consumers high bills [5]. Another definition of a microgrid is as a mini power system that provides electricity to local loads like housing estates, business centers, hospitals, or industrial parks. Microgrids can be powered by renewable energy sources such as wind turbines or solar photovoltaic systems, or by traditional generators. Because RESs emit no emissions and produce less pollution, they are beneficial. Electricity produced by wind and solar energy can surpass local energy needs in certain countries, where it can account for up to 20% and 8% of the total power demand, respectively[6]. Microgrids can be categorized based on their connection and operation modes. They can either be connected, or isolated to the grid. Isolated microgrids do not need a primary fuel source to function and can be located in geographic locations without traditional electric facilities. Grid connected microgrids can also import and export as needed because they are in conjunction with a primary grid. Microgrids also can utilize AC, DC, or both. AC microgrids are the most common microgrid since they can operate off of legacy technologies existing on the grid. DC microgrids are becoming more common in certain use cases, but still are not commonly seen in comparison to AC. Hybrid systems can use either AC or DC technology, which can optimize performance with different devices and energy sources and enhance flexibility and efficiency. Microgrids enhance usage efficiency for localized energy consumption, and represent a powerful mechanism to integrate renewable energy resources and

create greater sustainability. They are essential for the future due to their ability to accommodate the variable nature of RESs [7]. They are used in a variety of applications, including in rural electrification to provide power to off-grid communities; for reliability in the commercial sector when reliable power is needed; and in industry to reduce operational expense through self-generation. One benefit of microgrids is increased resilience of the grid, especially in times of power outages. They also lower dependence on fossil fuels, facilitate the transition to renewable energy, and result in carbon emission reductions. They may also increase energy efficiency, consequently reduce consumption costs and yielding economic benefits. However, there are challenges related to deploying microgrids, including economic challenges of high up-front costs with unguaranteed return on investment, and technical challenges related to stability, protection, and harmonics in more complex systems [8].

High-performance control strategies are essential to ensure the reliable and secure operation of microgrid systems. This can be achieved by decreasing the overshoot number which has a direct impact on system efficiency. In particular, this ensures safe power sharing as well as power transfer responses during mode transitions. Current and voltage sharing is a particular issue in microgrid operation. Besides voltage and frequency stability, some researchers have examined optimizing power sharing and response to enhance the resiliency of these networks to outside disruptions. The solution to these problems requires an advanced controller where the self-tuning functionality incorporates an optimization algorithm. Emerging technologies, which optimize power distributions and predict power demand like artificial intelligence and machine learning , have an increasingly important role in microgrid control [9]. As a result, microgrids will be an important aspect of the future energy landscape and developing more resilient, sustainable, and decentralized power systems.

2.2 Classification of microgrids

Based on their technical and operational features, some researchers have introduced a number of microgrid classifications based on their different characteristics. Those classifications usually follow principal criteria, such as their power type (AC, DC, or hybrid), control and monitoring architecture (centralized or decentralized), number of phases (single-phase or three-phase), and operation mode (isolated or grid-connected), as depicted in Figure (2-1). These categories determine the particular kind of microgrid and its possible uses, for example, commercial, industrial, and farm premises.

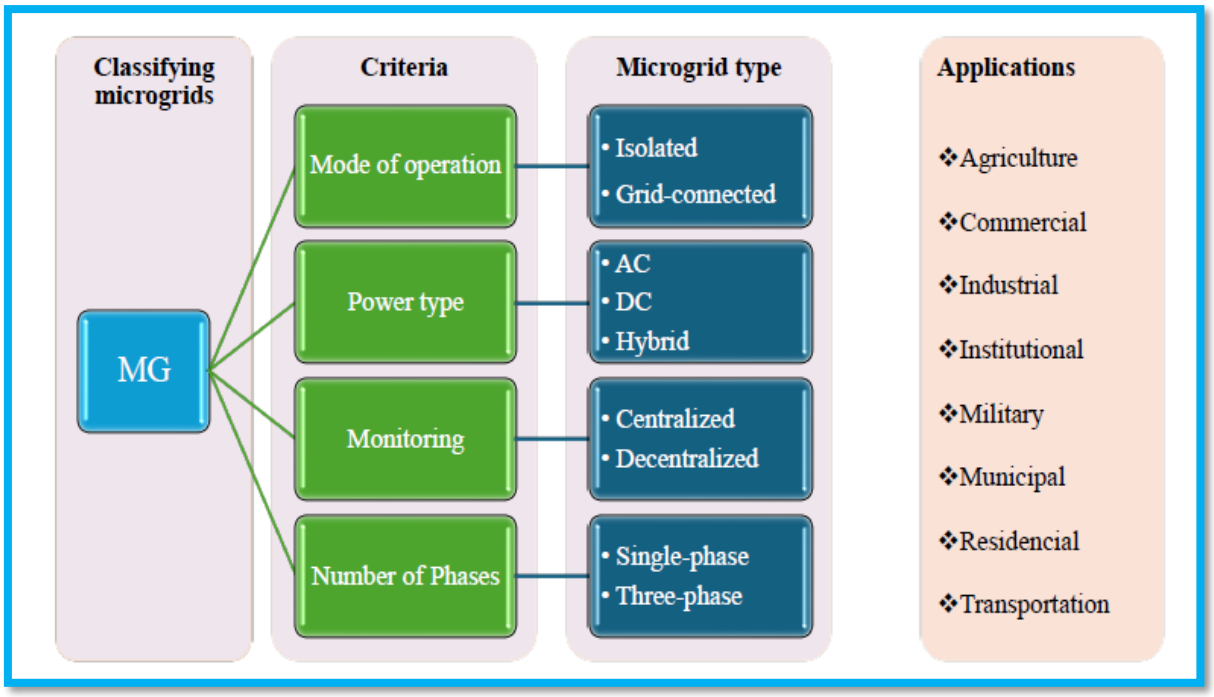

Figure (2-1) Standard operating classifications for microgrids [6]

2.3 Microgrid Structure

Microgrids are coordinated systems that use grid-based distributed energy resources that can be connected to or disconnected from the utility grid (UG) at the point of common coupling (PCC). The PCC is the distinct point where the entire microgrid system is connected to the primary utility grid. The elements that

constitute an MG are examined in the sections that follow. The main components of the microgrids system are the DER including PV, wind turbines, diesel generators, and other resources. The second component is the Energy Storage Systems (ESS) and this could be like lithium-ion batteries which are very important for maintaining power quality where the third component is the Power conditioning unit to enable and ensure compatibility between different sources and loads [10]. The following sections describe these primary components and their roles within the microgrid.

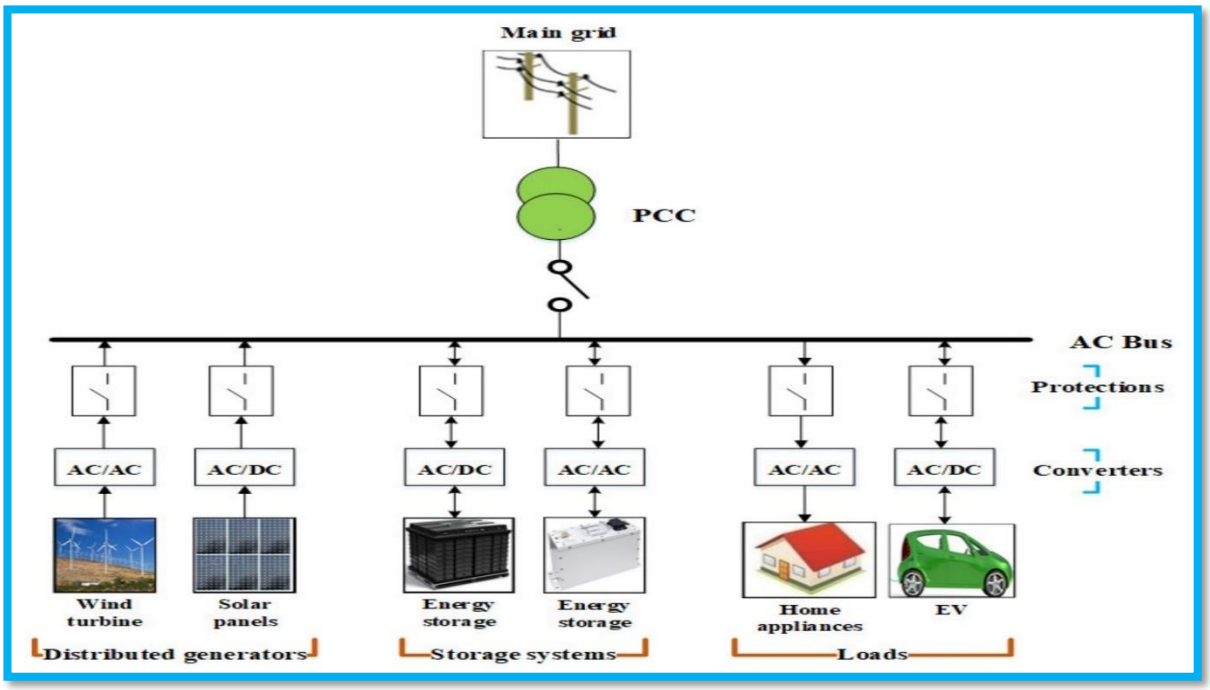

Figure (2-2) A microgrid's (MG) layout [1]

2.3.1 Distributed generators (DGs)

The microgrid provides a coordinated approach to integrating heterogeneous distributed generation resources, allowing for the unified operation of multiple energy sources regardless of their geographical placement. End users can get power from DGs such wind turbines, photovoltaics, hydro turbines, biomass and fossil fuel-based generators, and others. They considerably lower emissions. DGs can provide substantial environmental advantages in addition to producing and delivering energy efficiently. For DGs to successfully and smoothly connect to

MGs, they have a controller that controls frequency, voltage, and active/reactive power[11].

2.3.2. Storage Systems

Energy storage systems are crucial components of MGs, as they provide essential backup power to support renewable energy sources. When there is an abundance of generation from local DGs, ESSs store the excess energy to prevent wastage. Furthermore, they maintain system stability and minimize disruptions by injecting stored electricity into the grid during periods of high demand. By significantly mitigating the fluctuating effects of RESs, ESSs improve overall system performance, including frequency management and transient stability, to create a more reliable and dynamic power system.[12]. By considerably lowering the fluctuating effects of RESs, an ESS can improve system performance and enable a more economical MG operation. Other aspects of the system, including stability, PQ, power imbalance, dependability, and remote MG operation, can also be enhanced. Voltage imbalance (VU), frequency management, and transient and dynamic stabilities can all be improved by ESSs to create a dynamic power system.

2.3.3 Loads

Microgrids serve diverse load types, ranging from residential to commercial applications. To optimize system performance, these loads are categorized into critical loads such as medical equipment in hospitals or data centers and non-critical loads like decorative lighting or HVAC systems in non-essential areas. This prioritization ensures high reliability and power quality (PQ) for essential services, maintaining stability even during contingency events. [13]. Using protective systems, critical loads are cut off during grid outages, and local generation, the customers' own generating facility is then used continually.

2.3.4 Control Units

These units function as the microgrid's core intelligence, comprising power converter controllers that manage both islanded and grid-connected operations. The control architecture employs a dual-loop strategy: a fast inner current loop for precise grid current regulation and an outer voltage loop to maintain DC-link stability. The primary objective of these units is to ensure robust system stability and seamless performance under diverse dynamic conditions. [14].

2.3.5 Point of Common Coupling

The Point of Common Coupling serves as the critical electrical interface where the microgrid physically connects to or disconnects from the main utility grid. More than just a physical junction, the PCC acts as a strategic boundary for system operation and control. It is an essential component for effective protection, synchronization, and power flow management [15]. During grid-connected operation, the PCC facilitates the exchange of power between the microgrid and the main utility, ensuring that the local generation and demand are balanced. In the event of utility-side disturbances or faults, the PCC-located protection devices such as circuit breakers and relays trigger an islanding transition, isolating the microgrid to protect local Distributed Generation units and sensitive loads. Furthermore, the PCC is vital for synchronization; before re-establishing a grid-tied connection, it ensures that the voltage, frequency, and phase angle of the microgrid are aligned with the utility grid to prevent damaging inrush currents. Consequently, the PCC represents not only a physical link but also a dynamic control boundary that dictates the microgrid’s operational mode and maintains overall system stability.

2.3.6 Protection Elements

The microgrid's safety and dependability depend on protection systems. Their purpose is to identify and separate malfunctions and other disruptions. Protection devices, protective relays, measurement tools, and grounding are the usual

components of a protection system [16]. These components are essential for avoiding equipment damage and guaranteeing that vital loads receive a steady supply of electricity.

2.4 Mode of operation

A microgrid's efficiency, stability, and compatibility with other energy systems are all influenced by its topology. The overall performance of a microgrid is dependent on its operation mode and connectivity. Microgrids can operate in two ways: (i) connected to the grid and (ii) isolated.

2.4.1 Grid-Tied Mode

For grid-connected operation, MGs can purchase or sell energy from the UG, as per power grid demand. The integration of BESSs with MGs enhances system reliability, thus optimizes the system operation. The reliability of MGs can be guaranteed by BESSs that are able to control frequency and voltage fluctuations within limit values. When grid disruptions occur, BESSs are typically used in conjunction with RESs to provide standby generation, provide electricity to lower peak load demand, and regulate voltage and frequency to maintain the grid [17].

MGs connected to the grid are equipped with a PCC and a clever bi-directional switch. The bi-directional switch controls how the MG and main UG are connected in both directions. When the MG needs energy, it can draw it from the UG. It can also provide the UG extra power. When the microgrid is in grid-connected mode, it is in sync with the main electrical grid, enabling two-way energy exchange. The primary grid can act as a backup during variations in local generation or demand, which improves system stability and demand management. To maintain frequency and voltage at the point of common coupling, this mode necessitates a strong infrastructure and exact coordination.

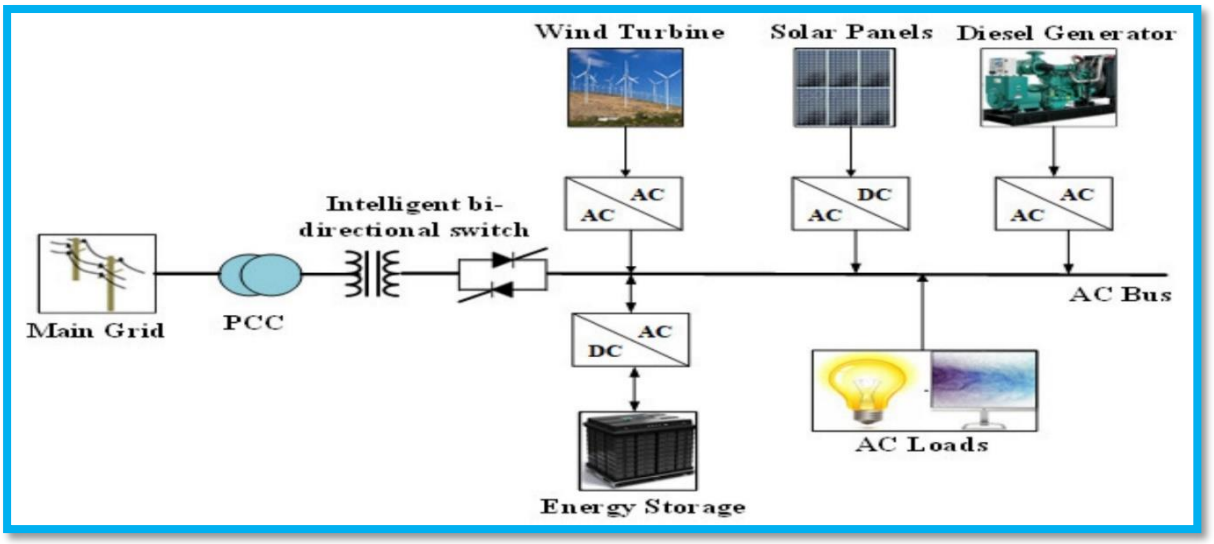

Figure (2-3) operation of MG in grid-tied mode [1]

2.4.2 Isolated Mode

MGs are usually connected to an electric power network at medium (or low) voltage levels and are connected to the UG via a PCC. Although the MG is not connected to the UG in the islanded mode, it may nonetheless reliably supply customers with power in response to DG bids. RES-induced power oscillations are lessened by ESS-integrated MGs, which also improve the power network's efficiency and dependability. In order to preserve power network stability and dependability in emergency situations where the MG is cut off from the UG due to network issues, the MG may function independently (in the islanded mode) with the assistance of DGs and the integration of battery ESSs [18]. In isolated mode, the microgrid functions as a self-sufficient energy ecosystem, which is vital for remote regions where grid extension is technically or economically unfeasible. This autonomous operation enhances supply reliability by eliminating dependence on external grid disturbances and provides superior voltage stability through localized control. By integrating ESS to buffer the intermittency of renewables, the isolated microgrid ensures a continuous, high-quality power supply, making it an ideal solution for critical infrastructure in off-grid locations. [19].

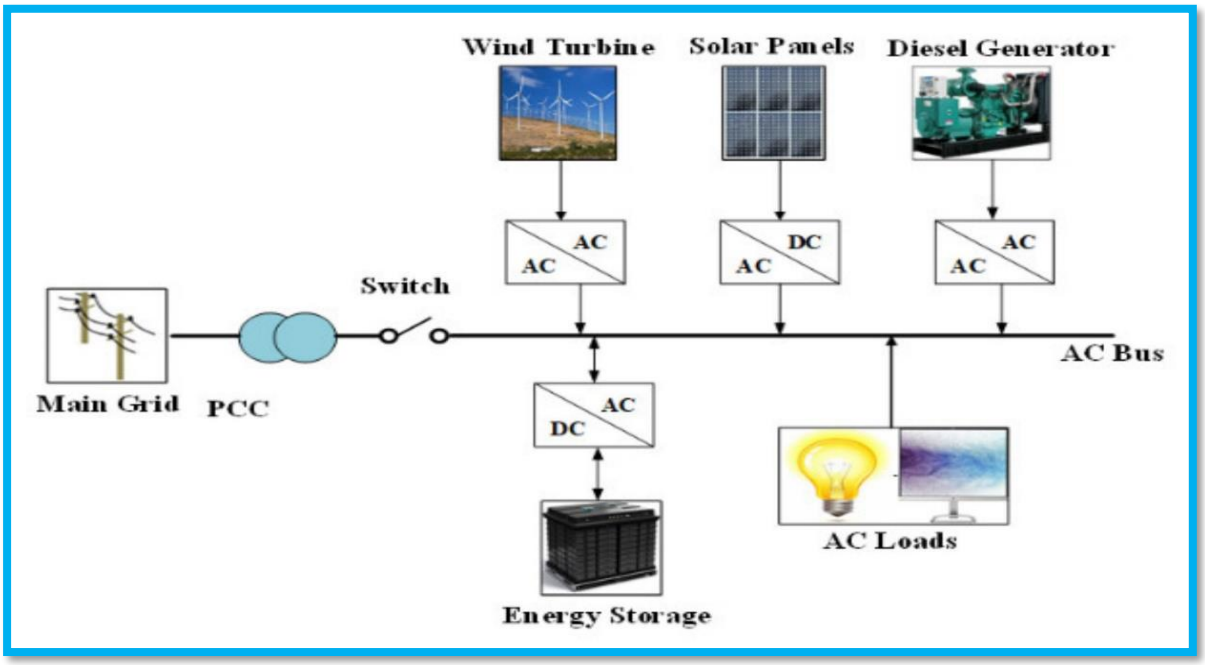

Figure (2-4) operation of MG in Isolated Mode [1]

2.5 Power type of microgrids

MGs are divided into three categories: hybrid AC–DC MG, direct current MG, and alternating current MG.

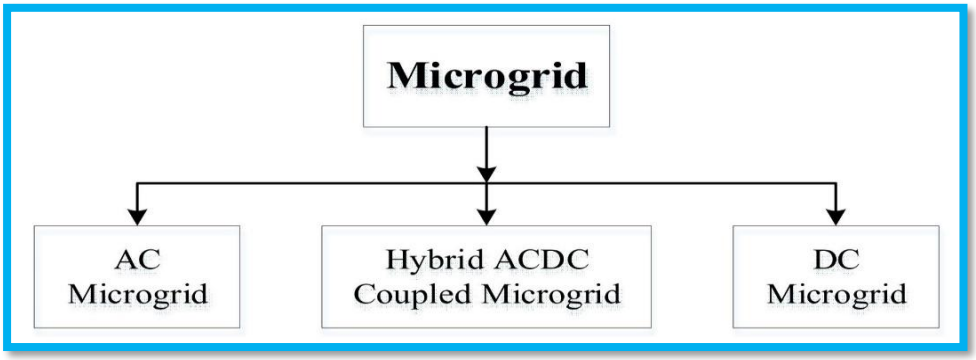

Figure (2-5) Microgrid categorization[9]

2.5.1. Alternating Current MG

A PCC connects an ACMG to the UG, and a switch regulates the MG's operating modes. To facilitate the integration of DC-based Distributed Generation (DG) units, such as Energy Storage Systems , into an AC-bus architecture, power electronic converters are required to perform the necessary DC-to-AC voltage transformation. [20]. The ACMG technique's primary drawback is that integrating

DGs with the UG necessitates large, intricate power electronic equipment, which causes a harmonic impact in the power network. Furthermore, it is necessary to synchronize and harmonize characteristics like phase angle, frequency, and voltage magnitude with the current UG. The use of ACMGs with UGs is limited by these constraints. Generally speaking, an ACMG needs more extra transformation steps than a DCMG.

2.5.2. Direct Current MG

Since DGs primarily produce a DC voltage, the DCMG scheme can be effectively integrated with them. Both RESs and ESSs use a DC voltage to function. Usually, DCMG systems are connected to the UG via a PCC. ESSs, PVs, EVs, and DC loads are connected to the DC bus using this method through DC–DC converters. Wind turbines, diesel engines, and other AC loads are connected to a DC bus using AC–DC converters. In order to increase system efficiency, the DCMG system's architecture is significantly simpler than that of an ACMG system because it does not require grid harmonization of DGs, harmonics, and reactive power flow [21].

However, using power electronic converters leads to issues with reliability and makes it harder to manage the flow of power from and to the distribution UG.

2.5.3. Hybrid AC–DC MG

This method combines the ACMG and DCMG techniques. The PCC is directly connected to the ACMG in this architecture. But to connect to the AC-bus system, the DCMG utilizes a two-way AC–DC converter. For the network to be dependable and efficient, each converter needs a control unit. Between the UG and network buses is the control unit Figure (2-8) To manage and regulate the DC bus voltage and power transfer between the AC and DC MG, a bidirectional converter is utilized [22]. A key advantage of hybrid microgrids is their inherent flexibility, as Distributed Generation units can be seamlessly integrated into either AC or DC buses without the complex synchronization requirements typically

associated with conventional AC grids. As a result, the control minimizes energy losses and is straightforward. Nevertheless, there are several issues with MG's control methods.

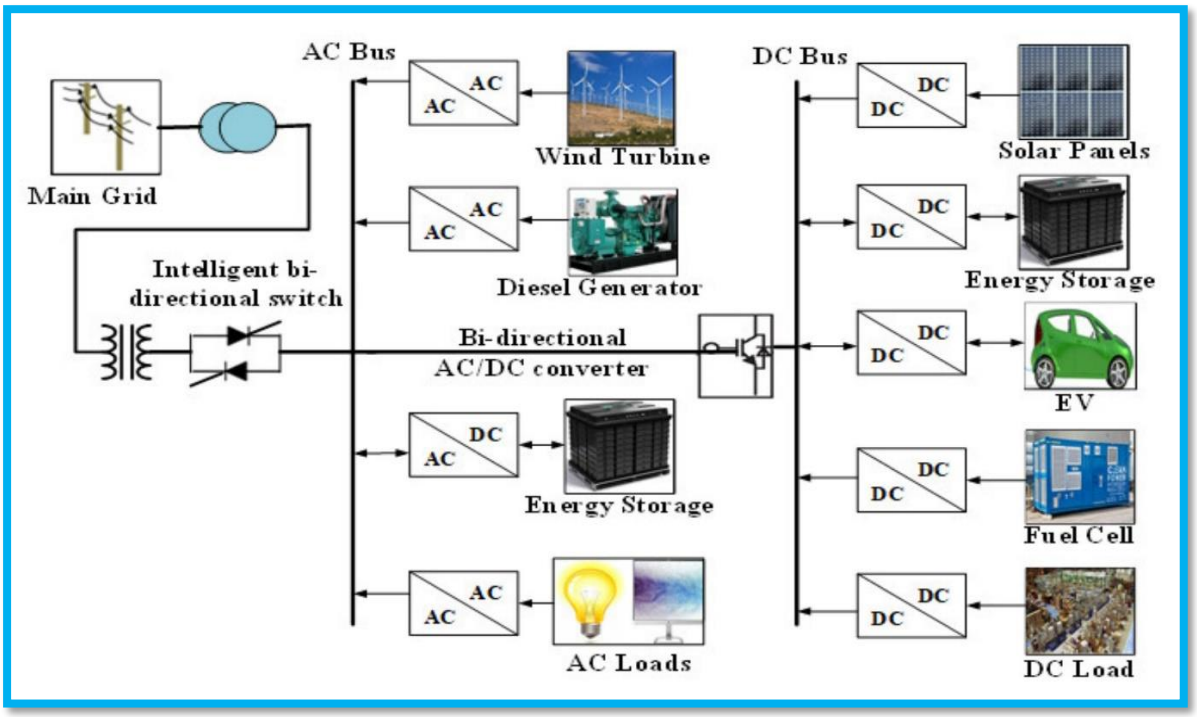

Figure (2-6) Hybrid MG structure - based power system [1]

2.6 Microgrid Energy Management System

Among its many tasks, the EMS keeps an eye on, evaluates, and forecasts DER power generation, energy and related market prices, load usage, and weather patterns. These features allow the EMS to meet all limits and achieve the best possible operation of MG. The EMS for coordinated MG systems is depicted in Figure (2-10) Every MG EMS in this MG hierarchy regulates the power of its own MG. Through the Energy Management System coordination, excess electricity generated by the microgrid is either exported to the main distribution system, shared with an adjacent microgrid, or stored within the Energy Storage System .In a similar manner, the EMS coordinates with the UG or an adjacent

MG to obtain the MG's power shortfall [23]. In order to stabilize and sustain cost-effective operation, the EMS keeps a steady power supply across the board.

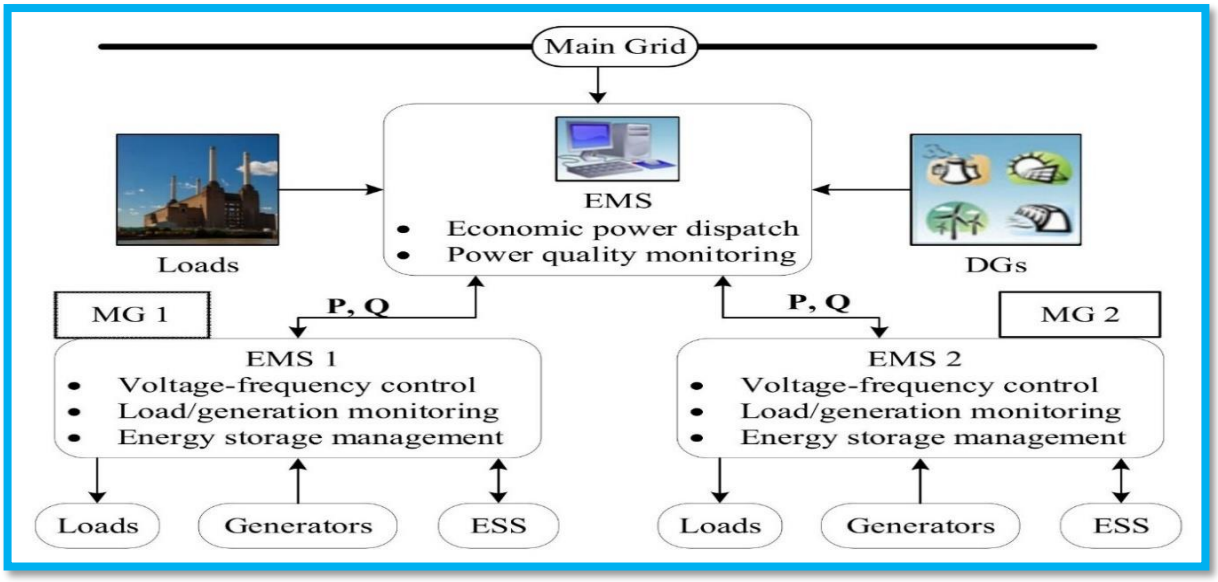

Figure (2-7) EMS for networked Microgrids[10].

2.6.1 Classification of EMS

An MG EMS's supervisory control method can be categorized as either hybrid, decentralized, or centralized.

2.6.1.1 Centralized EMS

The central controller in the centralized approach collects all data, including cost function, weather information, DER generating status, and users' energy consumption status [5]. Maintaining the energy balance of the entire power network is the major goal of a centralized EMS. The primary goals of this strategy are cost reduction and increased reliability. Furthermore, it handles the external EMS effectively Figure (2-11). The black and solid blue lines in Figure (2-11) represent the system's power flow and communication link, respectively. The EMS in the centralized model only performs one optimization, and MGs are connected to the UG over a shared bus. The centralized EMS method works well for optimizing standalone and single-owner MGs. EMSs based on central controllers have been examined and suggested for hybrid, AC, and DC MGs [24].

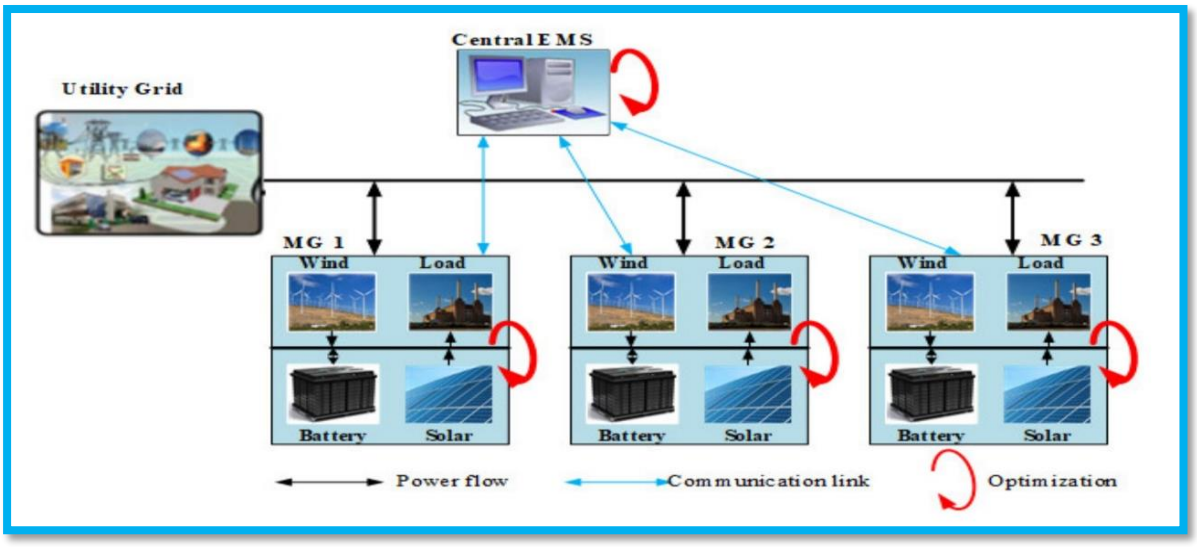

Figure (2-8) Centralized Energy Management System scheme [1]

2.6.1.2 Decentralized EMS

Each MG functions as a separate system in the decentralized EMS method, utilizing a local EMS to maximize its advantages. A decentralized EMS scheme is depicted in Figure (2-12) Every MG has the ability to trade power with the UG on their own. In certain cases, the nearby MGs and the local EMSs can work together to distribute the excess power [25]. Decentralized EMSs are typically optimized using multiagent systems (MASs). Grid-tied MGs made up of several rapidly changing DGs with multiple owners are a good fit for decentralized EMSs.

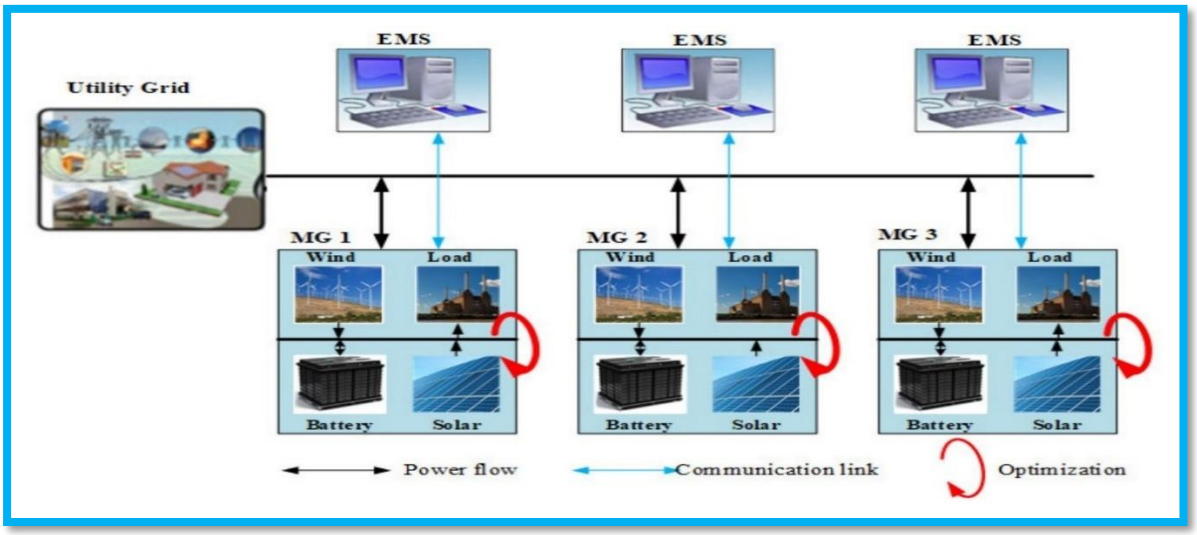

Figure (2-9) Decentralized Energy Management System scheme [1]

2.6.1.3 Hybrid EMS

To address the drawbacks of both centralized and decentralized EMSs and to capitalize on the advantages of individual EMS, hybrid EMSs have been developed. Under the hybrid method, each local EMS solely optimizes local sources and alerts the central EMS to any excess or insufficient energy Figure (2-13) The central EMS then permits an energy exchange between MGs and manages the resources of the overall system [26].

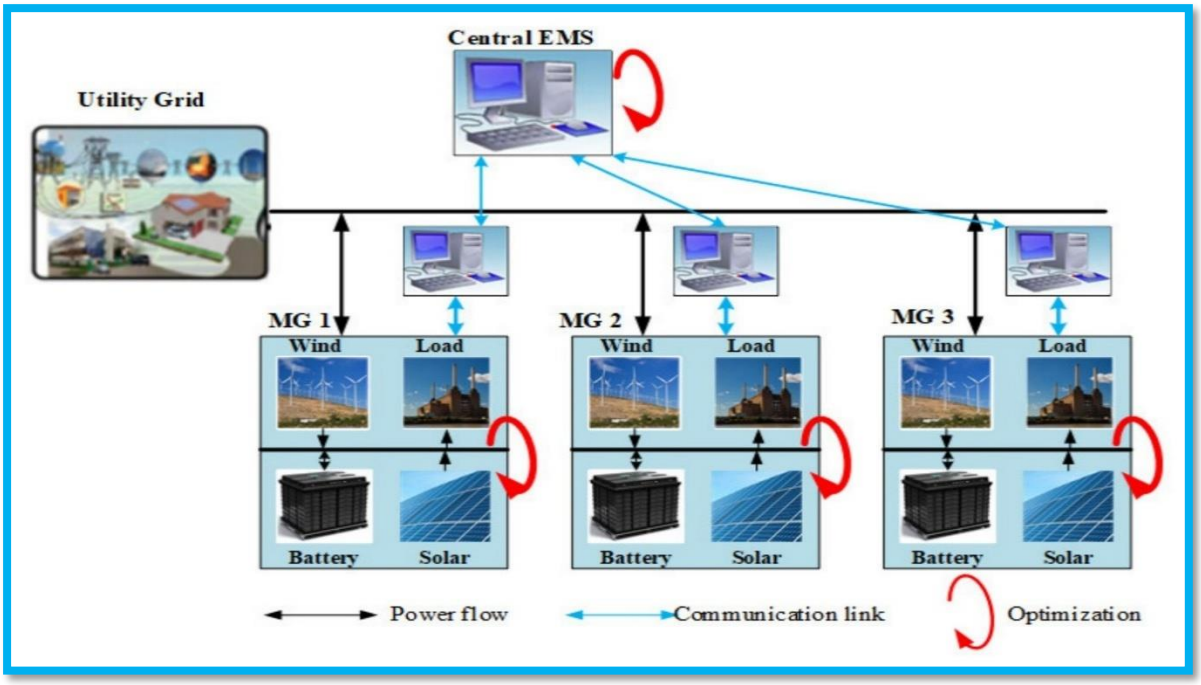

Figure (2-10) Hybrid Energy Management System scheme [1]

2.7 Control Techniques in Microgrids

2.7.1 Basic PID Control for Microgrids

In a microgrid system, transient phenomena of power sharing are the distribution of power amongst various sources as short-term disturbances occur. The process requires suitable control for ensuring dependability and stability of the system. A common control mechanism for regulating voltage, frequency, and power output is PID controller [27]. The PID algorithm is the most used control

technique in industry due to its simplicity, effectiveness, and wide operating range. In its basic form [28], engineers are able to program the PID function directly and easily, because it is so straightforward. The algorithm is based on three parameters, proportional (P) gain, integral (I) gain, and derivative (D) gain, tuned to deliver the best response. Traditional PID functions as a closed-loop system. A PID controller will sense information from sensors, compare the sensor measurement to a setpoint, and change the output to get the control variable to the setpoint such as temperature, speed, flow rate, voltage, and pressure [29].

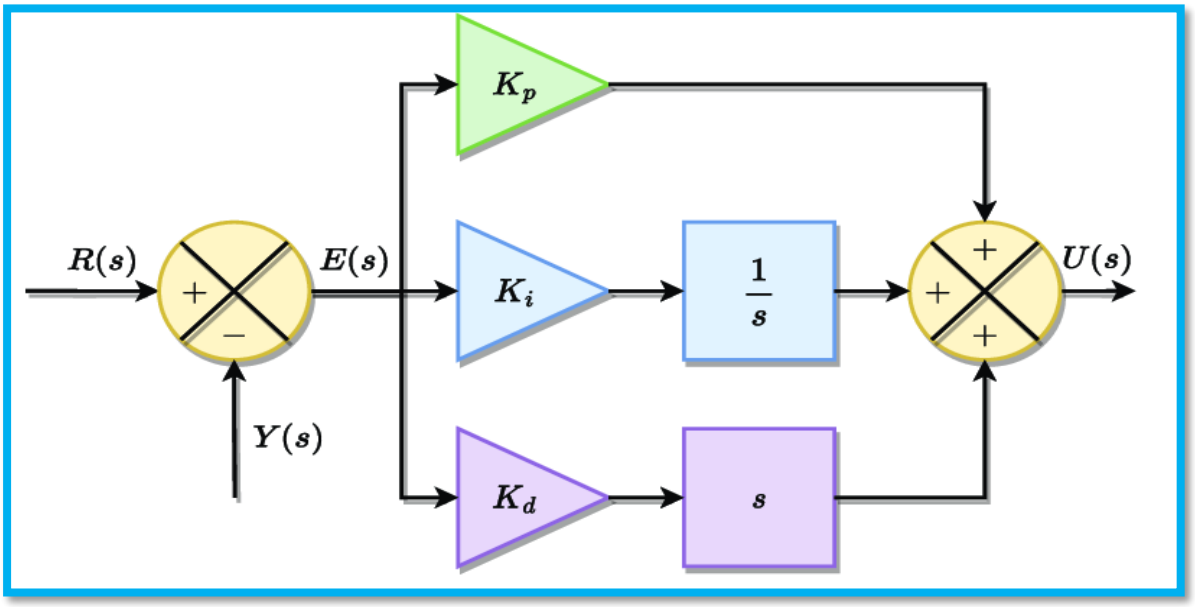

Figure (2-11) PID Controller Block Diagram [30]

PID control is the control algorithm that is most often applied in industry because it has built in reliability and simplicity, to name two advantages. The simplicity of PID control means that engineers can apply and run the controller with ease and confidence. Despite these advantages, there are several disadvantages to PID control. One of the main drawbacks is the manual tuning procedure, which is often complicated and highly time-consuming due to the complex interdependencies between PID gains and droop coefficients, especially when attempting to maintain stability across diverse operating points. In addition, most classical PID controllers do not usually give the required level of performance for

processes with significant non-linearities or time delays. Despite these disadvantages, engineers still favor PID control over more advanced methods, even when PID control does not always meet stringent control requirements or give optimal performance [31].

2.7.2 Conceptualizing Droop Control in Microgrids

Droop control is a decentralized inverter control method used in microgrids that eliminates the need for physical communication lines by allowing multiple power sources (such as inverters connected to solar panels or batteries) to function in parallel and share the load independently. The idea mimics the way traditional synchronous generators within a bulk power system regulate themselves: as the load on a generator is raised, naturally its speed decreases, and thus its output frequency decreases slightly. Inverters obtain this through simple mathematical formulas using droop control to allow independent and stable power sharing [32]. Microgrid droop control is significant, as discussed below, because it serves to provide system stability, self-sustained power sharing, and flexibility in scalability:

- **Autonomous load balancing:** This feature enables more than one inverter unit to be shared with active and reactive loads without a master controller or communication lines. Thus, the system is more reliable and scalable.

- **Grid-Forming Capability**: With isolated or islanded operation, the capability of the inverter to provide and support a regulated voltage and frequency for the microgrid enables it to behave like a grid-forming inverter.

- **Plug-and-Play Operation:** The microgrid can be accepted with additional distributed generating units without complex reconfigurations of control systems

- **Stability:** Droop control offers a type of virtual inertia that stabilizes the frequency and voltage of the microgrid under abrupt changes of generation or

load. The conventional droop control strategy serves as the foundational decentralized framework for power distribution in islanded microgrids. This method utilizes the P-f and Q-V relationships to achieve autonomous load sharing without critical communication links. The standard implementation within inverter-based DG units is illustrated in Figure 2.12, where local measurements of V and I are used to calculate the power components. These values then determine the reference frequency and voltage for the internal control loops, ensuring proportional response to load changes and maintaining AC bus stability.

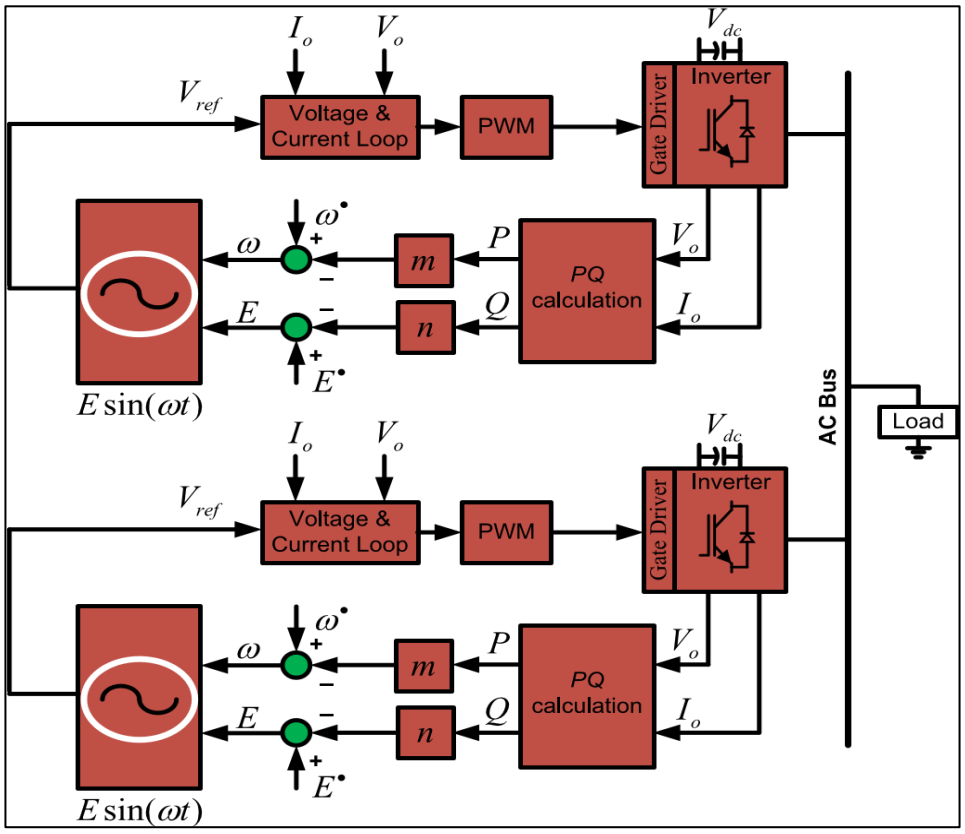

Figure (2-12) Block diagram of c conventional droop control.

2.8 Control of Microgrids

Microgrids provide significant benefits, including enhanced power quality and reliability for sensitive loads and increased utilization of different energy resources, such as renewable energy. Furthermore, because of their proximity to energy end consumers, microgrids are expected to benefit customers and service providers significantly. To improve control performance, DGs are typically

connected to microgrids via power inverters. Many control methods have been widely used worldwide to operate parallel-connected inverters for load sharing in DG grids, including:

- Centralized / Decentralized.
- Master-slave control.
- Average current-sharing control.
- Current power-sharing technique.
- Peer-to-peer control.

In this thesis, the focus is exclusively directed toward decentralized and peer-to-peer control strategies, as they represent the most robust and scalable approaches for modern microgrids. Unlike centralized systems that rely on a single controller, the decentralized droop control method implemented in this work allows each inverter to operate autonomously based on local measurements. This architecture ensures high reliability and eliminates the risks associated with a single point of failure, providing a seamless power-sharing mechanism between parallel units.

2.8.1 Decentralized control strategies for efficient operations and management

Decentralized control strategies provide as an alternative to centralized control strategies. In their most general form, they allow each generator unit in the microgrid to determine its output power without considering the power output of other units. Droop control is a widely used and better-known decentralized control strategy that can be implemented through primary control. There are different vertical arrangements for droop control. Still, the widely spread one combines P-f and Q-V droop control, where the active power frequency and the reactive power voltage droop control methods are used for distributed generator units. Recent developments have enabled the implementation of droop control for several inverter-connected distributed generator unit types. Such systems can

achieve stable operation in a grid-forming configuration, even if losses and/or unknown disturbances are acting on the system.

2.8.2 peer-to-Peer Control Architecture

The Peer-to-Peer (P2P) control strategy represents a truly decentralized approach where all Distributed Energy Resources within the microgrid operate with equal priority and autonomy. Unlike master-slave configurations, P2P architecture eliminates the dependency on a single coordinating unit, thereby enhancing the system's "plug-and-play" capability and overall survivability.

P2P control structure allows each Voltage Source Inverter to regulate its output based on local measurements of voltage and frequency. In this setup, there is no hierarchical dominance; instead, the parallel-connected inverters interact as "peers" to achieve balanced power sharing. This interaction is governed by the modified Droop-PID controllers, which ensure that any change in load is instantaneously distributed among all units according to their pre-defined capacities. This horizontal coordination, ensures that the failure of any single unit does not lead to a total system collapse, providing a robust foundation for the proposed PSO-ANN hybrid control framework.

2.9 Enhancing Stability in Microgrids

Microgrids represent small-scale power systems composed of DER with localized loads that can operate independently from the grid. DG growth has mainly increased interest in microgrids. However, the intermittent nature of renewable energy resources poses challenges to microgrid stability and control. Power system stability is defined as the ability of a power system to regain a state of equilibrium after being subjected to a disturbance. Increasing renewable energy resources in a microgrid can lead to potential issues related to stability, such as a decrease in the system of damping. Microgrid stability can be classified as small-signal stability or transient stability. Microgrid frequency and voltage

control are similar to the control method used in conventional grids, with frequency and voltage as two significant control variables. In a microgrid, controllable DGs are operated to maintain the adequacy of active and reactive power balance while operating within their generation limits. However, droop-based control methods of synchronous machines may also find limitations in microgrids with high levels of inverter-based resources. Stability is classified as a 'small signal' if the disturbances are small. The power system is subjected to constant small disturbances on occasion. Power systems with tightly interconnected connections and many interconnected machines can exhibit small-time electromechanical oscillations. These oscillations may persist for a long time and become significant because the system cannot dampen them. This makes small signal stability of the power system deteriorate, leading to an uncontrollable system. Voltage stability deals primarily with the ability of a power system to maintain steady voltages at all buses in the system after being subjected to a disturbance, which can also be classified into short-term and long-term voltage stability. Droop control used in voltage regulation of DG units may inadvertently increase the system's operating range, making them more prone to voltage instability.

2.10 Previous Study:

Several research papers investigated the optimization of transient power sharing in microgrids using various advanced techniques in conjunction with PID and Droop controllers. Below are some key works. The subsequent sections summarize and describe the implementation of each technique and the author contribution achieved in each work. Additionally, the pros and cons have been discussed and considered. The main focus of these advanced would be to optimize and schedule both PID controller gains as well as the Droop control coefficients for increased stability and performance- specifically using algorithms like PSO

for the tuning of the PID controller and/or the Droop control coefficients, as well as ANN for the adaptive control.

2.10.1 Traditional Controller Techniques

While PID controllers and conventional Droop control have historically served essential functions for load frequency control and power sharing in power systems, their inherent limitations, along with the increasing complexity of modern grids, have driven significantly more study in developing more complex and effective hybrid and advanced control methodologies**. Yue et al. (2023)** [39] examined the challenges in developing fast and robust power sharing for remote microgrids. The authors referenced that the power-sharing droop control method has typically not performed that well, for example, even when the gains of the droop are excessive, typically the system becomes unstable. The study confirmed that among the significant drawbacks of the classical droop method is the trade-off between power sharing speed and stability of the system. **Elvin Yusubov et al. (2025)** [40] assessed the robustness of metaheuristic PID controllers under the hierarchical control architecture of photovoltaic DC microgrids. The study identified that conventional PID tuning methods such as Ziegler-Nichols and Cohen-Coon fall short in handling the complex, dynamic behaviors of these systems. In line with the study, sacrificing conventional measures is necessary. **Waseem kh et al. (2024)** [41] centered on the important problem of DC voltage regulation in power plants, which they felt is required to ensure performance and reliability. The authors compared the four control systems: fuzzy logic, fractional order PID (FOPID), conventional PID and a hybrid fuzzy-PI system. The studies concluded to conventional controllers, for example, the conventional PID are not adequate enough to provide the performance and reliability of power plants, especially with the inclusion of renewable energy systems. **Ahmad et al. (2021)** [42] provided an extensive explanation of the fundamental concepts of conventional droop control. to control active and reactive powers in AC and DC

microgrids by means of voltage and frequency droop adjustments. the authors noted that this framework provides a decentralized power sharing scheme from different energy sources and does away with a centralized controller, a nature of conventional power systems. but the authors' work also quietly noted the drawbacks of this configuration such as a reliance on line impedances that are capable of affecting effective power sharing. **Mírez et al. (2020)** [15] gathered and compared the theoretical foundations and applications of the droop control method. The authors set the foundation for understanding how droop control is applied in microgrids by using synchronous generators to enable decentralized power sharing. This article illustrates the ease and advantage of the approach in providing and managing distributed energy resources, especially if operating in an islanded mode. **Fadi et al. (2024)** [43] analyzed how conventional PID controllers function in a grid-connected solar system. While PID is a straightforward method for stabilizing output power, the authors observed that rapidly varying weather conditions diminish the level of output power stabilization. The findings reveal limitations of using traditional control strategies in dynamically installed renewable energy systems; the authors point out the delay in PID response and difficulty of reaching and maintaining the stable maximum power point. **Mahmoud et al. (2023)** [44] contrasted and compared traditional control strategies in regulating the voltage within DC microgrids. PID control performance was studied, indicating an ease of setup, but issues arose concerning disturbance and nonlinearities in the system. The authors indicated that only fixed-gain PID controllers deliver performance that is always a compromise: fast response time will always be delivered at the expense of overshoot and precision or stability versus high precision and stability will always come with a compromise in response time and minimal overshoot. While the aforementioned studies demonstrate the fundamental operational stability provided by conventional PID and droop-based control strategies, a critical gap remains regarding their performance in highly dynamic environments. The

literature indicates that these methods rely heavily on fixed control parameters, which often fail to adapt to the non-linear, stochastic nature of renewable energy integration and sudden load fluctuations.

2.10.2 Optimized Controller Parameters using Algorithms

The modified controller refers to a conventional controller that has undergone some changes in order to address the shortcomings found when using traditional techniques. The impact of these changes on the performance and stability of the power system is examined in the sections that follow. **M. Regad et al. (2021)** [45] focused on using a PID controller tuned by PSO to control frequency in a microgrid power system that uses wind and PV sources**.** The authors utilized secondary means such as fuel cells and diesel generators. Energy storage systems were also used to support linked loads. This research concluded that PSO is a reliable optimization scheme for tuning PID controller gains for a particular objective function. The main purpose was to reduce variations in frequency of the system and overall power. PSO based PID controllers have better frequency and power performance than conventional controllers based on genetic algorithms**.** Under the supervision of PID and other simulated systems, the hybrid system detailed in the study integrates photovoltaic cells, wind turbines, fuel cells, diesel generators, and various energy storage devices**. Vincent N. Ogar et al. (2023)** [46] Emphasized the necessity of load frequency control for ensuring the security and reliability of power systems. They found PSO-PID to be an effective approach to increase LFC efficiency and strongly recommend it as grid complexity and renewable energy sources increase. **Nanda, A. et al. (2023)** [47]demonstrated the three-phase distributed energy freestanding microgrids' operational efficiency. Their study focused on systems that used solar photovoltaics as the main power source and a battery storage unit for system inertia and stability. The study examined the microgrid's performance under load imbalances and variations in solar insolation. **Ahmed Alshahir et al. (2021)** [48]

demonstrated a modified form of the MPSO algorithm that is designed to minimize the power-sharing ratios between a utility grid and a microgrid. Their indicated process aims to coordinate hourly networked systems with lower instantaneous power variances by taking various actions to minimize the variances of transient response parameters. This directly alleviates the concerns for dynamic grid integration associated with monitoring controller parameters to improve system sustainability and reliability. **Nihan Kahraman (2022)** [49] demonstrated a model designed to improve voltage and frequency stability and microgrid power responsiveness. The study proposed a self-tuning control strategy that employs an H-infinity controller optimized with the Artificial Bee Colony algorithm to enhance droop control. In comparison to other optimization methods and conventional droop control, the study showed significant improvements in power-sharing efficiency and dynamic response. **Farhad et al. (2022)** [50] explored a hybrid strategy to accomplish microgrid frequency regulation. They employed a hybrid Particle Swarm Optimization-Gravitational Search Algorithm (PSO-GSA)-based PID controller to study frequency regulation in islanded microgrid conditions. The objective function was time-dependent and a function of system frequency deviations, while the PID parameters were tested on a series of simulation experiments comprising power and frequency deviations and load deviations and standard function testing. **Mohsin Ali Tunio et al. (2020)**[1] proposed a new control system based on MPSO. The research methodology was aimed at transient response enhancement and optimal use of the maximum power sharing contribution in grid-connected microgrids. The primary reason that their work was new is the fact that it had a "best neighbor particles" (rbest) component, which other algorithms lacked and acquired the capability to search and choose the optimal global solution. **Majeed Kareem et al. (2024)** [51] noted the drawbacks of droop control with factors such as low dynamics, line impedance mismatches, and inaccurate load sharing. In response to these disadvantages, the authors conducted an evaluation of five

metaheuristic optimization techniques which included the Particle Swarm Optimization algorithm. The authors propose that these tools can enhance droop control parameters and improve the droop method's effectiveness and its applicable utility for the flexible microgrid. **Lai et al. in (2025)** [52] proposed a new enhanced droop method as a solution to reactive power imbalance issues in islanded microgrids. The authors used APSO method with virtual impedance control. The APSO process was set to optimize the PID controller parameters in the outer voltage control loop. The enhancement minimized circulating current between parallel inverters and greatly improved output voltage stability of the inverter. **Kaur et al. (2024)** [53] suggested a novel approach to droop control by using PSO algorithm. The approach was developed to achieve more accurate active and reactive sharing of electricity between distributed generating units in an islanded microgrid. Simulation results showed that the PSO algorithm outperformed conventional techniques of tuning the parameters of droop control, especially with changing loads. **Ghahramani, M. et al. (2019)** [54] were interested in applying a sophisticated PID controller in order to improve voltage and frequency control performance in isolated microgrids. The authors were interested in applying the Particle Swarm Optimization technique to tune the PID parameters in order to assist in controlling the overshoot of the voltage more efficiently and reducing the settling time. The findings using the PSO were that it was better than the conventional practices because it gave a far more dynamic and stable output with the simulations. **Al-Saedi et al. (2018)** [55] proposed a hybrid scheme that integrated droop control and the particle swarm optimization algorithm in order to improve power sharing in renewable-energy-based microgrids. The authors addressed the issue of power sharing mismatch as a result of the fluctuating line impedance and introduced a PSO to make dynamic adjustments to the droop settings in an effort to evenly distribute active and reactive power among the distributed sources. The results reflected the benefits of the PSO algorithm, showing that it had great potential to reduce load-sharing

inconsistency while enhancing stability in the microgrid. **Li et al. (2017)** [56] investigated voltage and frequency stability challenges when integrating renewable energy into microgrids. They proposed a control technique that integrated droop control along with the PID controller that was optimized with the PSO algorithm. Their attention was to balance correctly proper regulation of the voltage and proper power sharing with the right regulation of the frequency. They identified that the PSO-optimized hybrid system experienced faster recovery from disturbances and load change. This demonstrated the advantages of uniting state-of-the-art optimization techniques with conventional control methods.

2.10.3 Intelligent and Adaptive Controller Techniques

Microgrids today also possess complex, non-linear dynamics which continue to surpass those which traditional approaches such as PID control or droop control can manage, despite advances afforded by various algorithms, some of which are PSO. A significant emphasis of this research has thus been developing more intelligent, adaptive solutions. One novel approach to improving the performance and stability of renewable microgrids by means of an artificial neural network is employing the hybrid PSO-ANN framework. **Ghiasi, M., et al. (2022)** [3] investigated novel control techniques for voltage source converters in microgrid systems. They discovered through their investigation a novel technique, Particle Swarm Optimization, that would enable VSC performance and efficiency to be enhanced with regards to controlling microgrid dynamics. PSO is a natural move towards intelligent optimization as an evident alternative to parameter scheduling offered in an artificial neural network. Besides, Predictive Control, which is predicated on a general-purpose finite control set (FCS) model, was also used in the study to optimize the operating performance of the microgrid. **Dabbagh, M. A. et al. (2016)** [57] focused on creating an intelligent voltage and frequency controller for a remote microgrid setup using artificial neural networks . The

study demonstrated how ANN controllers can optimize system stability by adapting to changes in renewable energy source and load. **Javan, M. et al. (2015)** [58] suggested a novel control approach that maximizes the power sharing of hybrid microgrids using fuzzy logic and artificial neural networks . The research aimed at addressing the reliability issue of reactive power sharing through conventional droop control. **Nghia et al. (2023)** [4] increased dynamic load-sharing in microgrids through particle swarm optimization and artificial neural networks . The hybrid method utilizes the strengths of both methods: The PSO tunes a PID controller to optimality, and the ANN adjusts the controls for rapidly changing parameters dynamically in real time. **Abdulraheem et al. (2022)** [7] provided an intelligent control process for grid-connected renewable energy microgrids. The PMU based approach utilizes artificial intelligence (AI) techniques, a neural network combined with a fuzzy logic control system. The control system endeavors to improve the control actions for voltage and frequencies management in real-time microgrid data monitoring. **Nor et al. (2020)** [59] discussed thoroughly the utilization of artificial neural networks. Results illustrated that ANNs are particularly valuable for the management of complex and nonlinear power system conditions. Microgrid control performance can be significantly enhanced with the ability of an ANN to manage complex data and learn new conditions. Results illustrated that ANNs are a successful approach to build intelligent control strategies with the ability of quick adaptation to ensure system stability following an unexpected disturbance**. Olabi et al. (2023)** [60] proved the value of artificial neural networks in their research. The research proved that these networks were applicable in improving the power generation and reduction of the impacts of under shading through smart anticipation and an optimization method. The artificial neural networks must deal with random and dynamic conditions, in order to improve performance in renewable energy microgrid systems leading us to the relevance of this research in microgrid smart controls. **Ben Cheikh et al (2018)** [8] used artificial neural networks to create a

maximum power point tracking (MPPT) method for photovoltaic systems. Through this work, it was shown that the efficiency of power extraction was significantly better even under dynamic environmental conditions. This work is particularly important because it showed the possibility of using ANNs to achieve maximum power extraction and overall system efficiency, both of which are the basis of stability and functionality of microgrids driven by renewable energy sources**. Maher G.M. Abdolrasol et al (2021)** [11] presented a practical solution for the VPP system management of RES. The proposed approach is also related to smart microgrids since PSO and ANNs have been incorporated into the approach. This novel approach unites the strengths of both algorithms and produces an optimal energy scheduling plan ultimately leading to reduced power consumption along with reduced reliance on the master grid. With consideration of real-time weather and load demand, the study also explores the potentiality through which the hybrid ANN-PSO algorithm can increase the effectiveness of VPP systems, or indeed any that are fundamental to modern microgrid operation. **Kaushal and Basak (2020)** [61] investigated the application of ANNs in power quality issue handling for microgrid systems that are appropriate for PV systems. The research demonstrated performance of ANNs towards major power quality issues such as frequency stability, imbalance, and voltage sags. The research demonstrates the capability of intelligent control measures in enhancing the robustness and reliability of modern microgrid systems. **Kumarappan and Vigneysh (2025)** [62] proposed the use of a feedforward neural network (FFNN) to novelly address the problem of power sharing typical of traditional droop control. The authors prove that their method can stabilize voltage and frequency within the microgrid, as well as promote active and reactive power sharing in challenging situations and with troublesome line impedances. Making coordination and ensuring sharing of power is a major issue with microgrids and distributed energy resources, and the authors provide a solution for this issue. **Karimi et al. (2024)** [63] proposed a technique for correction of frequency

deviations in droop-controlled microgrids. They utilized shallow neural networks that mapped the droop control power reference values to resistive time-varying load power directly. The correction eliminated nearly all steady-state errors and improved frequency stability in the microgrid considerably. This paper demonstrates the feasibility of neural networks to supplement traditional control methods and improve the sensitivity of the methods to real-time load dynamics.

Kashyap et al. (2024) [64] utilized a droop-controlled bidirectional converter driven by artificial neural networks to integrate a DC microgrid with an energy storage system. The study demonstrated how optimization using ANNs could impact the management of the power imbalance associated with renewable energy sources, consequently ensuring power reliability and supporting the maintained stability of voltage in the system. This optimization method offers a plausible pathway for integrating intermittent energy resources into a microgrid, and there is promise it could enhance overall reliability of the power system.

Zadeh Bagheri (2024) [65] provided an adaptive droop system control approach, including fuzzy logic and neural networks. The solution can provide efficient coordination of electrical power flow for dispatchable decentralized energy resources in AC and DC microgrids. The paper demonstrates how the method can handle sudden changes in the system, including switching from islanded to grid-connected mode operation, and the hybrid approach provides operation stability and robustness against unapproved external disturbances to the microgrid.

Adiche et al. (2025) [66] propose a hybrid control scheme that blends droop control with an ANN-based adaptive PI controller. They aimed to demonstrate the capability of artificial neural networks in augmenting and outperforming conventional PI controllers, leading to better performance of power sharing and voltage regulation of microgrids, including dynamic systems. Their approach shows how the PI controller can be induced to counteract the different nonlinearities and disturbances that are faced in microgrid control by adding the capacity for the PI controller to adapt its gains in real time, leading to a more

robust and responsive approach. **Hassan et al. (2019)** [2] proposed an adaptive secondary controller for microgrids utilizing a biologically inspired reinforcement learning methodology. This article improves the performance of the secondary control layer to correct higher-level (PID and droop) control on deviations. While this article does not combine ANN, PID, and droop into a single block, it suggests that an intelligent algorithm can be utilized to enhance a higher control layer and that is a smart way of improving stability. The study is similar to the trend of introducing an adaptive, self-learning type controller that can provide improved performance over traditional control types.

Table 2.1 Comparison of Optimization Methods for PID Controller and Droop Parameters in Microgrids

Ref.	Year	Technique	Advantages	Disadvantages
[68]	2025	GA -PID	-Efficient in test a wide range of possible solutions - High resilience to system disruptions.	- Time-consuming and computationally expensive. - requires an advanced simulation environment.
[64]	2018	SSA -PID	-Simple to integrate into intricate systems. -Effective in enhancing system functionality.	-The solution space might not be thoroughly explored. -prone to problems related to convergence.
[69]	2023	CS-PID	-Effective system stability tuning. - Good convergence to a feasible solution.	- high cost of computation. - might choose a less-than-ideal option.

[70]	2025	ACO-PID	-Excellent performance and quick reaction. - Ensures increased system robustness.	- Increased design considerations - Initial parameter sensitivity.
[72]	2024	GA-Droop Control	-Effectively investigates a wide range of droop parameter combinations. - produces a robust and stable control system.	-Tuning can require a lot of computation and time.
[72]	2024	GOW-Droop Control	-Excellent search features for optimal droop configurations. - Offers superior power-sharing options.	-Needs to have its parameters carefully adjusted in order to produce a good outcome.
[73]	2023	ACO-Droop Control	-Able to adapt to complex and nonlinear dynamics with ease.	-prone to stagnation issues, which could result in tuning that is not optimal.
[67]	2017	PSO-PID	-Fast and effective PID parameter tuning -Easy to understand and apply	-Can get stuck in local optima. -Sensitivity to initial parameters.
[71]	2019	PSO with ANN	-Better performance compared to stand-alone solutions. -Extremely flexible in dynamic and nonlinear circumstances. - learns from data in an efficient way.	-Design and development are extremely complex -high processing load that uses a lot of resources.

[72]	2024	PSO-Droop Control	-Efficiently calculates the optimal droop coefficients. - enhances power sharing and stability.	-Initial parameter sensitivity. - Can get stuck in local optima
[74]	2022	ANN-Droop Control	-An extremely robust and stable control system. -quickly adjusts to changes in the system.	-incredibly difficult to create and calculate.
//////	2026	PID-Droop with PSO-ANN	-Superior Performance -Real-Tim Adaptation. -Comprehensive Stability	////////////////////////////////// //////////////////////////////////

2.11 Summary

In this chapter, a comprehensive overview of microgrid control strategies is provided, highlighting the primary challenges of voltage/frequency stability and sudden load changes. The literature review reveals a diverse range of protocols, from advanced meta-heuristic and artificial neural network techniques to conventional PID and droop controllers. However, a specific technical limitation is identified in traditional approaches; while conventional PID and droop controllers are reliable, they often lack adaptive capabilities and require manual parameter tuning to cope with dynamic load variations. Consequently, there is a need for a multi-layered, holistic framework that integrates the precision of classical control with the adaptability of modern optimization. The ideal approach identified is a hybrid strategy that synergistically combines these benefits to enhance frequency stability and power sharing.

The proposed approach leverages the learning capability of an Artificial Neural Network in understanding the dynamics of a system and utilizes Particle Swarm Optimization to learn and optimize the PID and droop controllers' parameters in an intelligent manner. The integration of both systems is intended to generate a control scheme that is resilient and flexible. The PSO-ANN integration enhances their performance to achieve optimal results in real-time, while the PID controller exhibits good voltage and frequency control and the droop controller has good power sharing. The method will maximize the overall system efficiency, improve resilience and uncertainties and maintain operations stability across the system through intelligent parameter tuning of the PID and droop controllers. This is a significant step towards a stronger, more efficient control strategy for contemporary microgrids with non-deterministic renewable energy sources.

CHAPTER THREE

MATHEMATICAL MODEL

CHAPTER Three

Mathematical Model

3.1 Introduction

This chapter presents a detailed mathematical and technical background of the suggested three-phase microgrid system and its control schemes. The three-phase Voltage Source Inverter and its related LC filter with a damping resistor (R_d) physical description precede. The chapter proceeds to examine the dynamic models of the system's significant components. In this presentation of robust cascaded control structure, control ideas are presented in both stationary (abc) and rotating (dq) coordinate frames. This methodology relies on three-phase Park transformation for obtaining precise and independent control of active and reactive power for balanced systems. Besides, a proper DC bus voltage model simulating short voltage dips is built, emphasizing the direct impact of such oscillations on stability and operation of the entire three-phase system. The chapter first introduces the decentralized droop control strategy for power sharing, and subsequently continues to elaborate on the basic voltage and current control loops. The prime contribution of this work is therefore established: an innovative optimization framework is utilized that employs the Particle Swarm Optimization algorithm for the purpose of determining the optimal PID controller gains as well as the decentralized Droop coefficients. The data gathered in this procedure is used to train an artificial neural network to produce a smart, adaptive controller capable of varying its gains dynamically to provide optimal performance. Finally, this whole methodology provides the groundwork for the following chapters, which simulate and estimate system performance in detail by connecting theoretical models with a real control and optimization process.

3.2 Methodology

The approach of the research is a comprehensive, multi-stage process that is a combination of contemporary metaheuristic optimization algorithms with conventional control techniques to improve three-phase microgrid performance. The basic paradigm is based on a single hybrid PSO-ANN algorithm. The algorithm simultaneously tunes all the most important controller parameters to make the main control layer more improved: the droop coefficients (m and n) (for frequency and voltage stability and proper load sharing) and the PID parameters (to improve dynamic response, quality metrics like THD, overshoot, and settling time). By optimizing all these parameters to operate on the dq reference frame, reactive and active power can be controlled decoupled and accurately. The Artificial Neural Network module is optimized using the optimal values for all the combined parameters by PSO module so that an adaptive real-time response can be achieved for varying load conditions. The ultimate objective is to optimize the microgrid completely and harmoniously by regulating a number of variables simultaneously, including power quality, dynamic response, stability, and three-phase load sharing. Simulation was carried out using the MATLAB platform and an algorithm that has been especially constructed to precisely replicate the real three-phase system. Analysis of the system's dynamic response and steady-state operation under different operating conditions, including load fluctuation and disturbances, was carried out to validate the efficacy of the suggested methodology. The following two separate yet interrelated flowcharts provide a detailed pictorial illustration of the integrated methodology adopted in this work, showing how cooperative control parameter optimization leads to revolutionary microgrid improvements. The following figure is a graphical overview of the main elements of the research methodology, from advanced control to three-phase physical modeling. This figure, referred to as Figure (3-1), is a concise and step-by-step overview of the entire process, from basic modeling of the microgrid

system to the detailed performance analysis. It highlights the rational flow of work from structuring the cascaded control system to optimizing it using the framework suggested. For ensuring optimal performance of the system, PSO-Based Parameter Optimization and the resulting Adaptive Control System Development are highlighted through the flowchart. The methodical approach is a perfect guide for system designing and implementation as well as guiding the reader through the research.

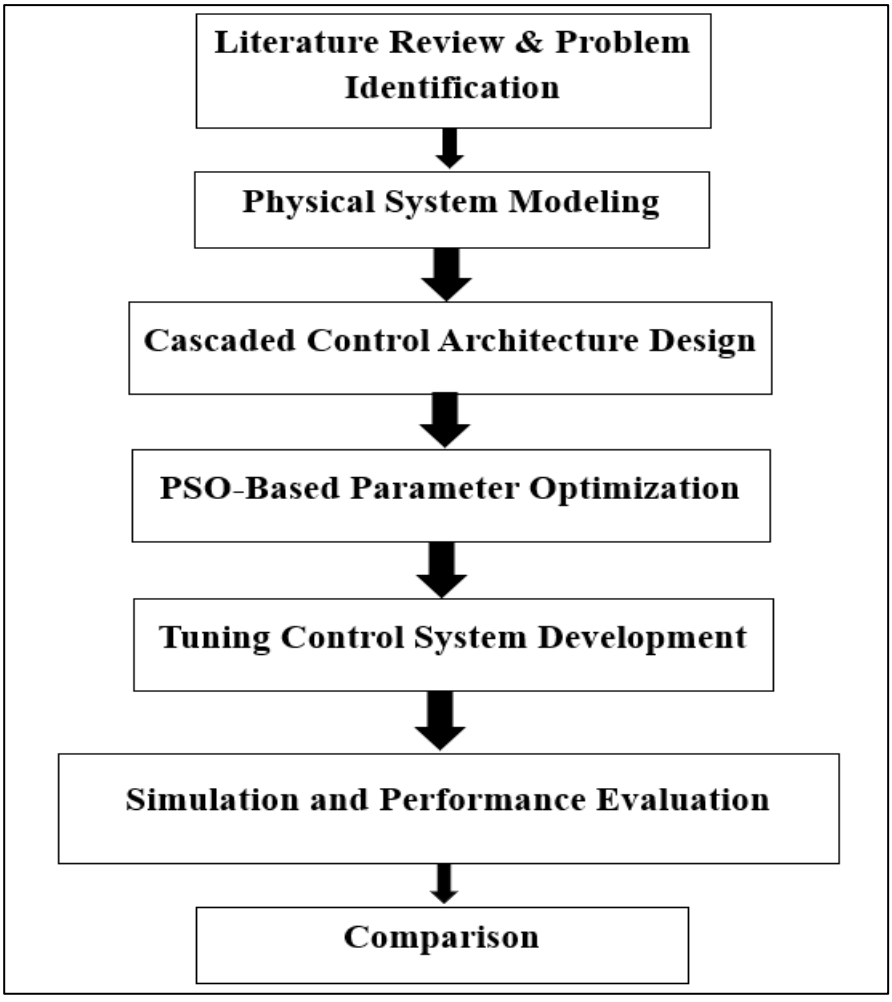

Figure 3-1 Overall System Development Block Diagram

The subsequent figure provides a comprehensive presentation of the Main Contribution of the research, since it complies with the general methodology of the research. The optimization method adopted in optimizing the performance of the microgrid is incorporated in Figure (3-2). The hybrid PSO-ANN method is employed in order to optimize the control system through a two-way process that

only acts on the tunable parameters. This optimization targets both the PID controller gains and the decentralized Droop coefficients used in the outer control loop, responsible for voltage, frequency, and proper load sharing. The inner loops that control current, based on constant PI controller gains, are actually supported by this optimization. This integrated strategy is required as tuning parameters of the outer loop has a significant effect on the overall stability and decoupling contributed by the current controllers. The strategy thus illustrates a holistic optimization that merges the external system performance improvement (Droop-based) with inner pre-set regulation optimization. The flowchart conveniently illustrates how the alteration of each parameter set produces distinct, quantifiable performance advantages, from improved frequency stability and reduced THD to improved dynamic responsiveness and active power sharing. This overall approach underscores the focus of the research on developing standalone microgrids in a complete manner.

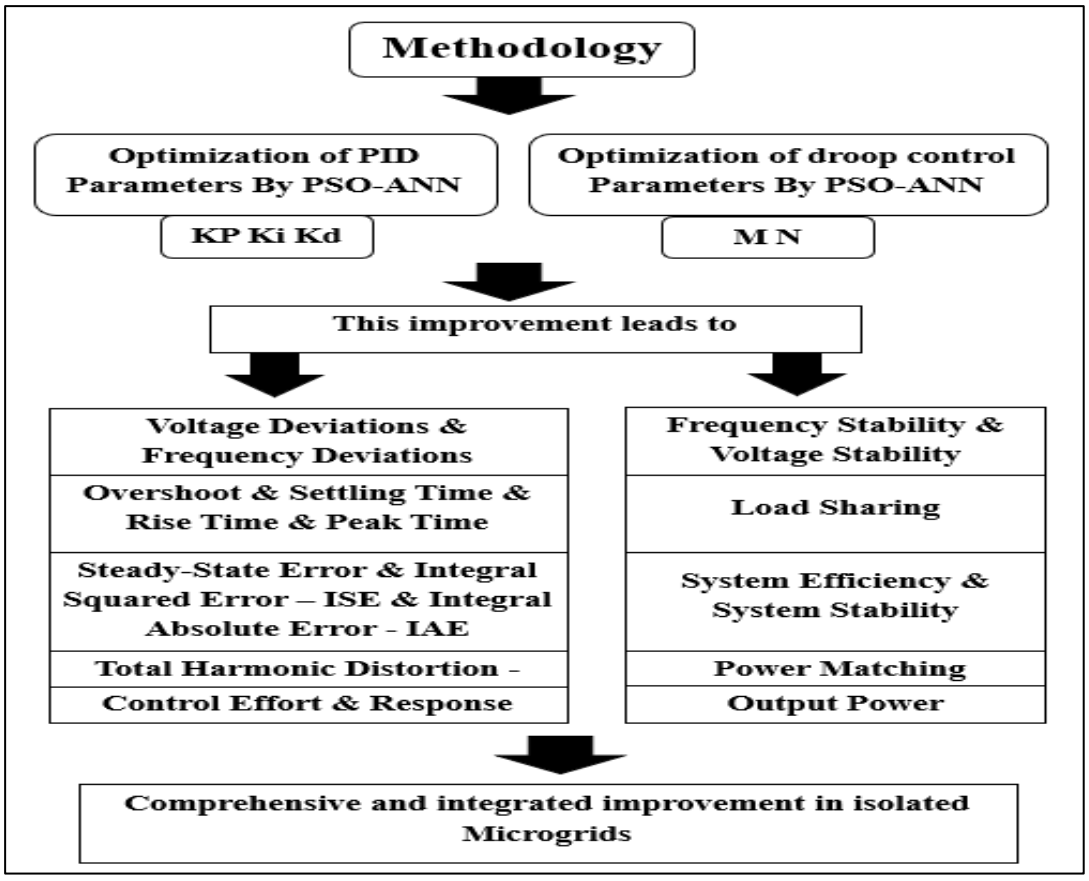

Figure 3-2 Hybrid PSO-ANN Optimization and Performance Metrics

3.3 Physical Representation and Mathematical Modeling of the Microgrid

A strong and precise mathematical model that emulates the dynamic performance of the physical elements of the microgrid is necessary for trustworthy microgrid simulation. Mathematical models that constitute the physical model of the simulated microgrid system are discussed in detail in this section. The two DG units are supporting a common three-phase AC load and each is modeled as a three-phase Voltage Source Inverter in Figure (3-3). As they are the primary interface between the DC power sources and the AC microgrid, they play a fundamental role in the system stability and power quality. Three-phase VSI, three-phase LC filter, and DC voltage source make up each DG unit. For the purpose of realism in simulation, the DC supply voltage is not held constant but rather is simulated to provide for small drops in case of instantaneously varying demand. A Pulse-Width Modulation (PWM) signal is used by the VSI to transform the DC voltage into a three-phase AC voltage of variable frequency and amplitude. An LC filter is placed at the output of each VSI for providing a high-quality sinusoidal output. The filter can be mathematically represented in terms of its internal winding resistance (R_f), capacitance (C_f), and inductance (L_f). A damping resistor (R_d) is added in parallel with the filter capacitor to effectively damp high-frequency oscillations and enhance the system's dynamic response. This addition is an essential part of proper modeling.

Table (3-1) outlines the primary configuration settings utilized for the simulation model, for example, LC filter values. A transmission line, far from being a perfect conductor, connects the inverters to point of common coupling. Rather, it is defined by its resistance (R_{line}) and inductance (L_{line}). In order to accurately simulate voltage dips and power losses along the network, these line impedances are needed. The last part of the physical system is the three-phase AC load at the PCC. It is fed with active and reactive power from the two DG units. Each of these items has a vectorial mathematical formulation in terms of differential

equations, which is a simple building block in circuit theory. These equations describe the three-phase dynamics of the system in continuous time, i.e., current through inductors and voltage across capacitors. Overall microgrid system dynamics are described using the state of the system, which is obtained upon solving these coupled dynamic equations in every simulation time step. This approach with detailed modeling allows for thorough analysis of the control methods under real operating conditions. The simulation of microgrid was carried out in MATLAB, a versatile tool of dynamic system analysis. The software supports simulating the entire system and can test the performance of its control algorithms for different load conditions. Stability, power-sharing accuracy, and transient performance overall can be validated by simulation through analyzing the dynamics of the system, i.e., response to active and reactive power changes. The control system of this microgrid adopts a decentralized, peer-to-peer strategy. As each distributed power unit can stand alone without depending on a central controller or a communication network, this technique is perfect for isolated microgrids. The natural division of the different functional components of the control system can be seen in the following figure. In order to determine the active and reactive output power of the inverter, the initial block, the Active & Reactive Power Calculation, currently calculates microgrid readings. The control system uses these variables as its main source of feedback signals. The calculation is derived from the three-phase power equations $P=3/2(V_dI_d+V_qI_q)$ and $Q=3/2(V_qI_d-V_dI_q)$ and the dq-frame voltage and current readings [75]. Upon measurement, the P and Q are then input to the Droop Control block. Having pre-determined power levels measured and a set of pre-determined droop equations, the middle block in the power-sharing approach produces new reference signals for the voltage magnitude and frequency. Connecting the power output directly to the respective frequency and voltage is how the droop mechanism makes each inverter contribute in proportion to the load.

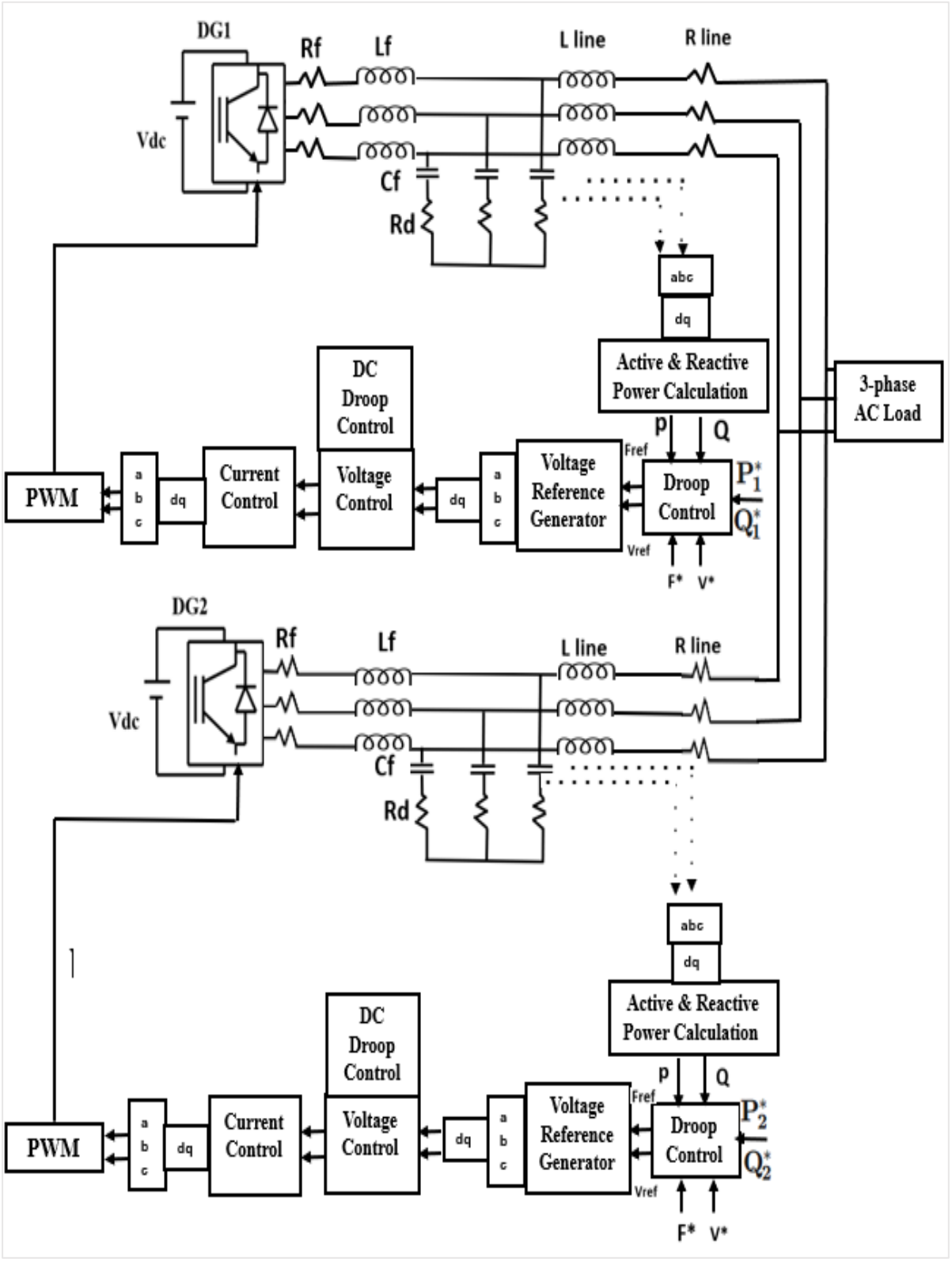

Figure 3-3 Microgrid System: Physical Components and Control Flow

After droop control, the Voltage Reference Generator computes these new reference values (V_{ref} and F_{ref}) and makes them ready for the inner control loops. With full Park-Clarke transformation, the dq-frame is essential to this function because it separates the three-phase AC signals to two DC components that can be separately controlled, so that P and Q may be controlled individually. A cascaded inner control system consists of two interconnected loops: a current control loop and a voltage control loop. The voltage control loop directly regulates the filter capacitor voltage (final inverter output voltage) to the value of V_{ref} from the Droop block. Most notably, the PI controller in this loop accomplishes this by generating the requisite current reference (I_{ref}) necessary to correct the voltage error. The current control loop then utilizes the voltage control loop's output (I_{ref}) as its reference input. The loops are performed in the dq-frame, allowing for enhanced voltage control and improved disturbance response. Lastly, the PWM block receives the input from the current control block. The PWM block implements the decisions of the higher-level loops by generating the actual switching signals for the transistors of the inverter, which physically regulate the power flow from the inverter to the microgrid. There are some very important variables that dictate the system's behavior that are found in the droop control block. The active and reactive power outputs of the inverter, measured as the letters P and Q, act as real-time feedback for the system. They are used to correct the control signals. The P* and Q* variables, on the other hand, are references, or setpoints, for the active and reactive. Although the droop control is decentralally realized, these reference values can be set to create a pre-determined ratio between the power shared by the inverters. Additionally, the nominal grid values, V* and F*, for the microgrid's nominal voltage and frequency (400V and 50Hz) are provided to the droop block. These are employed in order to calculate the required corrections using the droop equations starting from these points. The voltage reference and frequency reference, V_{ref} and F_{ref}, are generated by the droop block, which are required by the subsequent control stages. The main idea

behind the droop method is to change these output values incrementally from their nominal values as a function of the measured power such that they can share the power proportionally and correctly among the microgrid's inverters.

Table 3-1: Simulation parameters and the physical system [49][82].

Parameter	Symbol	Value	Unit
Nominal Frequency	f_{nom}	50	Hz
Nominal RMS Voltage	$V_{nom\text{-}rms}$	400	V
DC Bus Voltage (Battery)	V_{dc}	800	V
Filter Inductance	L_f	2	mH
Filter Capacitance	C_f	40	μF
Winding Resistance	R_f	0.5	Ω
Damping Resistor	R_d	7.07	Ω
Line Resistance	R_{line}	0.04	Ω
Line Inductance	L_{line}	0.5	mH
Sampling Time	T_s	$1 \cdot 10^{-4}$	s
Total Simulation Time	T_{total}	2.5	s

3.3.1 Voltage Source Converter (VSI) Model

The three-phase Voltage Source Inverter is the main power electrical interface utilized to interface the AC microgrid and the DC source. VSI within this model has been shown as a real system with a dynamically controlled three-phase AC output voltage. The foundation of the VSI is that its peak output voltage is set according to the rating of the DC bus voltage, which is the energy source. It assumes the VSI is powered by a battery source. The DC bus voltage is thus dynamically modeled rather than as an idealized constant source simplification. Dynamic modeling of this manner enables simulation of the real voltage drop whenever the system undergoes an instant increase in load. The recording of this dynamic voltage profile is critical to simulate transient behavior and test the stability of the VSI under physical conditions [76]. The nominal DC bus voltage

is set to 800 V to satisfy the specifications for AC output. The operation of the VSI involves supplying it with PWM switching signals from the control loops, which sets the target AC output voltage and manages the flow of power between the DC link and the microgrid.

3.3.2 LC Filter Model

The three-phase LC filter is a key building block to convert the raw PWM voltage of the VSI into a filtered, sinusoidal three-phase waveform. The dynamic behavior of the filter is simulated by a system of coupled differential equations that control the inductor current and capacitor voltage for each of the three phases (a, b, and c). These are derived from Kirchhoff's current and voltage laws and numerically solved in the simulation using forward Euler method with a time step Ts. Incorporating an explicit damping resistor R_d in parallel across the filter capacitor is also critical because it enhances the system's dynamic response and effectively eliminates high-frequency oscillations. Through the use of the formula based on the characteristic impedance of the LC filter, the value of such a resistor is mathematically determined. [76]

$$R_d = \sqrt{\frac{L_f}{C_f}} \quad \text{.....3.1}$$

The following equations represent the physical model of the filter:

- Inductor current equation (i_{inv}):

$$\frac{di_{inv}}{dt} = \frac{1}{L_f}\left(V_{inv} - V_{cap} - R_f \cdot i_{inv}\right) \quad \text{.....3.2}$$

- Capacitor voltage equation (V_{cap})

$$\frac{dV_{cap}}{dt} = \frac{1}{C_f}\left(i_{inv} - i_{line} - \frac{V_{cap}}{R_d}\right) \quad \text{.....3.3}$$

Where L_f is the filter inductance, C_f is the filter capacitance, R_f is the inductor's internal winding resistance, and R_d is the damping resistor. The variables are represented as three-phase vectors to reflect the system's nature:

- $V_{inv}= [V_{inv, a}, V_{inv, b}, V_{inv, c}]^T$ is the inverter's output voltage.
- $V_{cap}= [V_{cap, a}, V_{cap, b}, V_{cap, c}]^T$ is the voltage across the filter capacitor.
- $i_{inv}= [i_{inv, a}, i_{inv, b}, i_{inv, c}]^T$ is the current flowing through the inductor.
- $i_{line}= [i_{line, a}, i_{line, b}, i_{line, c}]^T$ is the current flowing to the line.

Figure (3-4) shows the physical components and their connections to give a visual depiction of this filter design. This configuration effectively reduces harmonics while ensuring a constant output voltage. Each time step's state variables are quantitatively determined using the forward Euler method in the manner described below:

- **Inductor current update:**

$$i_{inv}(k+1) = i_{inv}(k) + \frac{di_{inv}}{dt} T_s \text{.....3.4}$$

- **Capacitor voltage update:**

$$V_{cap}(k+1) = V_{cap}(k) + \frac{dV_{cap}}{dt} \cdot T_s \quad \text{..... 3.5}$$

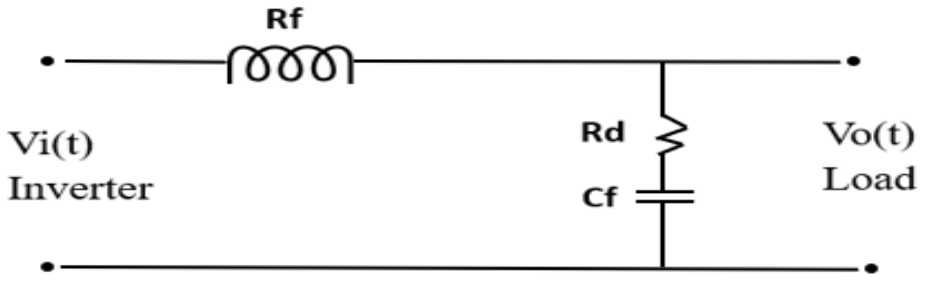

Figure 3-4 Physical Model of the LC Filter

3.3.3 Transmission Line Model

The three-phase model of the line accounts for the effective impedance that actually exists between the inverter and the PCC. This is needed for accurate voltage regulation and three-phase power sharing analysis. Line behavior, as it was represented by a simple R-L circuit, is based on a vectorial differential equation of the line current (i_{line}). The line current is derived by numerically integrating the equation at each time step[75]. The mathematical representation for the line is as follows:

$$\frac{di_{\text{line}}}{dt} = \frac{1}{L_{\text{line}}}\left(V_{\text{cap}} - V_{\text{bus}} - R_{\text{line}} \cdot i_{\text{line}}\right) \quad \text{..... 3.6}$$

Where the variables are represented as three-phase vectors:

- $i_{line} = [i_{line,a}, i_{line,b}, i_{line,c}]^T$ is the line current.
- $V_{cap} = [V_{cap,a}, V_{cap,b}, V_{cap,c}]^T$ is the voltage across the filter capacitor.
- $V_{bus} = [V_{bus,a}, V_{bus,b}, V_{bus,c}]^T$ is the voltage at the common bus.
- R_{line} is the line resistance.
- L_{line} is the line inductance.

Similar to the LC filter model, this equation is numerically solved using the forward Euler method, which updates the state variables at each time step.

$$i_{line}(k+1) = i_{line}(k) + \left[\frac{1}{L_{line}}\left(V_{cap}(k) - V_{bus}(k) - R_{line} \cdot i_{line}(k)\right)\right] \cdot T_s \quad \text{... ..3.7}$$

3.4 Control System Structure and Modeling

A robust and efficient control system design is of prime importance for the microgrid's stable operation, especially under the harsh conditions of an islanded system. The proposed control structure applies a decentralized architecture, which allows each inverter to operate independently using only local measurements (a peer-to-peer approach), thus enhancing system reliability and

scalability by avoiding a single point of failure and communication delays present in centralized schemes. The basic approach followed is a Grid-Forming Control, where the VSI acts as the main voltage source, establishing the voltage and frequency of the microgrid. This functionality is essential for autonomous and black-start capability when disconnected from the main grid. To achieve high stability and fast transient response, the overall strategy follows a cascaded control approach fully implemented in the rotating dq-frame[62].

This arrangement hierarchically separates the slower dynamics of power regulation from the faster ones of voltage and current control, which allows for independent and decoupled control of active and reactive power with high precision. These concepts are elaborated in the mathematical modeling of this cascaded structure in the subsequent sections, starting from the necessary frame transformation right up to the specialized inner and outer control loops.

3.4.1 Synchronization and dq-Frame Transformation

The implementation of fast and precise current and voltage control within the inverter requires that the measured three-phase AC quantities be translated into constant two-axis DC components. This step is critical for simplifying the control effort because it converts oscillating sinusoidal signals into a stationary form that PI controllers will be able to regulate. The step necessary to achieve such conversion is given by the park transformation, translating the instantaneous three-phase values (V_{abc} and I_{abc}) from the stationary frame onto the synchronous reference frame, from the abc-frame to the rotating dq-frame. Most importantly, the transformation is driven by the phase angle theta derived from the outer droop control loop to perfectly synchronize it with the operational frequency and voltage of the microgrid [75]**.** Some of the advantages of using the dq-frame from a control implementation perspective include:

• **Efficient System Control**: The transformation separates the active and reactive power control, enabling independent regulation of voltage and current in each axis to offer dependable and efficient power sharing within a balanced microgrid.

• **Simplified Controller Design**: By converting the AC quantities to DC components, the controllers can use a simple and effective PI control rule for better system responsiveness, which also simplifies the overall architecture of the control.

• **Targeted Regulation**: dq-frame allows the controllers to focus on the crucial parts of the system that need to be regulated for maintaining steady voltage and frequency under different load conditions. The equations for this transformation are applied to the measured voltage and current signals.

3.4.1.1The Park Transformation Equations

The measured three-phase voltage and current signals are transformed into the rotating dq-frame components using the following equations:

Voltage Transformation:

$$\begin{bmatrix} Vd \\ Vq \end{bmatrix} = \frac{2}{3}\begin{bmatrix} \cos(\theta) & \cos\left(\theta - \frac{2\pi}{3}\right) & \cos\left(\theta + \frac{2\pi}{3}\right) \\ -\sin\theta & -\sin\left(\theta - \frac{2\pi}{3}\right) & -\sin\left(\theta + \frac{2\pi}{3}\right) \end{bmatrix}\begin{bmatrix} Va \\ Vb \\ Vc \end{bmatrix} \quad \ldots\ldots\ldots \text{3.10}$$

Current Transformation:

$$\begin{bmatrix} Id \\ Iq \end{bmatrix} = \frac{2}{3}\begin{bmatrix} \cos(\theta) & \cos\left(\theta - \frac{2\pi}{3}\right) & \cos\left(\theta + \frac{2\pi}{3}\right) \\ -\sin\theta & -\sin\left(\theta - \frac{2\pi}{3}\right) & -\sin\left(\theta + \frac{2\pi}{3}\right) \end{bmatrix}\begin{bmatrix} Ia \\ Ib \\ Ic \end{bmatrix} \quad \ldots\ldots\ldots\ldots \text{3.11}$$

These transformations are fundamentals that will help in realizing precise and decoupled control of active and reactive power for balanced systems. Further, this robust approach to modeling proves the accuracy and reliability of our work, ensuring integrity for the subsequent control loops.

3.4.1.2 Power Calculation in the dq-Frame

Active power P and reactive power Q from the inverter output are obtained by using the transformed dq-components herein. These computed power values are pivotal since they become the feedback signals for the outer droop control loop. In such a way, by defining P and Q in the rotating frame, the control scheme decouples the active and reactive powers, enabling independent regulation of the frequency and voltage [77]. Expressions for the active and reactive power are given by:

$$P = \frac{3}{2}\left(V_d I_d + V_q I_q\right) \text{ …….. 3.12}$$

$$Q = \frac{3}{2}\left(V_q I_d - V_d I_q\right) \text{ ……3.13}$$

These power expressions are fundamental to the control system because they provide the feedback signals (P and Q) that the outer droop loop requires. This calculation confirms, for stability in the microgrid, the necessary decoupling between active and reactive power. The scaling factor 3/2 in both equations is a conversion constant for Power Invariance; it provides a means of making the power calculated in the two-axis dq-frame numerically equal to the actual power of the three-phase system, which is essential for coherence and precision in the power balance calculations of the system.

3.4.2 The Cascaded Control Architecture

The overall control approach is implemented in a cascaded control architecture, which is at the heart of achieving high dynamic performance, stability, and reliable power-sharing characteristics within VSIs operating in the dq-frame. It is this hierarchical structure that is optimally designed for managing the system dynamics with widely varying time constants and that is composed of two major loops. This is the outer control loop, which consists of Droop Control and the Voltage Control (V_{ref} and F_{ref} Generators). It is responsible for the slow dynamics of power regulation and hence for ensuring stability within the system.

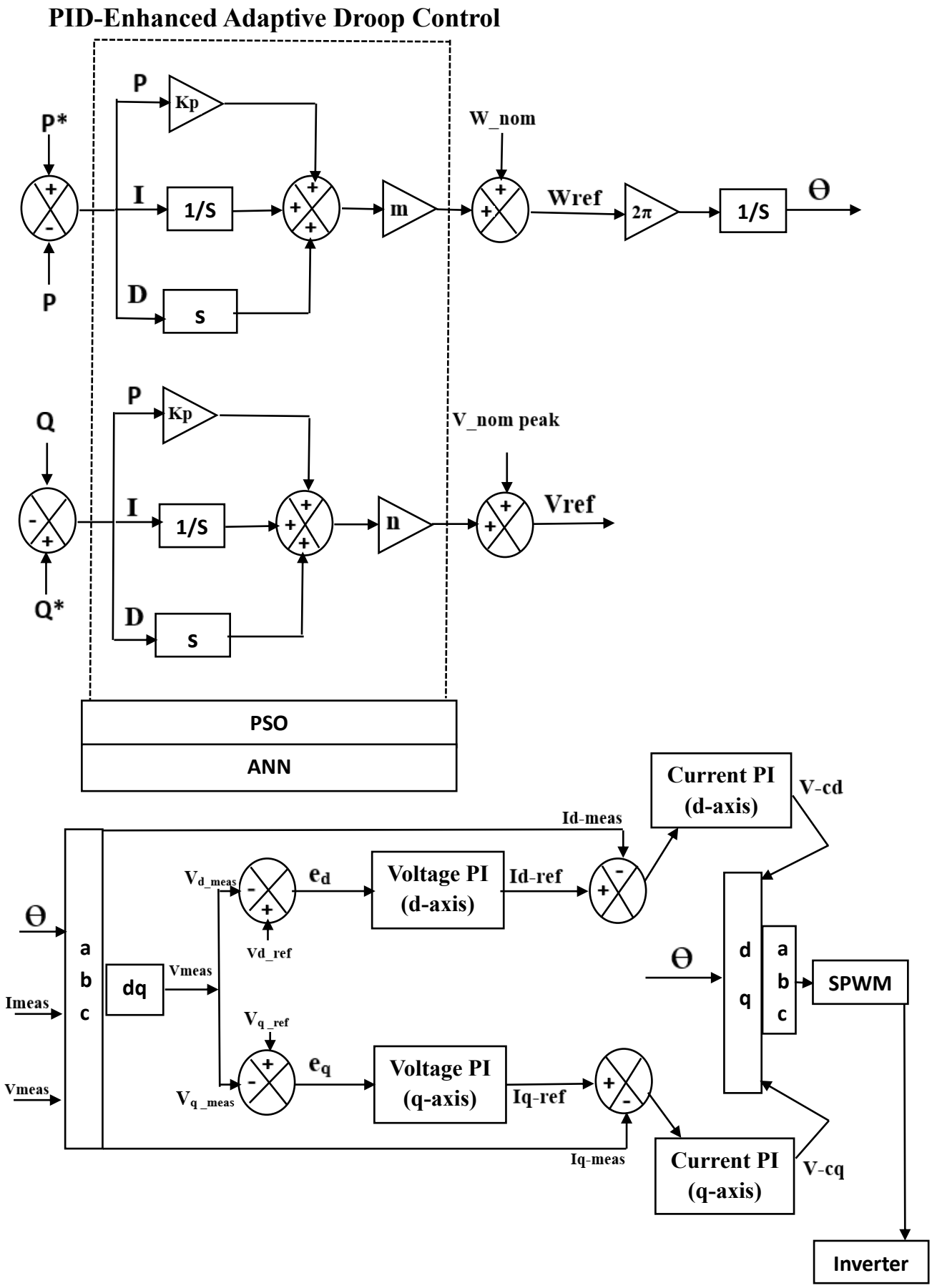

Figure 3-5 Adaptive Cascaded Control for Microgrid Inverters

3.4.3 The Outer Control Loop: Droop Control Mechanism

The outer control loop implements mainly the Droop Control mechanism, which is the basic strategy for decentralized power sharing among parallel inverters in an islanded microgrid. The droop mechanism emulates the behavior of conventional synchronous generators, creating a relationship between power flow and system frequency/voltage based on decentralization without requiring high-bandwidth inter-inverter communications. This inherently provides the Grid-Forming capability, where the inverters can establish and regulate the voltage and frequency of the isolated network.

The droop strategy aims to share the total load demand among all parallel inverters proportionally, depending on their rated power capacity. This is done by intentionally injecting errors into the frequency and voltage references based on the deviation of the measured active and reactive power from their respective references. For this proposed system, a PID-Enhanced Adaptive Droop Control structure replaces the traditional linear droop characteristic, incorporating a Proportional-Integral-Derivative controller into the power error signals before multiplying them by the droop coefficients. This adaptation greatly enhances transient performance, enhances power-sharing accuracy, and contributes to overall stability during severe load changes [75].

3.4.3.1 Active Power Droop and Frequency Regulation

The Active Power Droop mechanism is responsible for regulating the system frequency, W, in relation to the deviation between the measured active power, P, and its reference, P*. In a traditional linear droop system, this relationship is defined solely by a fixed droop coefficient, m ,as mathematically established by the conventional droop characteristic:

$$\omega = \omega_{nom} - m \cdot P \quad \text{..... 3.14}$$

However, to enhance the transient performance and power-sharing accuracy of the microgrid, the work herein uses a PID-Enhanced Droop structure. In this adaptive approach, the power error (ΔP = P* - P) is first fed to a Proportional-Integral-Derivative controller and then multiplied by the droop coefficient, m. The resulting frequency deviation is subtracted from the nominal frequency, Wnom, to determine the new angular frequency reference of the system, W_{ref}. This PID term is very important because it provides a dynamic tuning of the droop characteristic, which consequently limits the power oscillations and enhances transient stability. The relationship for the active power droop is given by:

$$\omega_{ref} = \omega_{nom} - m \cdot \left[K_p \cdot (P^* - P) + K_i \int (P^* - P) dt + K_d \frac{d(P^* - P)}{dt} \right] \text{..3.15}$$

Where W_{ref} is the angular frequency reference; W_{nom} is the nominal angular frequency; m is the active power droop coefficient (gain); and K_p, K_i, and K_d are the proportional, integral, and derivative gains of the PID controller, respectively. The integral of W_{ref} provides the phase angle θ required for the Park-Clarke transformation.

3.4.3.2 Reactive Power Droop and Voltage Regulation

The Reactive Power Droop mechanism serves to regulate the voltage magnitude, V, of the microgrid according to the deviation between the measured reactive power, Q, and its reference. As in the case of active power droop, such a relationship is crucial to guarantee accurate reactive power sharing among parallel inverters. In a traditional linear droop system, this voltage regulation is defined by the conventional droop characteristic:

$$V_{ref} = V_{nom} - n \cdot Q \quad \text{..... 3.16}$$

In order to maintain consistency and enhance overall system stability, this work will also apply the PID-Enhanced Adaptive Droop Control structure to the reactive power loop. The reactive power error ΔQ = Q* - Q is first fed through a

PID controller and then multiplied by the reactive power droop coefficient n. The resulting voltage deviation is subtracted from the nominal peak voltage $V_{nom\ peak}$ to get the voltage reference V_{ref} for the inner voltage control loop. This adaptive term significantly improves the transient response of the voltage regulation and prevents large voltage swings during sharp changes in reactive load. The relationship for the reactive power droop is given by:

$$V_{ref} = V_{nom\ peak} - n \cdot \left[K_p \cdot (Q^* - Q) + K_i \int (Q^* - Q)dt + K_d \frac{d(Q^* - Q)}{dt}\right] \quad \text{.....3.17}$$

where V_{ref} is the voltage reference for the inner loop, $V_{nom\ peak}$ is the nominal peak voltage magnitude, and n is the reactive power droop coefficient (gain), while K_p, K_i, and K_d stand for the proportional, integral, and derivative gains of the PID controller, respectively.

3.4.3.3 Power Sharing Mechanism and Droop Equations

The control mechanism of Droop is essentially a method of achieving distributed power sharing among multiple paralleled inverters without depending on a dedicated high-bandwidth communication network [76]. Using the frequency and voltage as virtual communication channels, the system automatically regulates the output power of each inverter to be inversely proportional to its respective droop coefficient, m or n. This proportionality in power sharing is obtained by accordingly adapting the droop coefficients, m and n, of active and reactive power, respectively, depending on the inverters' rated capacity. For example, if there are two inverters, Inv 1 and Inv 2, in a microgrid that are supposed to share the load in some proportion, say K_1: K_2, which could be 60%:40%, as seen mostly when the ratings are not equal, then the droop coefficients of these two inverters must be inversely related by

For Active Power Sharing:

$$\frac{P_1}{P_2} = \frac{m_2}{m_1} = \frac{K_1}{K_2} \quad \text{.....3.18}$$

For Reactive Power Sharing:

$$\frac{Q_1}{Q_2} = \frac{n_2}{n_1} = \frac{K_1}{K_2} \quad \text{.....3.19}$$

The overall droop mechanism, integrating the PID-Enhanced adaptive structure, ensures that these proportional sharing rules are maintained accurately, even under dynamic and transient conditions common in islanded microgrids. Complete equations governing the references for the inner loops are combinations of the active and reactive power droop equations defining the required angular frequency W_{ref} and voltage magnitude V_{ref}. The droop characteristics of the inverters are non-identical because of their non-identical droop coefficients. The identical slopes of the curves in Figure (3-6) give a consistent response to changes in load, illustrating how equal and accurate load sharing can be implemented more easily with a traditional management strategy with matched parameters.

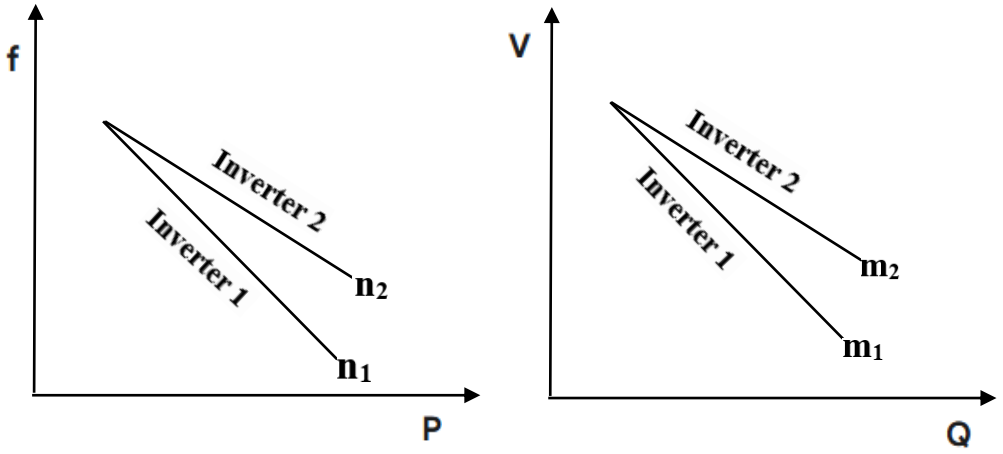

Figure3-6 Conventional Droop Characteristics for Asymmetric Microgrid Inverters

Table 3-2 Comparative Analysis of Classic Droop Control and PID-Based Droop Control Characteristics

Feature	Classic Droop Control	PID-Based Droop Control
Control Logic	Proportional (P) only. A simple linear relationship between power and frequency/voltage.	Proportional-Integral-Derivative (PID). A multi-component controller that acts on the error.
Steady-State Error	Exists. The frequency and voltage permanently deviate from their nominal values due to the linear relationship.	Eliminated. Frequency and voltage return to their nominal values as the Integral (I) term gradually reduces the error to zero.
Dynamic Response	slower reaction to abrupt changes in load. may result in oscillations and overshoots.	quicker and more reliable reaction. Large swings are avoided and oscillations are dampened by the Derivative (D) term.
Complexity	Easy to apply.	Designing and adjusting the PID gains is more difficult.
Performance	Simple functionality, appropriate for non-essential uses.	Superior performance, highly suitable for modern, high-performance microgrids.

3.4.3.4 Droop Coefficient Settings for Proportional Power Sharing

With the full mathematical model and control structure established for the microgrid inverter system, this section summarizes the key design parameters and coefficients used specifically for the droop control strategy. These parameters include the droop coefficients (m and n) and the power sharing ratios, which are essential for achieving the desired decentralized power sharing characteristics between Inverter 1 and Inverter 2. The initial droop coefficients and share ratios for the two inverters, necessary to achieve the specific proportional power sharing allocation, are listed in Table (3-3):

Table 3-3 Conventional Droop Coefficients for Inverter 1 and Inverter 2 [72].

Parameter	Symbol	Inverter 1 Value	Inverter 2 Value	Unit	Description
P-f Droop Coefficient	m	$5 \cdot 10^{-5}$	$6.6 \cdot 10^{-5}$	Hz/W	Droop coefficient for active power.
Q-V Droop Coefficient	n	$1 \cdot 10^{-5}$	$3 \cdot 10^{-5}$	V/VAR	Droop coefficient for reactive power.
P-f Share Ratio	-	0.6	0.4	-	The intended proportional sharing of active power

3.4.4 The Inner Control Loops: Fast and Precise Regulation

The Inner Control Loops form the heart of the cascaded structure, operating at considerably higher bandwidth than the outer droop loop to ensure a fast and accurate tracking of the reference signals, W_{ref} and V_{ref}, and effective suppression of harmonics. These are implemented entirely in the rotating dq-frame, were simple, highly effective Proportional-Integral controllers can process DC quantities. It contains two nested loops: the outer voltage regulation loop and the inner current regulation loop. The main purpose of the mentioned nested configuration is to filter the output voltage ripple and to protect the inverter switches against overcurrent surges. It is just this precise control of the output voltage and current that ultimately enables the stable Grid-Forming capability of the inverter. The operation and mathematical modeling for each loop are discussed in detail in subsequent sections.

3.4.4.1 Voltage Regulation Loop

The Voltage Regulation Loop is the outermost layer of the inner control structure. It primarily serves to regulate the measured output voltage V_{dq} to a reference voltage V_{ref}, which is provided by the droop control loop. This regulation is independently implemented along the d- and q-axes using individual PI controllers. The voltage loop error signals ($e_{v,\,d}$ and $e_{v,\,q}$) are processed by the

PI controllers in order to produce the current reference signals ($I_{d\text{-}ref}$ and $I_{q\text{-}ref}$), which are applied to the subsequent inner current loop. Also, the output of $I_{d\text{-}ref}$ comes from the d-axis voltage PI controller, and the output of $I_{q\text{-}ref}$ comes from the q-axis controller [78]. The equations governing the output of the d-axis and q-axis voltage PI controllers are

d-axis Current Reference:

$$I_{d-ref} = K_{p,v} \cdot e_{v,d} + K_{i,v} \int e_{v,d} dt \quad \ldots\ldots 3.20$$

q-axis Current Reference:

$$I_{q-ref} = K_{p,v} \cdot e_{v,q} + K_{i,v} \int e_{v,q} dt \ldots\ldots\ldots 3.21$$

3.4.4.2 Current Regulation Loop

The Current Regulation Loop is the innermost and fastest control layer, operating to ensure that the measured inverter output current precisely tracks the current references generated by the voltage loop. Its major tasks include the protection of VSI switches from overcurrent conditions, active damping of harmonics, and assurance of a high dynamic response. Current error signals ($e_{I,\,d}$ and $e_{I,\,q}$) are processed by dedicated PI controllers[78][75]. Due to the coupling effect inherent in the inductor and the rotating dq-frame, a standard PI output must be supplemented with decoupling terms (wLI_{meas}) in order to eliminate cross-coupling between the axes d and q. This decoupling ensures that the control over the current in one axis is completely independent of the other. The final output voltage references of the current loop, $V_{cmd,\,d}$ and $V_{cmd,\,q}$ are then computed by adding the PI output with these decoupling terms and the necessary voltage feedforward terms ($V_{meas,\,d}$ and $V_{\,meas,\,q)}$ for full compensation. Current Loop Output with Decoupling:

1. d-axis Inverter Voltage Reference:

$$V_{\text{cmd},d} = K_{pI} \cdot e_{I,d} + K_{iI} \int e_{I,d} dt - (\omega L) I_{\text{meas},q} + V_{\text{meas},d} \ldots .3.22$$

2. q-axis Inverter Voltage Reference:

$$V_{\text{cmd},q} = K_{pI} \cdot e_{I,q} + K_{iI} \int e_{I,q} dt + (\omega L) I_{\text{meas},d} + V_{\text{meas},q} \ldots 3.23$$

3. Inverse Park Transformation

The calculated inverter voltage references ($V_{inv,\,d}$ and $V_{inv,\,q}$) are in the rotating dq-frame. To realize these signals in the physical three-phase system, a final Inverse Park Transformation (or dq to abc conversion) must be applied. This conversion generates the three-phase instantaneous voltage references (V_a, V_b, and V_c) that are fed directly to PWM unit to control the switching of the VSI. The equation for this final conversion is:

$$\begin{bmatrix} Va \\ Vb \\ Vc \end{bmatrix} = \begin{bmatrix} \cos(\theta) & -\sin\theta \\ \cos\left(\theta - \frac{2\pi}{3}\right) & -\sin\left(\theta - \frac{2\pi}{3}\right) \\ \cos\left(\theta + \frac{2\pi}{3}\right) & -\sin\left(\theta + \frac{2\pi}{3}\right) \end{bmatrix} \begin{bmatrix} Vin,d \\ Vin,q \end{bmatrix} \ldots\ldots .3.24$$

3.5 PID and PI Controllers

PID and PI controllers are fundamental feedback control mechanisms used to regulate a system's output by minimizing the error (discrepancy) between a measured process variable and a desired setpoint. The control method employs a cascaded structure in the sense that the choice of type of controller is optimized for operation of its loop. The outer loop, following the traditional droop control, is joined with a PID controller for enhancing the dynamic and transient response of the system for active and reactive power sharing. Most importantly, the constants of this outer PID controller and also the droop parameters were not arbitrarily selected, but were instead calculated and optimally tuned by a mix of metaheuristic algorithms and training through ANN to guarantee optimal performance. Simultaneously, PI controllers are used in the inner voltage and

current loops for accurate and stable control in the rotating dq-frame, effectively providing zero steady-state error for the transformed DC values.

3.5.1 PID Controller

Proportional-integral-derivative, or PID, controllers are the most widely used and adaptable industrial controllers. It determines an error value by comparing a measured process variable to a desired setpoint using a control loop mechanism. The controller modifies the inputs for process control in an effort to reduce the error [30]. The PID control law is based on three terms:

- The proportional term (P) reacts to the error that is occurring at the moment. It provides an instantaneous correction response by producing an output proportionate to the fault. Although it produces a faster reaction, a bigger proportional gain (K_p) might cause instability and overshoot.
- Integral Term (I): Over time, this term reacts to the cumulative mistake. The long-term discrepancy between the setpoint and the actual value is known as steady-state error, and it is eliminated using this technique. Even a tiny, persistent fault will finally be fixed thanks to the integral term.
- Derivative Term (D): This term reacts to the error's rate of change. Based on its current pattern, it forecasts mistake behavior in the future. The derivative term enhances the stability and transient response of the system by reducing overshoot and dampening oscillations. The system may be more susceptible to noise if the derivative gain (K_d) is higher.

The PID controller can be represented in two forms: the standard continuous-time form for theoretical analysis and the discrete-time used for digital implementation in control hardware.

1.Continuous-Time PID Controller Equation

This is utilized to portray the relationship between control signal and system error at any point of continuous time (t) in the theoretical analysis of control systems.

$$u(t) = K_p e(t) + K_i \int_0^t e(\tau)\, d\tau + K_d \frac{de(t)}{dt} \quad \dots 3.25$$

The control signal, u(t), is based on the system error, e(t), and consists of a summation of three distinct control actions.: an integral term, a derivative term, and a proportional term. Their gains, K_p, K_i, and K_d, respectively, are used to scale the terms. A control action that is proportional to the current error is provided by the proportional gain (K_p). For steady-state errors to be eliminated, the integral gain (K_i) must act on the accumulation of the error over time. The derivative gain (K_d) provides a predictive control action that reduces oscillations and improves transient response as a result of the rate of change of the error.

2.Discrete-Time PID Controller Equation

The majority of digital implementations on microcontrollers and software employ this form. It is an approximation of the continuous integration and differentiation functions by computing the control signal at discrete-time instances (k) with a specified sampling time (T_s) [30]. This particular formulation is according to the adopted dynamics and control logic employed in the simulation model.

$$u(k) = K_p e(k) + K_i T_s \sum_{j=0}^{k} e(j) + \frac{K_d}{T_s}[e(k) - e(k-1)] \dots 3.26$$

At the current times step u(k), the control signal is computed in terms of the previous errors, the current error e(k), and the previous error e(k−1). For the proportional, integral, and derivative terms, scaling factors are the gains, K_p, K_i, and K_d. Both the continuous integral and continuous derivative are approximated as discrete summations and differences, respectively, by Ts. The application of an iterative loop construct and explicit use of the Ts variable to compute integral and derivative terms in the code supports the use of this discrete-time approach.

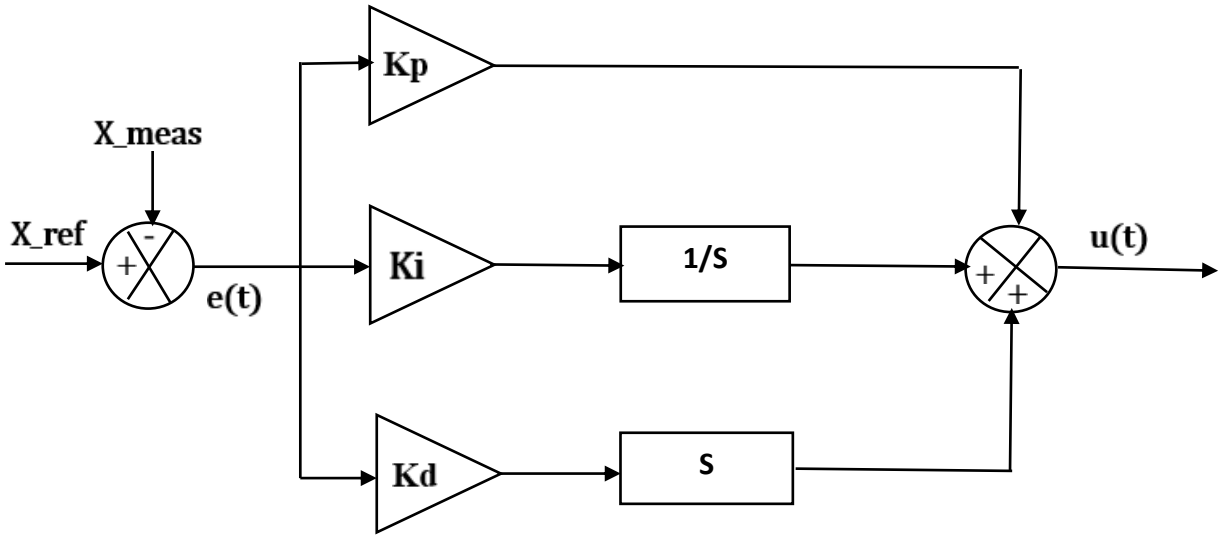

Figure 3-7 Block Diagram of a Proportional-Integral-Derivative Controller

The constant gains made up of the PID gains establish a reference level of system performance. The two VSI converters (Inverter 1 and Inverter 2) are electrically modeled with the identical physical parameters (filter and line elements) as outlined in Table (3.1). However, for the unequal load-sharing of 60% and 40%, the control parameters are intentionally tuned to be disparate. Specifically, classical PID gains are defined with characteristic values for each inverter and are given in Table 3.4. These differences in control parameters underlie the system's ability to address unbalanced power contribution despite Distributed Generation units' physical symmetry.

Table 3-4 Conventional PID Controller Parameters

Parameter	Symbol	Inverter 1 Value	Inverter 2 Value
Proportional Gain	K_p	0.052	0.077
Integral Gain	K_i	3.12	22.3
Derivative Gain	K_d	$4.22 \cdot 10^{-4}$	$5.41 \cdot 10^{-4}$

3.5.2 PI Controller

Simplified PID controllers without the derivative term are called proportional-integral (PI) controllers. In situations where the derivative action is

either unnecessary or undesirable, including in high-noise systems, it is frequently employed [30].

- **Proportional Term (P):** Same as in the PID controller.
- **Integral Term (I):** Same as in the PID controller.

The PI controller eliminates steady-state error and responds quickly without the derivative term, but it is unable to predict mistakes in the future. Compared to a well-tuned PID controller, this makes it less effective at handling systems with high degrees of inertia or quick changes. It may also cause higher overshoot and a longer settling period [75]. The PI controller can be represented in two forms: the standard continuous-time form for theoretical analysis and the discrete-time used for digital implementation in control hardware.

1.Continuous-Time PI Controller Equation

This form describes the relation between the control signal and the system error at any continuous point of time (t) and occurs in theoretical control system analysis. It cancels steady-state error by combining the integral and proportional components.

$$u(t) = K_p e(t) + K_i \int_0^t e(\tau) d\tau \quad \ldots.3.27$$

The control action, u(t), is a weighted function of the system error, e(t), and assumes two main actions. First, the proportional action results in a control action proportional to the present error, amplified by the proportional gain (K_p). Second, the integral action raises the accumulated error to a power, prompted by the integral gain (K_i). This critical part is necessary to ensure that the system will ultimately achieve the desired value by eliminating the remaining steady-state error.

2.Discrete-Time PI Controller Equation

For digital implementations of software and microcontrollers, this is the most common form. Using the sampling time period (T_s) to estimate the continuous integral, it determines the control signal at discrete time periods (k). This formulation is utilized in the inner voltage and current loops in the model simulation.

$$u_k = K_p e_k + K_i T_s \sum_{j=0}^{k} e_j \quad \dots\dots 3.28$$

At the instant in time now, uk, the control signal relies on the instant error, e_k, and the total of all past errors. The cumulative error is controlled by the integral gain (K_i), and the real-time reaction to the current error is controlled by the proportional gain (K_p). By adding the current error (scaled by T_s) and the previous integral value at each time step, the code is performing the task of making the system capable of eliminating steady-state errors. The integral term accumulates the error at each step.

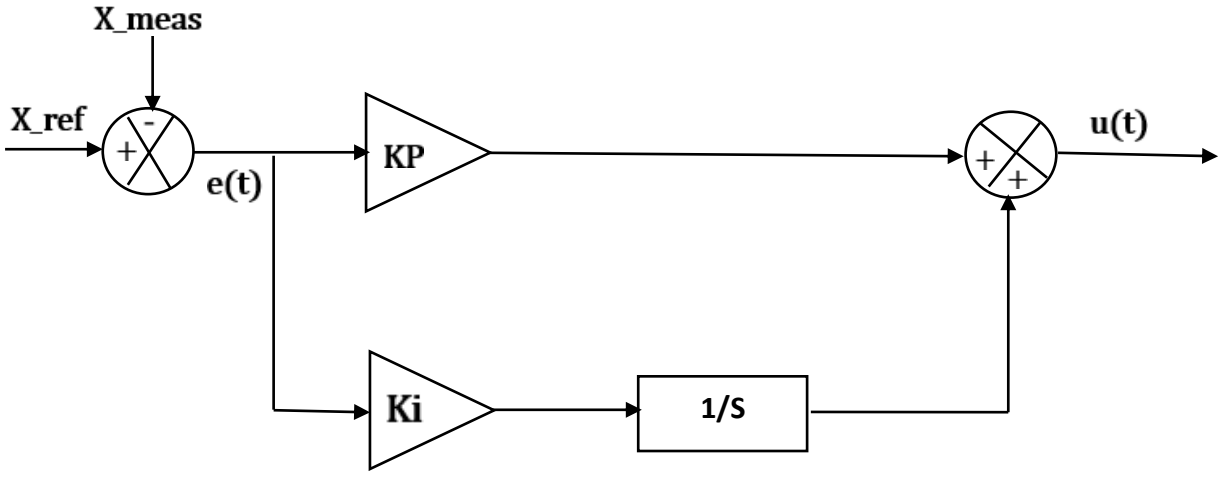

Figure 3-8 Block Diagram of a Proportional-Integral Controller

The inner control loops' continuous gains decide the system's dynamic accuracy. As seen in Table (3-5), the Proportional-Integral controller gains are systematically set to various values for the inner voltage and current control

loops. The motivation for this difference is that the voltage loop requires high integral action (high K_i) to track the reference signal accurately, while the current loop requires a quicker, less oscillatory response. These distinct sets of parameters validate the utilization of single PI controllers to provide the desired transient and steady-state performance for each inner loop.

Table 3-5 Inner Control Loop Parameters

Parameter	Symbol	Value	Description
Voltage PI Proportional Gain	K_{p_v}	10	Proportional gain for the inner voltage loop.
Voltage PI Integral Gain	K_{i_v}	50	Integral gain for the inner voltage loop.
Current PI Proportional Gain	K_{p_i}	10	Proportional gain for the inner current loop.
Current PI Integral Gain	K_{i_i}	80	Integral gain for the inner current loop.

3.5.3 Key Differences and Applications

The derivative word is the primary distinction. This term offers the PID controller a "predictive" capability that the PI controller does not have [27].

Table 3-6 PID vs. PI Controller: A Comparative Analysis

Feature	PID Controller	PI Controller
Components	P, I, D	P, I
Error Handling	Responds to current, past, and future error	Responds to current and past error
Response	Faster and more stable transient response	Can have more overshoot and a longer settling time
Noise Sensitivity	Highly sensitive to noise due to the derivative term	Less sensitive to noise
Complexity	More complex to tune due to three gain parameters	Simpler to tune due to two gain parameters

Typical Application	Systems requiring a fast, highly stable response (e.g., robotics, motion control)	Systems where steady-state error is the primary concern and noise is a factor (e.g., flow control, temperature regulation)

In the context of a microgrid model, the inner control loops (for voltage and current) use a PI controller because they are high-bandwidth loops that must respond quickly and eliminate steady-state error. Meanwhile, the outer, slower loop might benefit from the full PID to better handle power sharing and transient stability.

3.6 Particle Swarm Optimization

Particle Swarm Optimization is a metaheuristic algorithm that draws inspiration from the collective behavior of fish schools or flocks of birds. The method iteratively searches a search space for the optimal solution. Every possible solution is represented by a "particle" that travels through the search space under the direction of both the swarm's best-known position (g_{best}) and its own best-known position (p_{best}). [46][71].

3.6.1 The Algorithm's Core Process

The optimization process is based on an iterative movement. The main goal is to find the optimal values for the five controller parameters: K_p, K_i, K_d, m, and n. Each particle represents a set of these five values.

- **Initialization**: A swarm of particles is positioned at random within a predetermined search space to begin the procedure. The lower bound (lb) and upper bound (ub) for every parameter define this region. The code initializes 40 particles for the 5 parameters.

- **Evaluation**: A fitness function is used to assess the "fitness" or "cost" of each particle's position at each iteration. The purpose of this function is to measure the solution's quality. A better solution comes at a lesser cost.
- **Updating p_best and g_best**: The algorithm updates the personal best (p_{best}) and global best (g_{best}) locations to improve the process. Each particle remembers where it is at its best. If the expense of the new job is lower than the previous one, it moves its best. The method simultaneously tracks the best position found by each particle in the entire swarm, which is the overall best solution found so far (g_{best}).
- **Movement**: Two primary factors influence each particle's movement: the swarm's best position (g_{best}) and the particle's individual best position (p_{best}). The fundamental idea is that particles iteratively seek out the best answer for the entire swarm as well as their individual best-found solution.

The particle's velocity and position are updated using the following equations:

1.Velocity Update Equation:

$$v_i^{t+1} = w \cdot v_i^t + c_1 \cdot r_1 \cdot \left(p_{best,i} - x_i^t\right) + c_2 \cdot r_2 \cdot (g_{best} - x_i^t) \quad \dots 3.29$$

Where w (pso. w = 0.7) is the Inertia weight, which controls how much a particle's previous velocity influences its new velocity. A higher w favors global exploration. c_1 (pso.c_1 = 1.5) is the Cognitive coefficient that determines how much the particle is influenced by its own experience (p_{best}). c_2 (pso.c_2 = 1.5) is the social coefficient, which determines how much the particle is influenced by the best experience of the swarm (g_{best}). Finally, r_1 and r_2 are random numbers between 0 and 1, providing a stochastic element to the search.

2.Position Update Equation:

$$x_i^{t+1} = x_i^t + v_i^{t+1} \quad \dots .3.30$$

This equation updates the particle's new position by adding the new velocity to the present position. It simulates the physical movement of the particle towards more promising regions in the search space, led by the personal and global best experiences. The basic steps of the PSO method are depicted in a flow diagram in Figure (3-9), which is based on the thorough explanation of the algorithm. The logical progression of the algorithm's operation, from initializing the particles to repeatedly updating their positions and velocities to obtain the best solution, is depicted in this diagram.

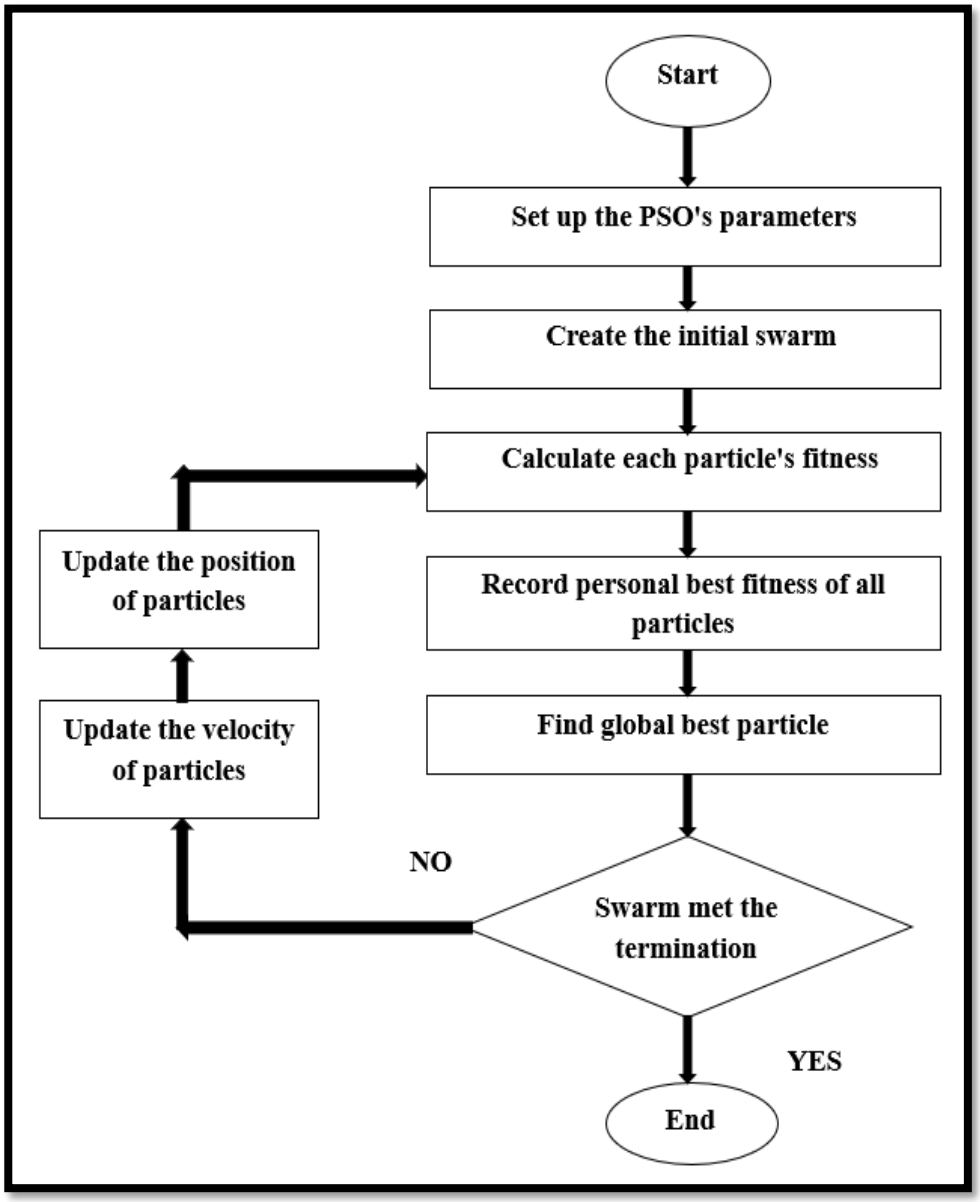

Figure 3-9 Flowchart of the Particle Swarm Optimization Algorithm

3.6.2 The Fitness Function

The cost function is the mainstay of the controller parameter tuning optimization procedure. Through the measurement of the cumulative errors across the simulation time, it was intended to offer a thorough assessment of system performance. These mistakes serve as the main indicator of the system's response quality. To guarantee a balanced performance that gives equal weight to precision and stability, the cost function is made up of two primary parts:

- **IAE (Integral of Absolute Error):** This element is a representation of the system's overall absolute inaccuracy. The optimization algorithm guarantees the most accurate overall performance of the system by minimizing it.
- **ISE (Integral of Squared Error):** The purpose of this component is to penalize significant errors especially. Since errors are being squared, the algorithm is very interested in minimizing overshoot and abrupt change because a large deviation from the reference value would lead to a large rise in cost.

The cost function utilized in the optimization process is represented by the following formula:

$$\text{Cost} = w_p \cdot \left(\text{IAE}_p + \text{ISE}_p\right) + w_q \cdot \left(\text{IAE}_q + \text{ISE}_q\right) + w_f \cdot (\Delta f) + w_v \cdot (\Delta V) \ldots\ldots 3.31$$

The total cost function serves as the objective function for the PSO algorithm. It is framed as a weighted sum of multiple performance indices to achieve a properly balanced tuning outcome. By combining the Integral of Absolute Error (IAE) and the Integral of Squared Error (ISE), the function minimizes the steady-state errors and penalizes large transient excursions like overshoot simultaneously. Crucially, high weights assigned to frequency and voltage deviations ensure the algorithm prioritizes grid stability, making the resulting

controller both robust and highly responsive. The weights for the total cost function were carefully selected to represent the relative significance of each control objective. We gave active power (w_p) a weight of 10 and reactive power (w_q) a weight of 20, as reactive power is more important for voltage stability. To demonstrate a particular design priority, other weights were given to critical frequency and voltage deviations. For example, a weight of 100 was used for frequency (w_f) and a weight of 150 for voltage (w_v). These high weights lead the algorithm to prioritize keeping the grid stable and thus produce a rapid, oscillation-free response which improves the overall system performance.

3.6.3 PSO Parameters and Search Range

The performance of PSO algorithm is highly dependent upon the parameters which are configured. The algorithm settings for this system are given as follows:

Table 3-7 PSO Algorithm Parameters [61].

Parameter	Value	Description
Number of Particles	40	The number of potential solutions (particles) searching the solution space.
Number of Iterations	35	The number of times the algorithm will update the particles' positions and velocities.
Inertia Weight (w)	0.7	Controls the influence of the particle's previous velocity on its current velocity.
Cognitive Coefficient (c_1)	1.5	Dictates the particle's attraction to its own best-found position.
Social Coefficient (c_2)	1.5	Determines the particle's attraction to the best position found by the entire swarm.

The range of search, which determines the boundaries of the controller gains, is as below:

Table 3-8 PSO Search Range

Parameter	Lower Bound	Upper Bound
K_p	0.05	0.1
K_i	3	50
K_d	4×10−4	6×10−4
m	1×10−5	12×10−5
n	1×10−5	6×10−5

Since they restrict the search to a stable and physically significant area, these ranges are crucial.

3.6.4 Stopping Condition

The code employs a simple and reliable termination condition for PSO algorithm: executing a fixed number of iterations. The loop is regulated with the command for iter=1: pso. n_iterations. The process of optimization is therefore ensured to execute precisely 35 times (because pso. n_iterations has been assigned the value of 35), regardless of whether the swarm has converged or not. When the last (35) iteration is reached, the best position of the swarm (g_best_pos) is obtained and stored as the best controller parameter set.

3.7 Performance Evaluation Criteria and Calculation Methods

The performance of each controller is evaluated using a set of quantitative metrics. These metrics are not simply observed from plots but are calculated mathematically from the simulation results. The MATLAB code uses built-in functions and direct calculations to derive these values, which are then compiled into the final comparison tables.

3.7.1 Transient Response Metrics (Using step info Function)

MATLAB's stepinfo function is used to automatically calculate some of the most significant transient response parameters directly from the output signal of the system. For performance assessment, the function studies the responses of the RMS Voltage and Frequency (at the PCC) to a step change in the load. The voltage response is primarily chosen to be the primary signal for this analysis due to its central role in stability and highest cost function weightage factor (the voltage weightage factor) among the whole list of the signals. However, the Frequency response is also quantitatively analyzed using the same transient metrics for a complete overall evaluation of the overall enhanced system stability [75].

- **Overshoot:** The amount by which the response exceeds the steady-state value. It is calculated as:

$$\text{Overshoot} = \frac{\text{Peak Value} - \text{Steady-State Value}}{\text{Steady-State Value}} \times 100\backslash\% \quad \dots 3.32$$

- **Undershoot**: The Undershoot value is defined as the absolute difference between the final steady-state value of the response and the lowest minimum value (trough) reached during the transient period.

$$\text{Undershoot (Value)} = \text{Steady-State Value} - \text{Minimum Value}$$

- **Settling Time:** The time required for the response to settle within a certain percentage (usually 2%) of the steady-state value [55]. The code calculates this using info. Settling Time
- **Rise Time:** The time it takes for the response to rise from 10% to 90% of its final value [55]. The code calculates this using info. Rise Time (though this specific metric isn't explicitly used in the final fitness function, stepinfo provides it).

- **Peak Time** is the time it takes for a system's response to reach its highest or maximum value. It's the point in time where the first peak of the response curve occurs.

The analysis is configured to use info. Overshoot, info. Undershoot, info. Settling Time, info. Rise Time, and info. Peak Time to obtain these values for both the RMS Voltage response and the Frequency response.

3.7.2 Integral-Based Error Metrics

These integral-based error metrics are crucial for a comprehensive analysis of transient performance and are directly used to evaluate controller performance. They are calculated as the integral of the error over time, and the code's fitness function is based on a weighted sum of these metrics. [78][79]

- **Integral of the Absolute Error:** This measures the sum of the absolute error over time. It is calculated as:

$$\text{IAE} = \int_0^T |e(t)|dt \quad \ldots 3.33$$

- **Integral of the Squared Error:** This penalizes large errors more heavily than small ones by squaring the error. It is calculated as:

$$ISE = \int_0^T e^2(t)dt \quad \ldots .3.34$$

The fitness function for the code employs a weighted sum of integral-based error metrics, i.e., IAE and ISE, to drive optimization towards system performance.

3.7.3 Steady-State Error

The final difference between the system output and its target is established by Steady-State Error. It's a critical value for estimating a controller's ability to produce a precise output. The code determines this error after the simulation for

all the major control variables (x), which is critical when calculating the long-term precision of the target of power-sharing [79].

The general formula used to compute the steady-state error (Err_x) is:

$$\mathrm{Err_X} = |\mathrm{X_{ref}} - \mathrm{X_{actual}(end)}| \quad \ldots.3.35$$

Where X represents the system's active power (P), reactive power (Q), voltage (V), or frequency (f). X_{ref} is the target reference value, and $X_{actual(end)}$ is the final simulated value of the variable at the end of the simulation. It must be noted that this error formulation calculates the steady-state error at the time of instantaneous measurement by performing an absolute difference at just the final time of the simulation. This SSE reading differs from the Voltage and Frequency Deviation readings calculated in terms of the average absolute deviation over the whole stable operating period since it only looks at the last point of convergence and not the performance of the controller throughout time in general.

3.7.4 Power Matching

The Power Matching is the most crucial action in analyzing the power-sharing mechanism and indicates proportionally how the two inverters are distributing the active (P) and reactive (Q) portions of the load. It entails measurement of the proportionate share of each inverter to both types of power throughout the simulation [80]. This is computed by the code as:

- **Active Power Matching**

$$\mathrm{Match\_P} = 100 \times \left(1 - \mathrm{mean}\left(\left|\frac{P_1}{P_{ref1}} - \frac{P_2}{P_{ref2}}\right|\right)\right) \ldots..3.36$$

- **Reactive Power Matching**

$$\mathrm{Match\_Q} = 100 \times \left(1 - \mathrm{mean}\left(\left|\frac{Q_1}{Q_{\mathrm{ref1}}} - \frac{Q_2}{Q_{\mathrm{ref2}}}\right|\right)\right) \ldots.3.37$$

A value closer to 100% indicates more accurate power sharing.

3.7.5 Voltage and Frequency Deviation

By measuring the amount by which the voltage and frequency deviate from nominal, these metrics quantify the stability of the system. The measure is the mean absolute deviation over the stable operation time of the simulation [79].

Voltage Deviation: The RMS voltage deviation at the PCC from the nominal voltage, averaged over a specified time.

$$V_{\_dev} = \text{mean}\left(\left|V_{nom,rms} - V_{bus,rms}\right|\right) \quad \ldots\ldots 3.38$$

Frequency Deviation: The average deviation of the system frequency from the nominal frequency.

$$F_{\_dev} = \text{mean}(|f_{nom} - f_{bus}|) \ldots\ldots\ldots\ldots 3.39$$

These deviations are the worthy indexes to the ability of the droop controller in providing system stability for various loading conditions. Primarily, the mean absolute deviation (mean function) is utilized to calculate these indexes for extensive statistical analysis of the overall performance of the controller during the stable operation period.

3.7.6 Total Harmonic Distortion (THD_V)

Total Harmonic Distortion of Voltage (THD_V) is the most critical metric for assessing the quality of the voltage waveform generated b

y the inverters. It quantifies the presence of undesirable harmonic components that are generated primarily by PWM process of the VSI [81]. Maintaining THD_V within the standard levels (e.g., 5% according to IEEE 519 [75]) is crucial to protect sensitive loads and ensure the overall quality of the microgrid output. The THD_V is mathematically expressed as the proportion of the RMS value of the

harmonic contents to the RMS value of the fundamental component (V_1) in percentage:

$$\mathrm{THD_V} = \frac{\sqrt{\sum_{h=2}^{N} V_h^2}}{V_1} \times 100\backslash\% \quad \ldots.3.40$$

Where V_h is the RMS voltage of the h-th harmonic component, and V_1 is the RMS voltage of the fundamental frequency component. The goal of the advanced PID-ANN-PSO controller, therefore, is to ensure that the voltage waveform maintains a THD_V value significantly lower than the conventional controller, thereby enhancing the overall power quality and reliability of the microgrid.

3.8 Artificial Neural Network Training

One type of machine learning model that learns and decides or predicts from data. Through the use of an Artificial Neural Network, this project incorporates adaptive intelligence in microgrid control system. The ANN is trained only once rather than repeatedly using the time-consuming and computationally expensive Particle Swarm Optimization algorithm for real-time prediction of the optimal controller values. Because of this, the system reacts to changing load conditions very quickly [36].

1. The Purpose of the ANN

The main function of the ANN is function approximation. It learns a complex and non-linear relationship between the optimal controller gains and system performance. The ANN is merely being trained to give an answer to the following question: "For a given set of system conditions (represented by a cost value), what are the optimum controller gains (K_p, K_i, K_d, m, n).".

2. Data Collection for Training

The ANN is not trained from scratch; it learns from the data generated by the PSO algorithm. During each iteration of the PSO, a set of controller gains is tested, and the resulting performance is measured by the fitness function. This creates a set of data pairs:

- **Input:** The cost value (a single number) calculated by the fitness function. This cost represents the overall performance of a specific set of gains.
- **Target:** The corresponding set of controller gains (K_p, K_i, K_d, m, n). This is a vector of five numbers that produced the input cost.

The code collects these data pairs into two arrays: pso_data_for_ann. inputs and pso_data_for_ann.targets. The ANN will learn to map the inputs (cost) to the targets (gains).

3. ANN Architecture and Training Process

The specific ANN used in the code is a feed-forward neural network with multiple layers. The architecture is defined as fitnet [10 8], which means it has:

- An **input layer** to receive the cost value.
- Two **hidden layers**, with 10 neurons in the first and 8 neurons in the second. These layers process the input and learn the complex relationships.
- An **output layer** that produces the five controller parameters as the final prediction.

Training process itself is an iterative cycle where the network's internal weights and biases are adjusted to minimize the error between its predictions and the actual target values. The code uses the train function in MATLAB, specifying the training parameters: net. trainParam.epochs = :300 This parameter specifies that the network is trained in a systematic fashion by exposing the entire dataset and executing it 300 times, which is sufficient iterations for the highly efficient

Levenberg-Marquardt algorithm to train the network parameters. The training is guided by an objective called the Mean Squared Error (MSE). The network continuously adjusts its weights to minimize the MSE, which is the average of the squared differences between the network's predicted gains and the actual optimal gains from the training data. To represent the architecture and data flow visually, the complete architecture of the feed-forward neural network employed is given in Figure 3.10, according to the fitnet [10 8] specification.

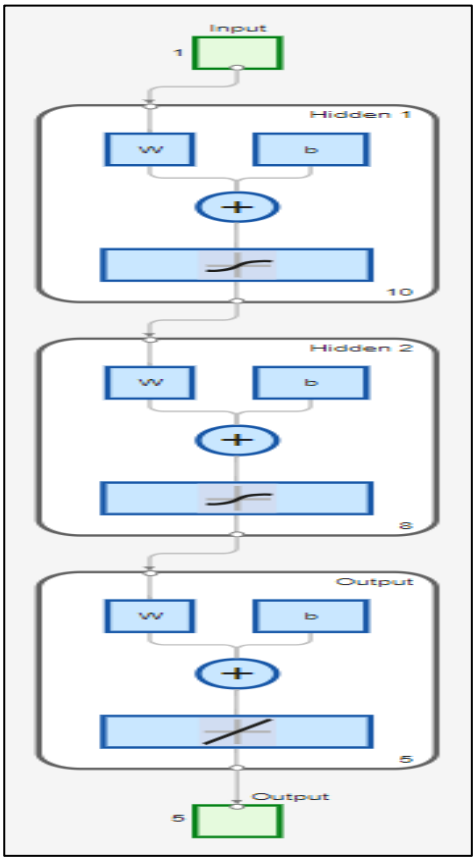

Figure 3-10: The Architecture of the Two-Hidden-Layer Feed-Forward Neural Network

To provide a comprehensive visualization of the intelligent control framework, the systematic execution of the neural network training phase is detailed. This process translates the optimized parameters derived from the Particle Swarm Optimization into a predictive model capable of real-time adaptation. The logical sequence of data initialization, weight adjustment using the Levenberg-

Marquardt algorithm, and the iterative learning cycle is illustrated in figure (3.11) below:

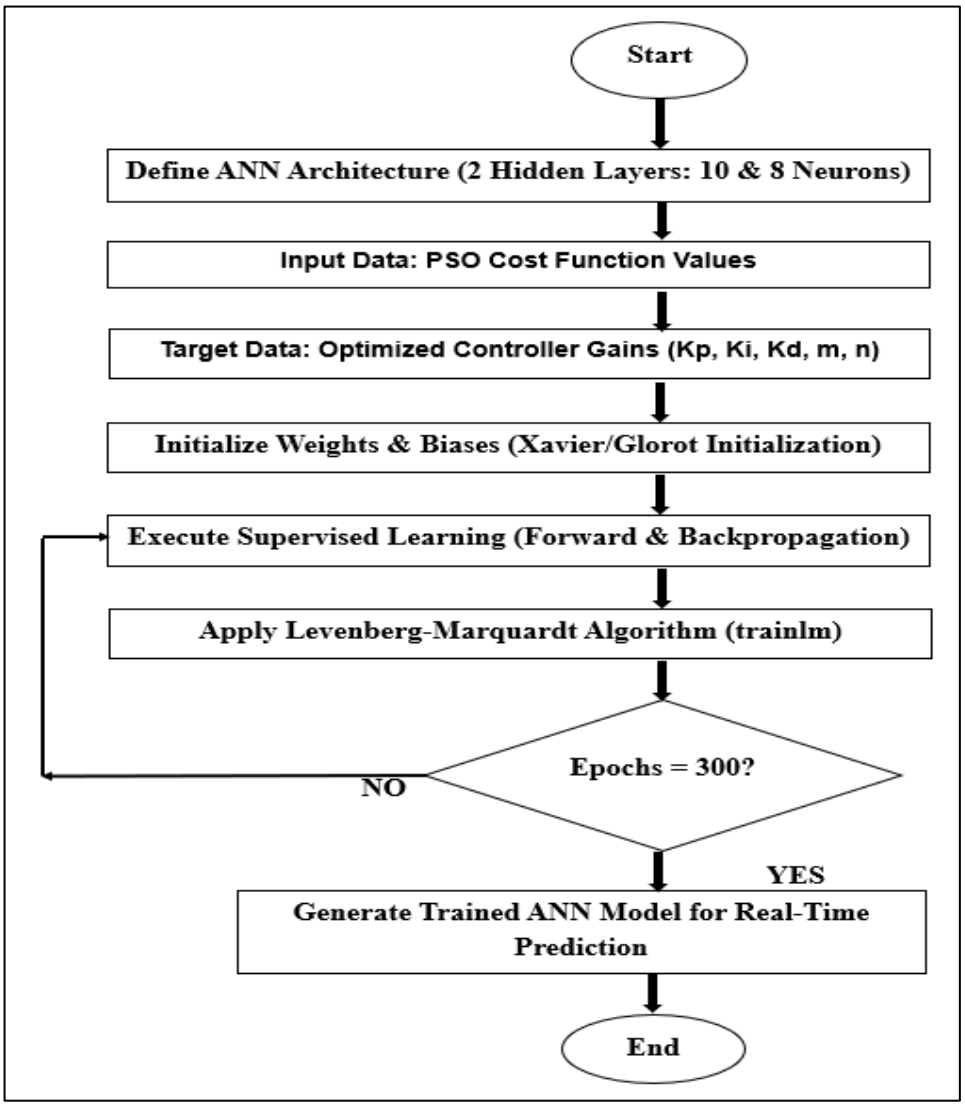

Figure 3.11: Flowchart of the Proposed ANN Training Process

3.9 Hybrid PSO-ANN Approach for Advanced Microgrid Control

Neural networks are sometimes called artificial neural networks or simulated neural networks. ANN is composed of connected nodes that are called artificial neurons. These nodes represent the neurons in the brain. Also, the nodes are connected by edges, which model the synapses in the brain. The function of this approach can be explained as described in the following section. The artificial neuron processes the signals received from the other connected

neurons and then sends a signal to other connected neurons. The sent signal is a real number, and the output of each neuron is computed by some non-linear function of the sum of its inputs, called the activation function. The strength of the signal at each connection is determined by a weight, which adjusts during the learning process [35]. ANNs are machine learning models designed to learn complex patterns from data. In power systems, ANNs can be trained to control system behavior in real-time, making them more adaptive to the changes that occur in the system. In hybrid approaches ANN can be used with PID-PSO and Droop control for more performance enhancement. For more declaration, as an example, ANNs can adjust the PSO-optimized PID controller gains and Droop coefficients based on changing grid conditions, improving the control system's response to transients [36]. Several studies show the effect of combining PSO-optimized PID and Droop with ANNs is the most effective method to develop the optimum control for power in transient condition sharing through microgrids by these combinations. A PID controller is used mainly to ensure that the system stability, and the PSO algorithm optimizes the controller parameters for system performance enhancement. Adding an ANN allows adaptive real-time adjustments, further improving transient responses and power-sharing accuracy [37].

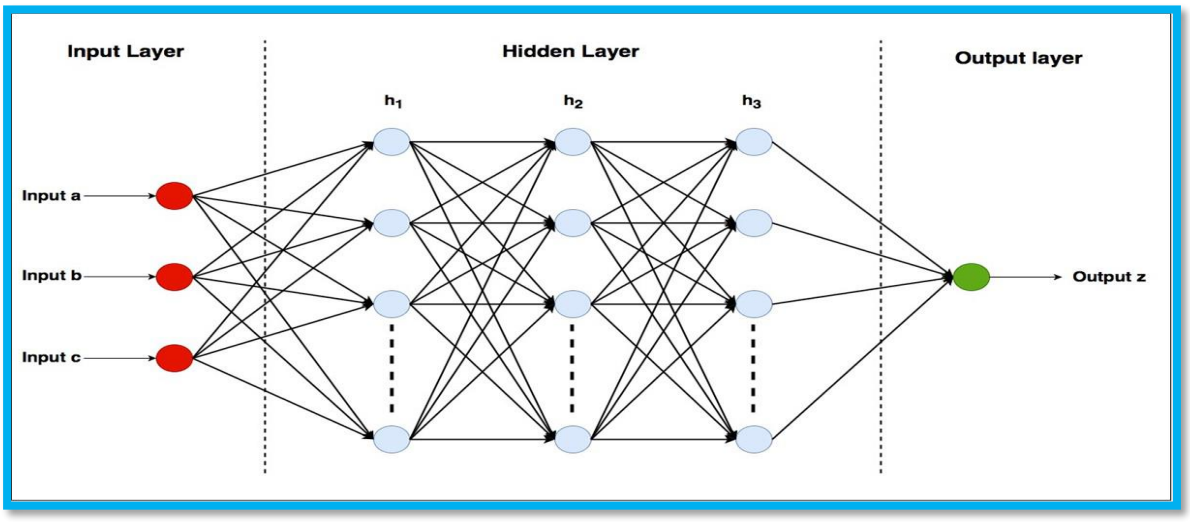

Figure (3-12) Basic ANN Structure [36]

Hybrid control strategies, such as the synergistic combination of droop control with PSO-ANN, have been proposed to improve microgrid resilience, specifically in regulating voltage and frequency during islanded operation. recently, the integration of ANNs with PSO- optimized PID and Droop controllers has had more effect on microgrids performance enhancement. ANNs, with their ability to learn from data, can dynamically adjust the PID gains and Droop coefficients parameters in real time, improving system behavior during transient events. These hybrid approaches have shown commitment in various studies, especially for managing combined, nonlinear systems like microgrids [38].

3.10 summary

This chapter presents the complete methodological structure for modeling, control, and optimization of a stand-alone microgrid. The study begins by defining an exact mathematical model of the physical system where two distributed generation units are represented by a VSI, an LC filter with a damping resistor, and a transmission line. These three elements are represented exactly with dynamic differential equations to create a true simulation setup. The control technique is based on a cascaded two-loop configuration that divides the tasks of accurate voltage/current regulation and power sharing. The outer loop employs a PID controller with the Droop control mechanism to decimate the active and reactive power errors and set up the reference signals for voltage and frequency (V_{ref} and W_{ref}). The inner loop employs PI controllers for fast and accurate output regulation (voltage and current). The entire control strategy is executed in the dq-frame to provide better performance.

One of the main contributions of this work is the use of intelligent optimization to tune the controller parameters. The PSO method computes optimal controller gains by maximizing a penalty-function that penalizes transient response faults. The controller is then able to make real-time parameter updates based on the data from this optimization to train an ANN. This hybrid approach, which combines

conventional control with current computational intelligence, significantly improves the stability and performance of the microgrid under a wide range of load conditions.

CHAPTER FOUR
RESULTS AND DISCUSSION

CHAPTER Four

Results and Discussion

4.1 Introduction

Ensuring stable and effective power sharing among distributed generation units in islanded microgrids remains one of the most significant challenges for control engineers. The system's response is heavily influenced by the quality of the controller design, particularly during transient states arising from sudden load changes. Such events can lead to high power overshoots, prolonged settling times, and undesirable deviations in voltage and frequency, thereby threatening the stability of the entire network. This chapter presents and analyzes the practical results obtained from the simulation environment designed in MATLAB, fulfilling the primary objective of this thesis: to improve the optimal control of transient power sharing in a microgrid using a hybrid controller combining PID and Droop control optimized with the particle swarm optimization algorithm and an Artificial Neural Network. To achieve this goal, a dynamic model of a microgrid system, consisting of two parallel inverters sharing a common load, was constructed. This model was designed using a detailed time-domain simulation, which accurately reflects the dynamic behavior and internal physical components, such as the LC filter, to capture the system’s transient response and stability. The performance of three distinct levels of control strategies will be compared, based on their response to sudden load changes. The first is the Conventional PID Controller, which serves as a baseline with manually tuned parameters and is expected to exhibit limited performance with noticeable overshoots and steady-state errors. The second strategy is the PID and Droop controller optimized with PSO. At this stage, the optimal parameters for both the PID controller and the Droop coefficients were found by executing a live PSO algorithm, with the objective of minimizing a cost function based on overshoot, settling time, and integral error. The final and most advanced strategy is the

Adaptive Controller based on an Artificial Neural Network (ANN-based Controller). Here, a trained ANN predicts the optimal PID and Droop gains in real-time based on the current load level, endowing the system with the ability to deliver optimal performance across a wide range of operating conditions. Numerical values and graphical plots, like transient response, power sharing accuracy, stability of voltage and frequency, and performance analysis under varying loads, will be used to compare the performance of each controller. The serious comparison endeavors to establish beyond reasonable doubt the greater efficacy and robustness of the proposed hybrid ANN-PSO approach towards achieving robust, effective, and adaptive control.

4.2 Analysis and Comparison of Simulation Results

This section gives a thorough explanation of the simulation results in the endeavor to compare the performance of the three control strategies under different operating conditions. Analysis will take into account significant performance metrics that have been extracted from the simulation outputs, such as voltage and frequency stability, transient response, and precision in power sharing. This section will examine graphs and figures closely in order to verify the thesis's main arguments. It will also show how the improved controllers perform much better than the baseline of the conventional Droop control integrated with a manually tuned PID controller.

4.2.1 Active and Reactive Power Sharing Performance

The microgrid system's active and reactive power-sharing capabilities under varied load conditions are thoroughly examined in this section. The subsequent subsections illustrate how improved control schemes, which enhance droop coefficients and external control parameters, offer fair and accurate power distribution among parallel inverters.

4.2.1.1 Individual Inverter Power Sharing

Performance results of active and reactive power sharing for two inverters for a step-load condition are given in figure (4-1). The figure presents a comparison of the proposed ANN-PSO approach with two established methods: PID-PSO and conventional. The study will show better power sharing precision and transient performance through simultaneous tuning of PID and droop parameters. The unequal active power distribution between the P1 and P2 inverters is depicted in Figure (a). The system is configured to have unequal power distribution, where the reference line confirms that Inverter 1 (P1) supports approximately 60% of the load, whereas Inverter 2 (P2) supports approximately 40%. In the first steady-state period ($t < 0.8$ seconds), the total loading is 10 kW, split between 6 kW for Inverter 1 and 4 kW for Inverter 2. In $t = 0.8$ seconds, there is a step change in load, raising the overall load to 16 kW. Specifically, Inverter 1 changes from 6 kW to 9.7 kW, and Inverter 2 changes from 4 kW to 6.3 kW. Both during the initial operation ($t = 0$) and the shift in load ($t = 0.8$ seconds), Conventional controller (red line) exhibits slow transient response, characterized by longer Rise Time and Settling Time. The overshoot visible at $t = 0$ is because the controller attempts to correct the colossal initial error between the initial state (zero power) and the reference value in a sudden way. By contrast, the PSO-optimized controller (blue trace) shows a significant improvement, demonstrating a much more responsive system and quicker settling time in both transient cases. While this speed is achieved with a significantly lower overshoot compared to the sluggish Conventional controller, the PSO method effectively minimizes both the transient duration and peak deviations, validating its superior effectiveness in optimizing the overall dynamic response. The ANN-PSO controller (green trace) performs the best with the least settling time, quickest rise time and minimal steady-state error in both transient cases. This provides the ability ANN to forecast optimum parameters, resulting in a much more accurate

and dynamic response that closely tracks the reference power with minimal error. Reactive power sharing (Q1 and Q2) is indicated in Figure (b). The system is programmed for unequal reactive power sharing, where the line of reference confirms that Inverter 1 (Q1) takes 60% of the load and Inverter 2 (Q2) takes 40%. In the first steady-state period ($t < 0.8$ seconds), the total reactive load is 2 kVAR, split between 1.20 kVAR for Inverter 1 and 0.80 kVAR for Inverter 2. A step-up in load occurs at $t = 0.8$ seconds, raising the total reactive load to 4 kVAR. To be exact, Inverter 1 rises from 1.20 kVAR to 2.4 kVAR, and Inverter 2 rises from 0.80 kVAR to 1.6 kVAR. The classical droop control (red line) settles slowly and exhibits a long rise time and a high initial overshoot. This short-term overshoot is characteristic of controllers which are trying to achieve rapid tracking. The PSO-optimized controller (blue line) exhibits a significantly faster response and achieves a quicker settling time than the Conventional method but again, the ANN-PSO controller (green line) outperforms both of them with the lowest settling time and by far the smoothest and most accurate transient response, effectively minimizing the transient duration. The exceptional performance observed is primarily attributed to the direct optimization of the active power control parameters. By achieving precise regulation in the active power loop, the system indirectly enhances reactive power sharing among the parallel inverters. This coordinated optimization maintains a stable voltage profile and significantly mitigates circulating currents, thereby maximizing the overall stability and resilience of the microgrid during transient events. The improved ANN-PSO controller's transient response affirms that an existing network can successfully adjust to load variations and deliver optimal control parameters, resulting in extremely precise and consistent power sharing.

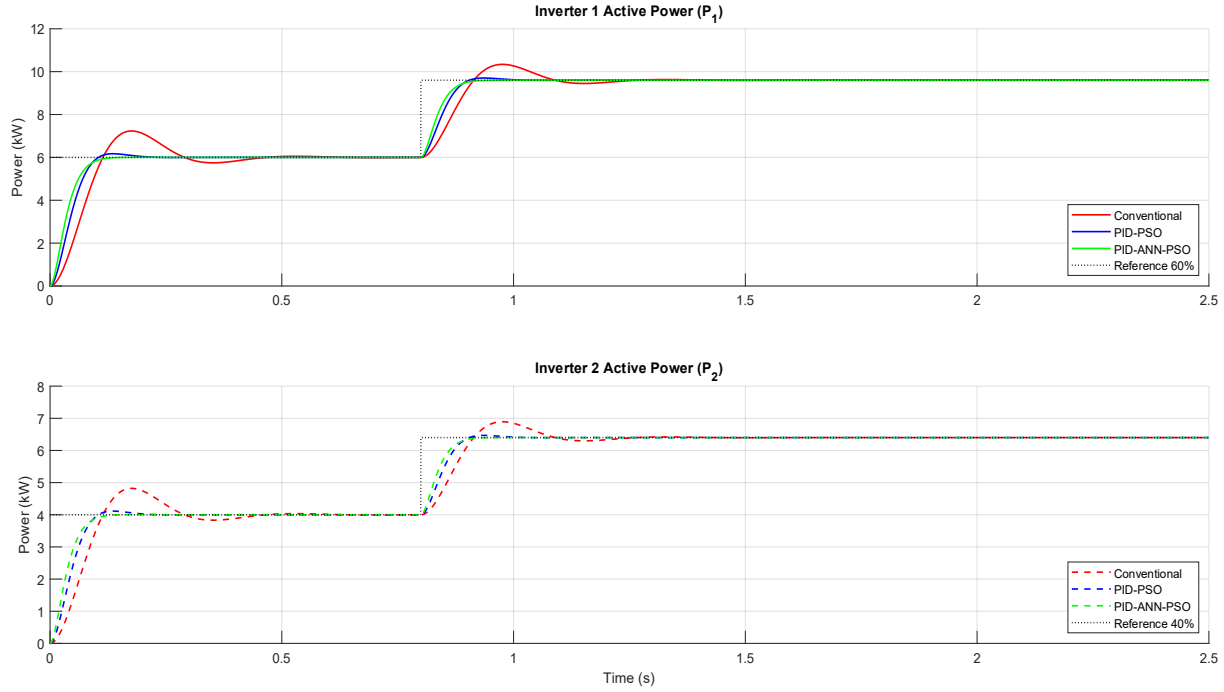

(a)

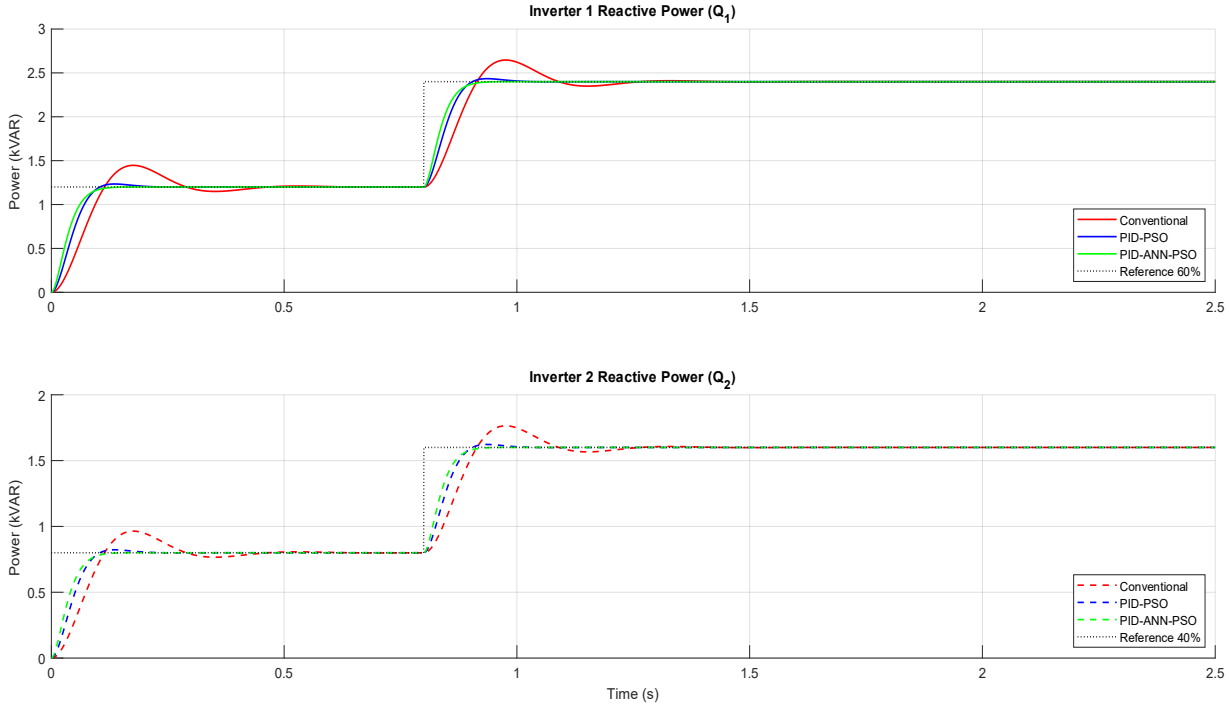

(b)

Figure 4-1 power sharing between inverter 1 and inverter 2 under step -load conditions (a) Active power (b) Reactive power

A further investigation on instantaneous power sharing errors demonstrates the improved performance of the proposed PID-ANN-PSO controller in active and reactive power sharing. Error analysis is extremely crucial for the evaluation of dynamic response as it represents the significant minimization of transient deviation from the desired reference. As can be seen in Figure (4-2), the traditional controller exhibits a slow return to zero error in both the transient events (t=0 and t=0.8 s). Importantly, the traditional controller has a finite non-zero steady-state error in both the first and final steady-state intervals, albeit small. The optimal controller based on PSO shows a considerably improved transient response compared to that with the conventional method, with approximately zero SSE in both stable operating intervals. But the ANN-adaptive controller truly excels, as shown in its error curve, which has the least deviation during the initial load step and ensuing load ramp at 0.8 seconds.

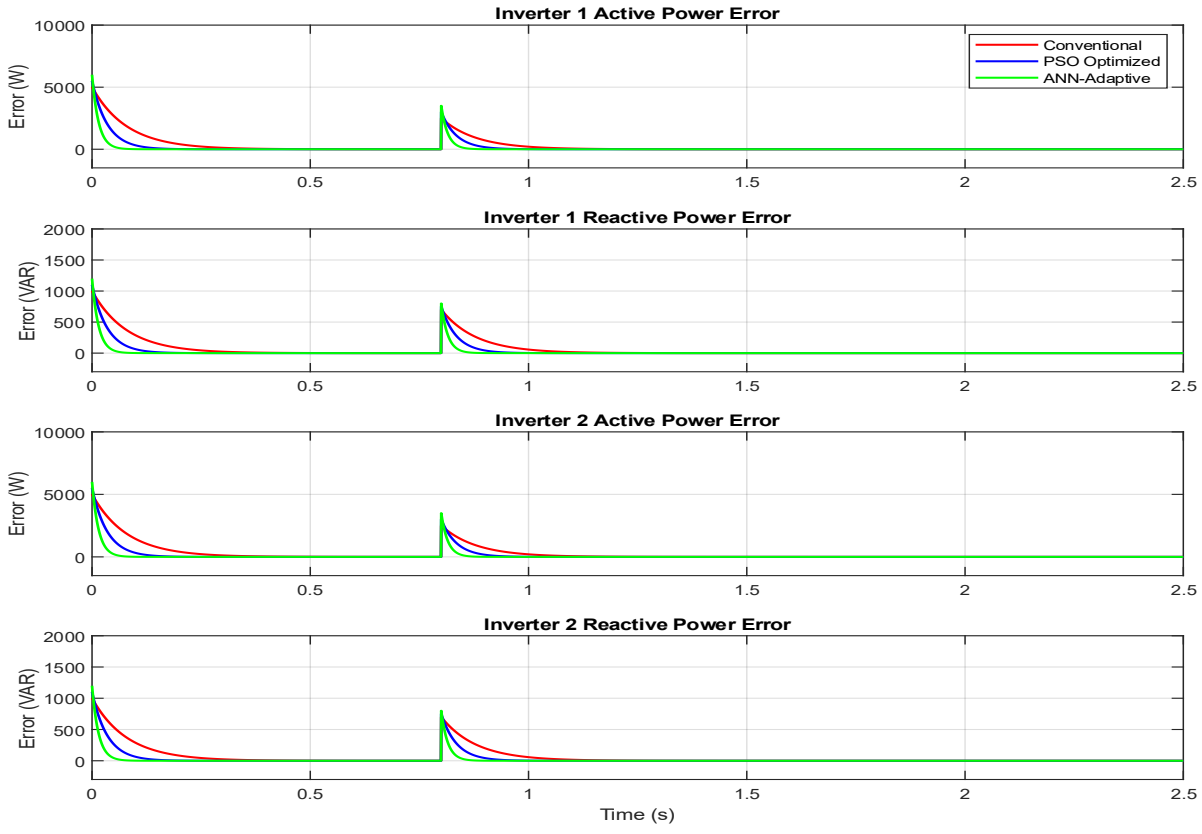

Figure 4-2 Instantaneous Power Sharing Error

This ability to adapt its PID gains and droop coefficients in real-time dynamically cancels out disturbances and maintains a near-zero steady-state error during both steady operating intervals. Adjusting both sets of parameters simultaneously allows the system to reach a speed and accuracy level that cannot be matched by conventionally used fixed-gain controllers. As a result of this dynamic flexibility, the microgrid is guaranteed to always have precise and stable power sharing as well as being highly responsive to change

4.2.1.2 Total System Power Delivery

In Figure (4-3), Total Active & Reactive Power Supplied vs. Load, the overall system performance of the suggested control strategies are compared directly and quantitatively. This analysis confirms the effectiveness of our method, which optimizes the PID and droop coefficients together to obtain optimum microgrid performance. The total active power delivered to the load is shown in the top subplot, where the total active load (P_{Load}) is plotted with the dashed black line, stepping from 10 kW to 16 kW at t=0.8 seconds. The conventional controller (red dashed line) has a slow rise time and noticeable overshoot in each load step. The PSO-tuned controller (blue dashed line) is a clear improvement over the conventional method, in that it is a faster response. But the PID-ANN-PSO controller (thick green line) performs the best under dynamic conditions with the highest rise time and earliest settling time at every step of load. This illustrates how the co-optimized parameters improve power delivery quality overall by allowing the microgrid to respond to abrupt changes in load more quickly and uniformly.

Also, the provided total reactive power is indicated in the lower subplot, in which the total reactive load (Q_{Load}) rises from 2 kVAR to 4 kVAR. The conventional controller gives the slowest transient response. The PSO-tuned controller (blue dotted line) exhibits better performance with a faster response. In contrast, the PID-ANN-PSO controller (green line) is much more tightly controlled with a very

short settling time. This result is particularly significant as it demonstrates how the direct optimization of active power control parameters effectively stabilizes the frequency-voltage coupling within the microgrid. While the primary objective was the enhancement of active power sharing, this direct improvement indirectly optimized the reactive power flow and voltage regulation.

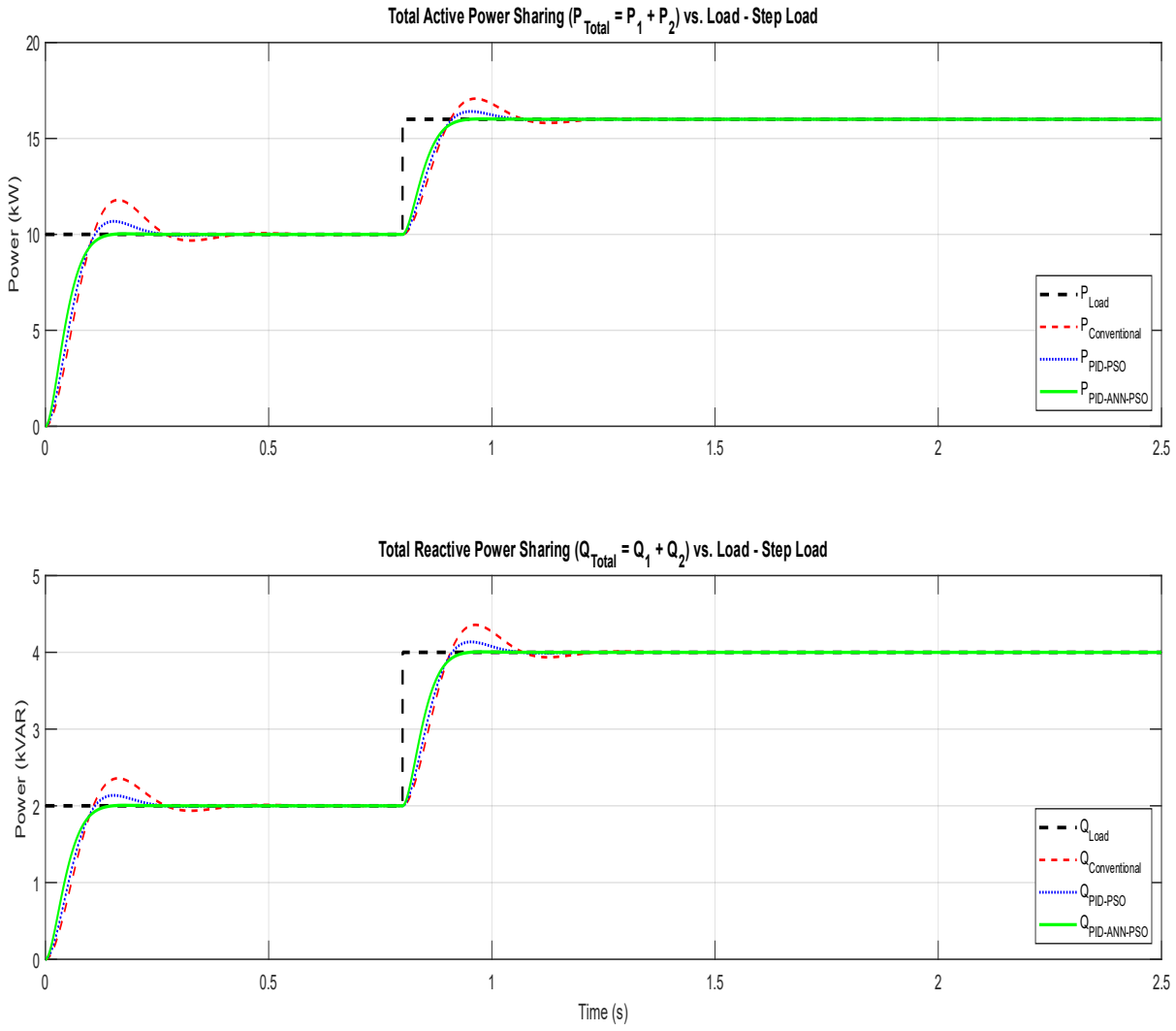

Figure 4-3 Total Active & Reactive Power Supplied vs. Load

4.2.1.3Active and Reactive Power Sharing Performance under Varying Load Steps

The results in Figure (4-4) show the improved performance of the suggested optimized controllers to achieve power sharing accuracy in both active and reactive power under a multi-step load condition. The test utilizes the system's dynamic capability for three consecutive load changes at times t = 0.1 s, t= 0.6 s, and t =1.1 s. Tuning the PID controller parameters and the droop coefficients is demonstrated to be beneficially useful, with the plot revealing how the system behaves in response to such inputs. The conventional controller reacts slowly to all step changes and settles at the new steady-state levels after an extremely long time. The PID-PSO and PID-ANN-PSO controllers, respectively, exhibit a much quicker transient response with highly reduced instantaneous tracking errors. The system's operation is characterized by three consecutive load changes (steps):

- During the first step (t = 0.1 s), the sum of active load is 6 kW (distributed as 3.8 kW for Inverter 1 and 2.2 kW for Inverter 2) and the sum of reactive load is 1 kVAR (distributed as 0.6 kVAR for Inverter 1 and 0.4 kVAR for Inverter 2).
- In the second step (t 0.6 s), the total active load increases to 10 kW (6 kW for Inverter 1 and 4 kW for Inverter 2), and the total reactive load increases to 2.5 kVAR (1.5 kVAR for Inverter 1 and 1 kVAR for Inverter 2).
- Finally, the total active load is 15 kW (9 kW for Inverter 1 and 6 kW for Inverter 2) and the total reactive load is 3.5 kVAR (2.1 kVAR for Inverter 1 and 1.4 kVAR for Inverter 2) at t 1.1 s.

The PID-ANN-PSO controller delivers the fastest and most stable response, achieving precise active power sharing while indirectly optimizing the reactive power distribution with minimal oscillations. This performance confirms that while direct parameter optimization significantly enhances the system's dynamic response and active power-sharing, it simultaneously yields an indirect yet

substantial improvement in voltage stability and reactive power quality, thereby validating the comprehensive effectiveness of the proposed control scheme.

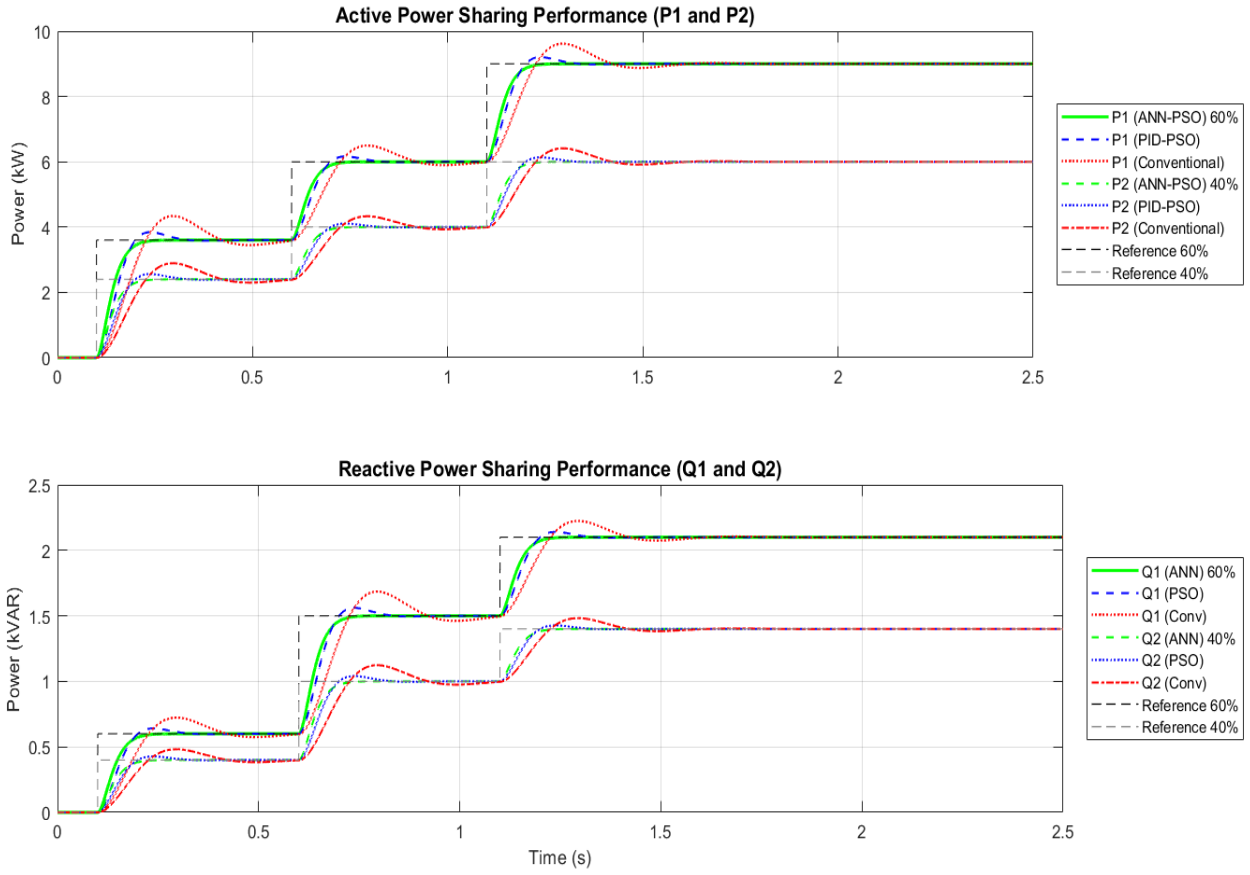

Figure 4-4 Comparative Performance of Active and Reactive Power Sharing under - Multi-Load Scenario

Figure (4-5) shows the Total Active Power Tracking Performance (P Total) of the microgrid system during a multi-step load condition, which includes three different demand changes (i.e., from 6kW to 10kW to 15kW). The plot compares the performance of three control methods: the Conventional PID, the PID optimized by Particle Swarm Optimization (PID-PSO), and the proposed Adaptive PID based on an Artificial Neural Network combined with PSO (PID-ANN-PSO). The results unequivocally demonstrate the superior performance of the PID-ANN-PSO controller. In all abrupt load changes, this adaptive method is

characterized by a considerably quicker dynamic response, with a more rapid approach to the new set point in comparison with the two other techniques. Importantly, it shows barely any oscillation, confirming excellent transient control and stability, and comes to rest precisely at the total load reference with fine steady-state accuracy. On the other hand, the Conventional and the PID-PSO control schemes both show inferior settling time as well as perceptible overshoots following the load steps, confirming that the synergy of the ANN's adaptivity capability and the optimization of PSO is of valuable advantage in enhancing the system's dynamic stability and power tracking accuracy under heavy loads

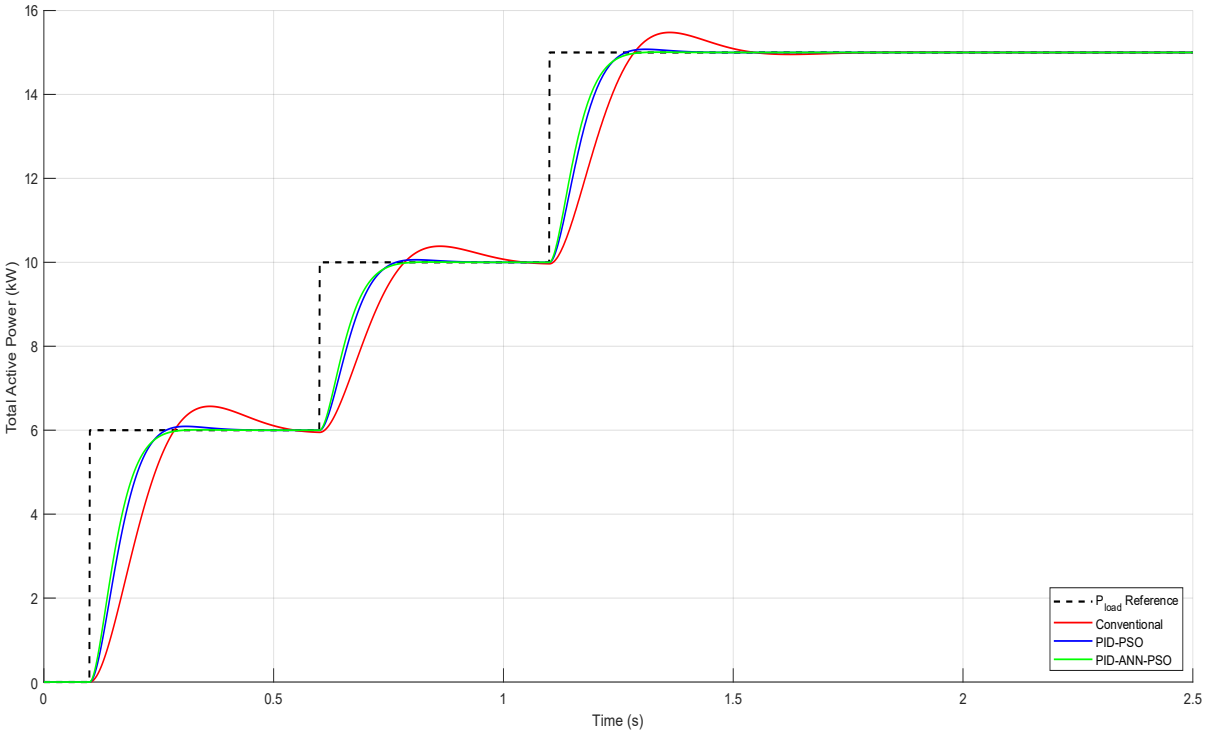

Figure 4-5 Total Active Power Response - Multi-Load Scenario

Referring to the Total Reactive Power Sharing Performance (Q_{Total}) in Figure (4-6), the system behavior is in close agreement with the Active Power results. The PID-ANN-PSO control strategy once again demonstrates the best and most stable dynamic response compared to the Conventional and PID-PSO controllers in tracking the multi-step load reference (from 1 kVAR to 2.5 kVAR, then 3.5 kVAR). The PID-ANN-PSO controller is characterized by minimal oscillation

and settling at the desired value with excellent steady-state accuracy at every load transition. These results consistently validate the efficacy of the adaptive and optimized control scheme. It is noteworthy that while the optimization was directly targeted at the active power control parameters, it indirectly led to a significant improvement in reactive power dynamics. By achieving a rapid and precise response in the active power loop, the system effectively stabilized the voltage-frequency coupling, thereby ensuring a fast and accurate transfer of reactive power between the inverters during dynamic operating conditions.

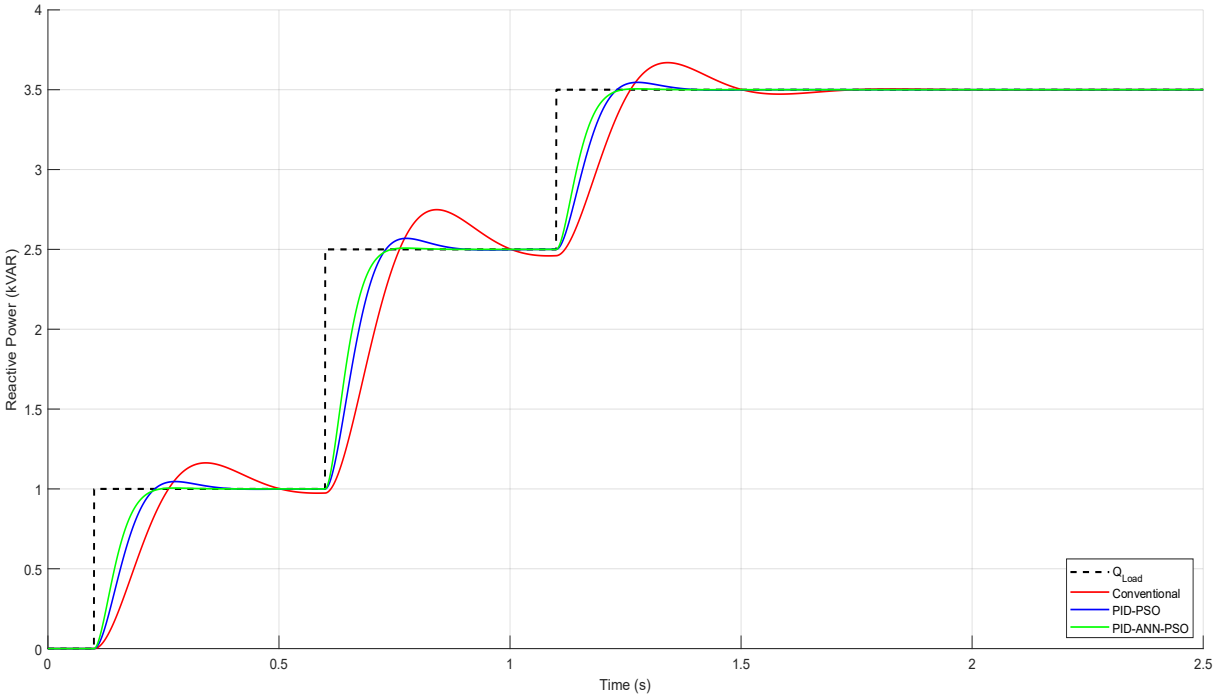

Figure 4-6 Total Reactive Power Response - Multi-Load Scenario

4.2.2 System Stability and Power Quality Analysis.

This section gives a comprehensive rundown of how the microgrid operates, focusing on two important aspects: system stability and power quality. The following sections will extensively evaluate the microgrid's dynamic response to load fluctuations, paying special attention to the stability of its voltage and frequency. Important internal operational metrics such as DC-link voltage stability and circulating power will also be examined, and a harmonic distortion

study will be used to assess the overall power quality. The purpose of this analysis is to show how the suggested control strategies can improve the performance and dependability of the microgrid.

4.2.2.1 System Stability Analysis (Voltage and Frequency)

Microgrid performance in islanded mode, when the system is disconnected from the main grid, depends critically on voltage and frequency stability. In this situation, the Q-V and P-f droop control methods are used to guarantee reliable operation and efficient power sharing amongst DG units. While this approach is traditionally predicated on the idea that frequency drops indicate active power rises and voltage drops indicate reactive power production, our suggested approach builds on these relationships (Figure 4.7) via a hybrid PID-ANN-PSO strategy. By optimizing the P-f loop, this method indirectly stabilizes the reactive power and voltage profile, ensuring robust performance through improved system synchronization. This mixed implementation simulates the response of typical synchronous generators without needing high-bandwidth communication, leading to a more responsive and stable system under different load conditions.

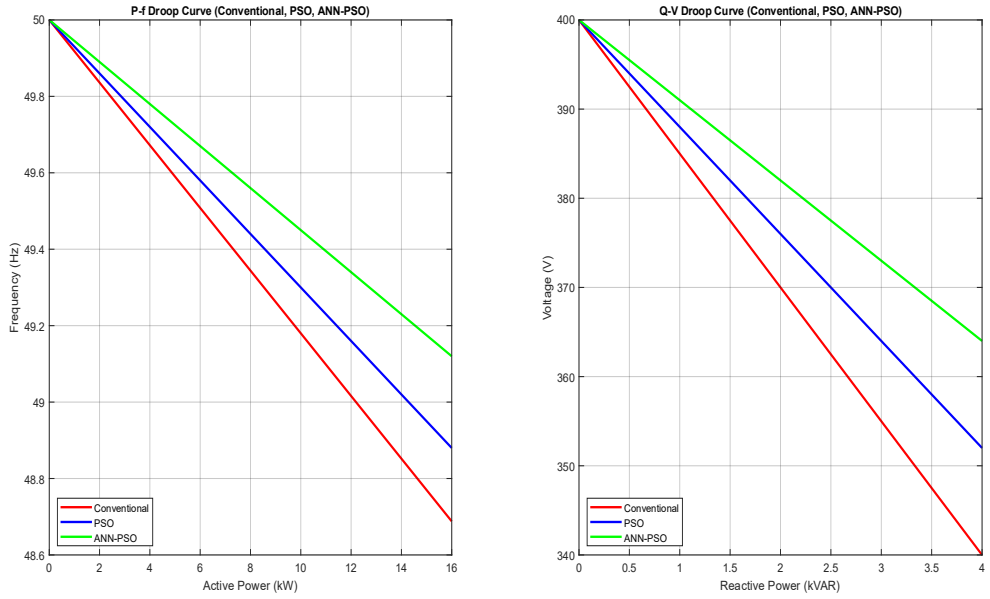

Figure 4-7 Comparative Analysis of Static P-f and Q-V Droop Characteristics.

The comprehensive view of system stability is presented in Figure 4.8, illustrating both the voltage and frequency stability curves under an abrupt load shift at time equals 0.8 seconds.

- **Voltage Stability Analysis**

The PCC Voltage Stability response, illustrated in the top curve of Figure 4.8, demonstrates the system's RMS voltage behavior in response to the step load change. The conventional droop method (red dashed line) suffers from the most significant voltage drop and the poorest steady-state recovery. Initially, the system maintains a stable profile near the nominal 400 V, with the proposed PID-ANN-PSO controller (green line) sustaining the highest precision. Following the abrupt load surge at 0.8 seconds, the voltage naturally dips to accommodate the increased demand. The conventional controller experiences the largest dip, falling towards 399.85 V, and takes the longest time to stabilize with visible oscillations. In contrast, the PID-ANN-PSO controller minimizes this transient dip and recovers rapidly, maintaining a superior steady-state voltage of approximately 399.93 V shortly after the disturbance. It is important to note that this enhancement in voltage quality is achieved indirectly; while the controller primarily optimizes the P-f control loop to ensure frequency stability, the resulting improvement in active power-sharing and system synchronization inherently enhances the overall voltage profile at the Point of Common Coupling (PCC) without the need for aggressive direct Q-V adjustments.

- **Frequency Stability Analysis**

The frequency stability response, as illustrated in the lower curve of Figure 4.8, demonstrates the system's dynamic reaction to the active power imbalance. Upon the load step at 0.8 seconds, a temporary frequency drop is observed across all control strategies. The Conventional controller (red dashed line) exhibits the most significant deviation, reaching a minimum frequency nadir of approximately

49.78 Hz before struggling to recover. In contrast, the improved controllers show a much more resilient response; the PID-PSO (blue line) limits the drop and begins recovery sooner, while the proposed PID-ANN-PSO (green solid line) achieves the best performance with the least deviation, maintaining a nadir of approximately 49.91 Hz. Following the transient period, the proposed hybrid controller enables the system to settle significantly faster, stabilizing the frequency near the nominal value by t = 1.2 seconds, whereas the conventional method continues to show oscillations. This superior response, achieved through the simultaneous tuning of the droop coefficient (m) and PID parameters, ensures high frequency quality and robust dynamic stability for the microgrid throughout the 2.5-second simulation period.

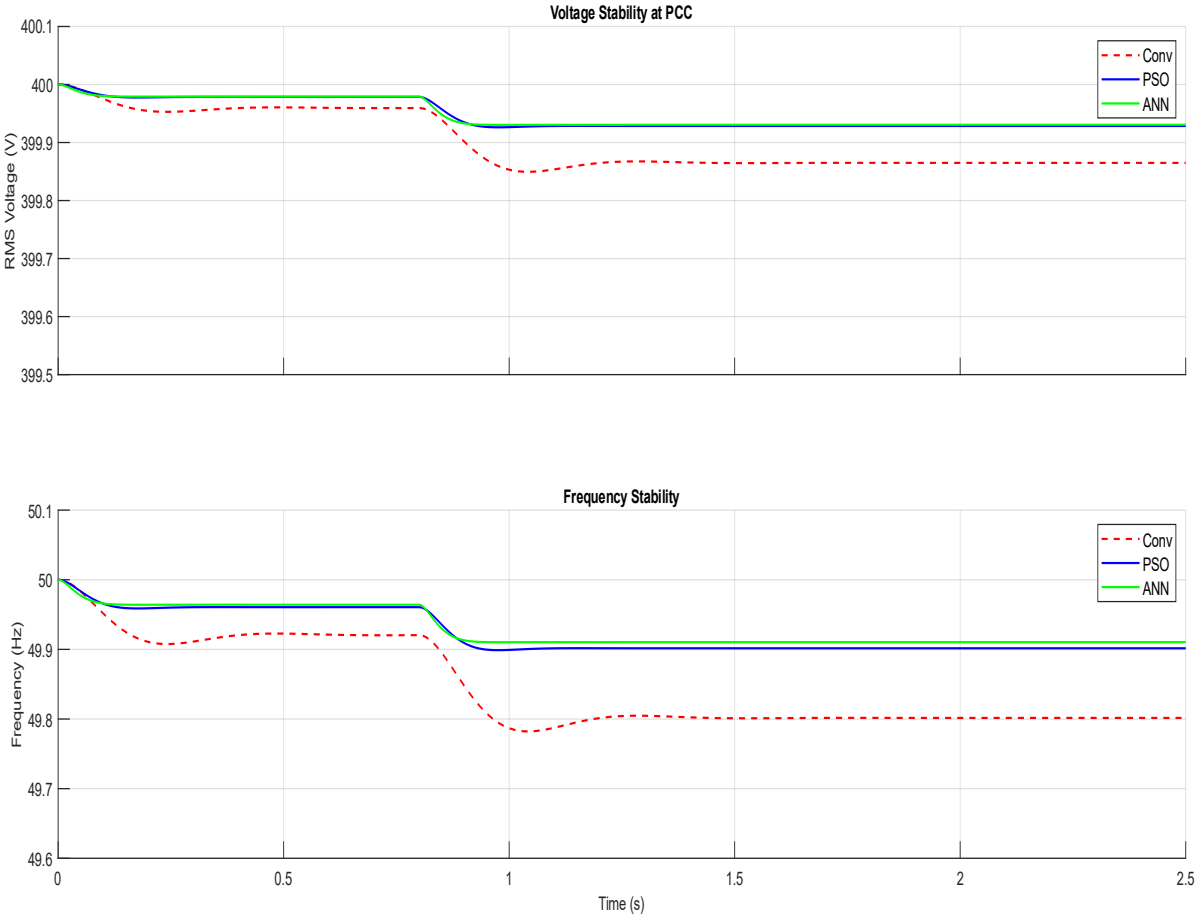

Figure 4-8 Voltage & Frequency Stability at PCC

4.2.2.2 Total Harmonic Distortion Analysis

Total harmonic distortion and the microgrid's output voltage quality are closely linked, making the latter a crucial performance indicator. In Table 4.1, the THD percentages for the three control systems are clearly presented and compared. The conventional controller, according to the tabulated data, has the highest THD, indicating a low-quality output voltage with a high harmonic content. On the other hand, the THD is significantly lower for the controllers with optimal parameters, such as the PID-PSO and particularly the PID-ANN-PSO. In order to increase power quality, it is highly effective to simultaneously modify the droop coefficients and the parameters of the PID controller integrated with the Droop loop. The PID-ANN-PSO controller delivers the lowest THD value as recorded in the table.

Table 4.1 THD Comparison for Conventional and Intelligent Controllers.

Algorithm	THD (%)
Conventional	5.1
PID-PSO	3.3
PSO- ANN	2.9

Figure (4-9) provides visual support for this conclusion by displaying the voltage waveform with time. The high THD value of the conventional controller is consistent with its output (shown in red) seeming deformed and less sinusoidal. The ANN-PSO controller's waveform (shown in green) is far cleaner and more like an ideal sine wave, proving the output voltage's improved quality and confirming the combined optimization approach's efficacy in reducing harmonic distortion.

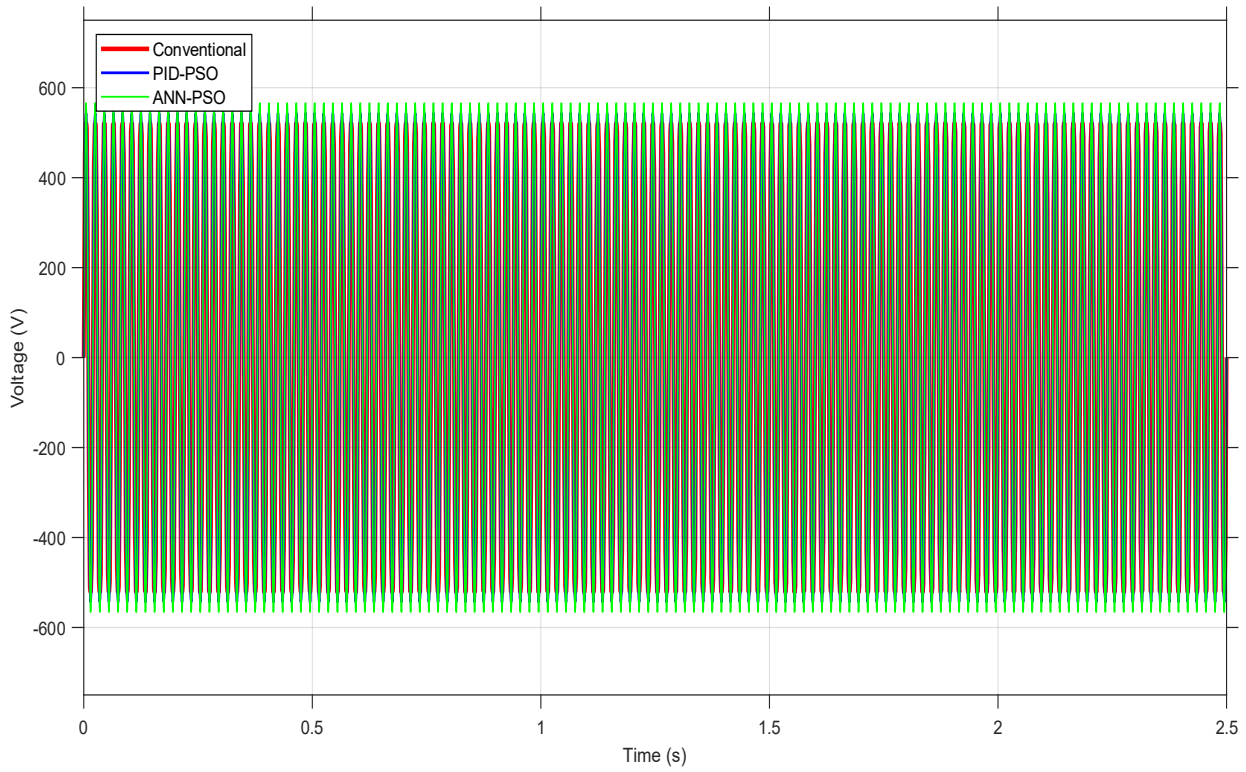

Figure 4-9 Harmonic Content in Output Voltage

4.2.2.3 Zero-Load and DC-Link

The internal stability and power sharing of the microgrid's inverters are crucially revealed by this research, which is based on a fresh set of data. Circulating power is the undesired power flow between the parallel inverters when there is no load, as seen in Figure(4-10a). This power must be swiftly forced to zero by an efficient control strategy. The graph makes it evident how the enhanced control techniques, which are accomplished by fine-tuning the droop coefficients and internal control parameters, efficiently reduce these oscillations and quickly bring the circulating power down to zero. The improved performance of the suggested control mechanism is directly reflected in this increased damping capabilities.

The DC bus voltage response under a step load change is illustrated in Figure (4-10b), demonstrating the system's ability to maintain a stable DC link at 800 V. The abrupt load transition at 0.8 seconds induces a transient voltage dip across all controllers. The Conventional controller (red dashed line) exhibits the most significant drop, falling to approximately 760 V. The PID-PSO controller (blue dotted line) shows an improved response by limiting the dip to about 772 V. However, the proposed PID-ANN-PSO (green solid line) demonstrates superior transient resilience, restricting the voltage drop to only 780 V and achieving the fastest recovery to the nominal level. This enhanced performance confirms that the dynamic tuning of control parameters effectively strengthens internal stability and sustains DC voltage quality under disturbance.

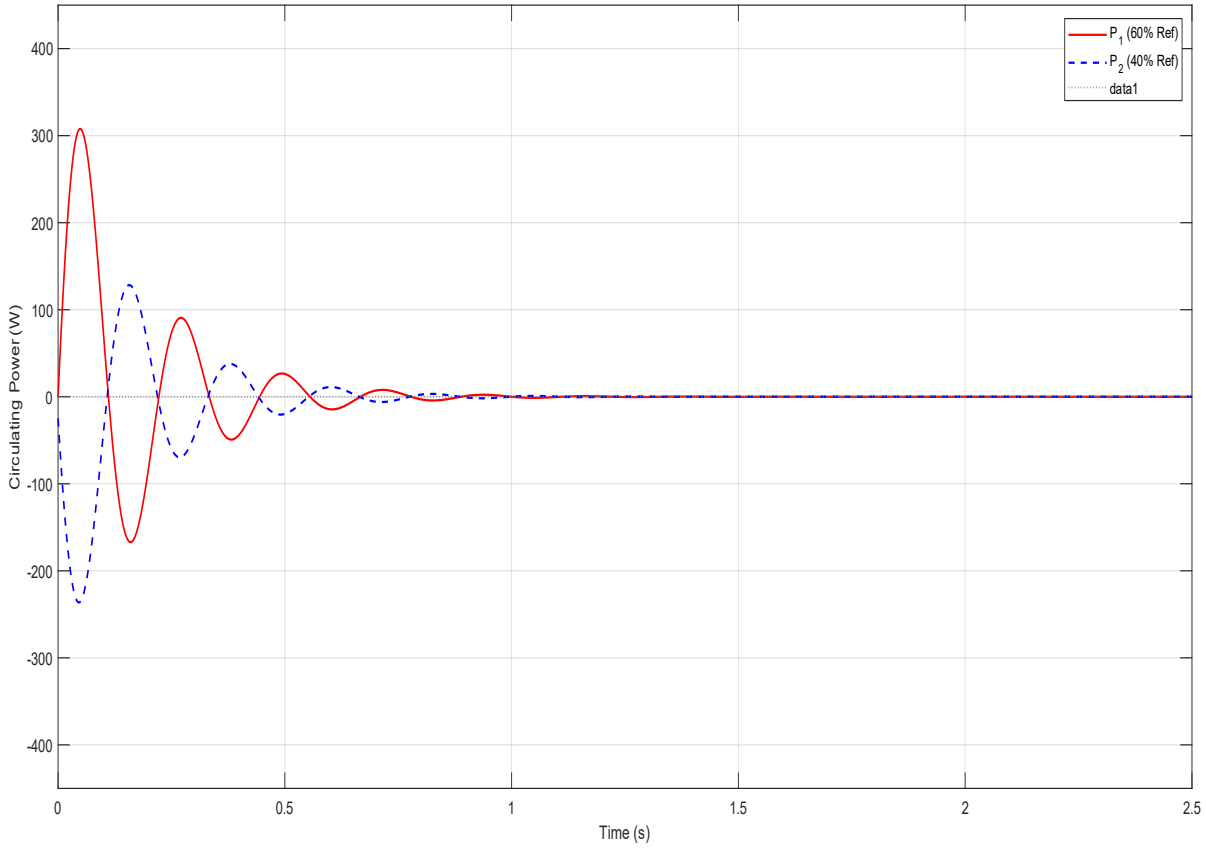

(a)

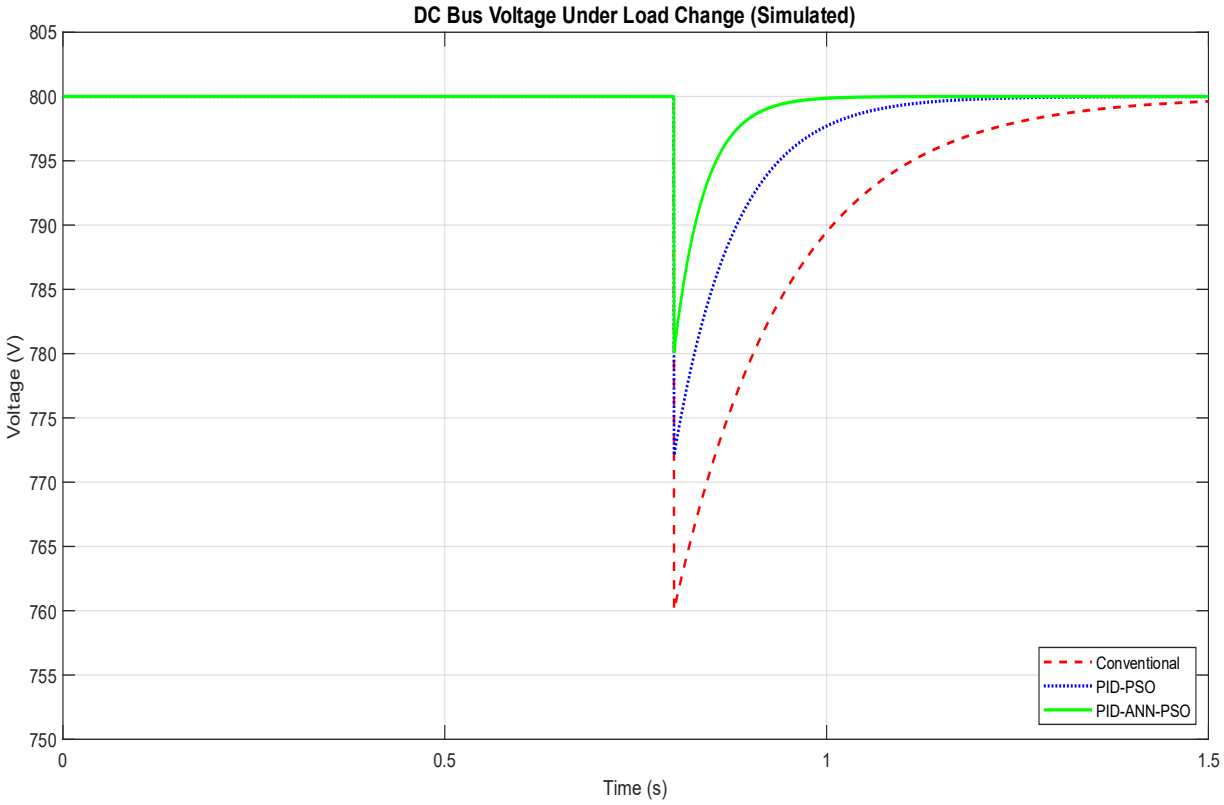

(b)

Figure 4-10 (a) Circulating Power (b) DC Link Voltage

4.2.3 Control Effort and Phase angle difference Analysis

This section provides the overall findings achieved by the proposed PID-ANN-PSO optimization of the PID control and droop coefficients. The study is structured to demonstrate the dynamic system performance against sudden load disturbances. Specifically, the analysis discusses two key aspects: the Control Effort, defined by the magnitude and dynamic efficiency of adaptively adjusted controller parameters, and the Transient Response, which quantifies the system's speed and stability using indices such as Active and Reactive Power Rise Time. The outcomes collectively validate that the optimized parameters yield a very effective and superior dynamic response compared to conventional techniques.

4.2.3.1 Evaluation of Control Effort Magnitude and Dynamic Efficiency

Figure (4-11) presents an important explanation of the Control Effort Magnitude imposed by each controller on Inverter 1 (contribution of 60%) and Inverter 2 (contribution of 40%).

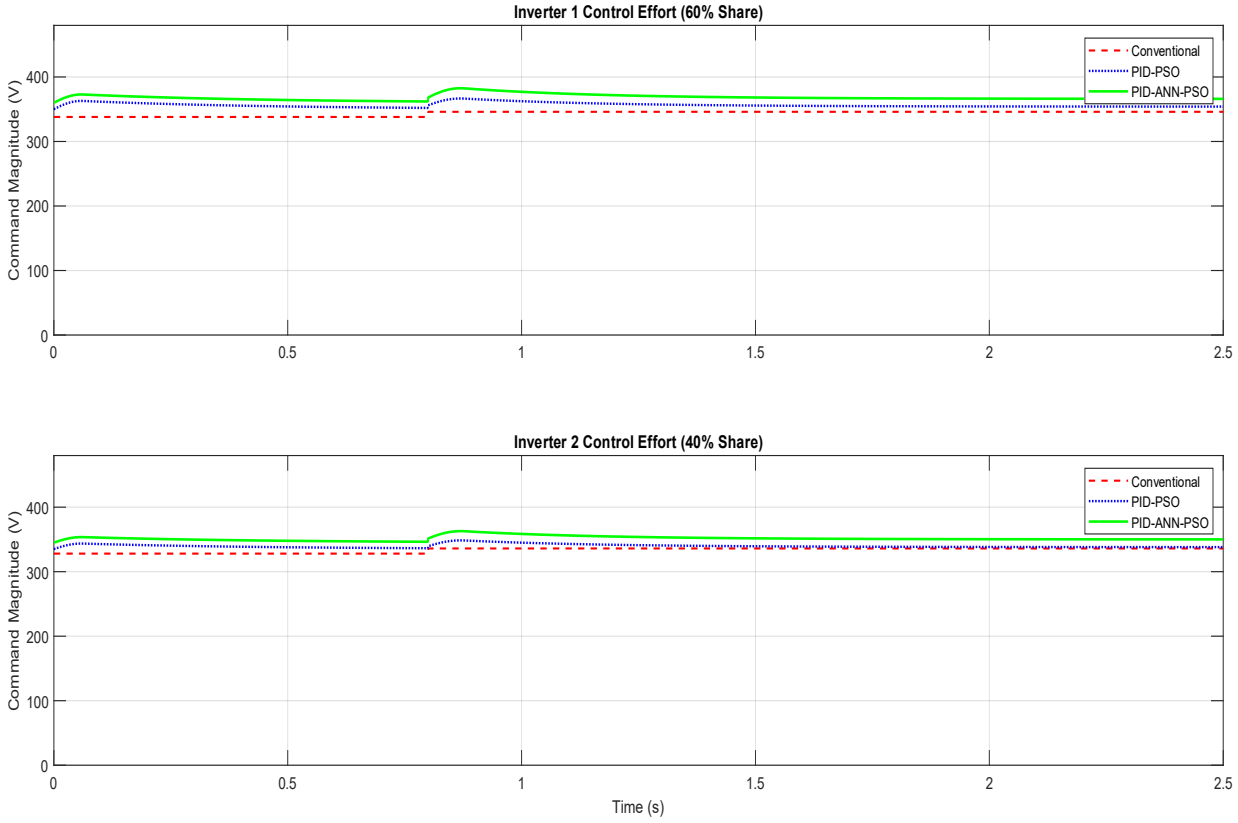

Figure 4-11 Comparison of Inverter Control Effort Magnitude for Inverter 1 (60% Share) and Inverter 2 (40% Share) During Step Load Change

The magnitude of the command signal is indicative of the internal power or force utilized by the controller in compelling the required power-sharing performance, especially during transient conditions. The figure clearly shows that the Conventional controller (Red dashed line) yields the minimum overall control effort, both at initial conditions (t=0) and during the step change (t=0.8 s). This minimum effort is, nonetheless, the cause of its slowest transient response and largest steady-state error of power sharing, as shown in previous figures.

Conversely, the projected PID-ANN-PSO controller (Green solid line) demonstrates the greatest peak control effort in both inverters immediately following the load step, with a controlled peak not exceeding 380 V for Inverter 1 and 365 V for Inverter2 . Such a significantly higher command magnitude is the only reason that the active power response becomes better (fastest settling time and zero steady-state error). The system is applying maximum corrective force to achieve the fastest dynamic stability. While the PID-PSO controller (Blue dotted line) shows an intermediate effort, the compromise achieved by the PID-ANN-PSO, forgoing low-effort transient for maximum speed and final accuracy, is the most effective approach to stabilize the dynamic behavior of the microgrid.

4.2.3.2 Phase angle difference

The phase angle difference, as visualized in the accompanying figure (4-12), plays a crucial role in visualizing the microgrid's stability and synchronization, as a lesser difference directly correlates with a more reliable system. This figure serves as a simple gauge of inverter cooperation across different operational states. Before the load change at t=0.8s, the phase angle accumulation is minimal but already shows differentiation: at t=0.7s, the conventional controller has accumulated about 0.85 degrees, the PID-PSO is at about 0.75 degrees, and the proposed PID-ANN-PSO demonstrates the lowest initial accumulation at about 0.65 degrees. Immediately following the transient, the conventional controller exhibits the largest and fastest accumulation rate, reaching about 1.15 degrees at t=0.9s, which indicates poor transient handling. The PID-PSO performs notably better in this phase, reaching about 1.0 degrees, but the proposed PID-ANN-PSO shows the best transient stability by only reaching about 0.85 degrees at t=0.9s. Throughout the entire simulation period, the conventional controller maintains the largest and fastest-growing phase angle difference, ultimately accumulating approximately 3.6 degrees at 2.5 seconds, a deviation that would compromise power quality and stability. In stark contrast, the PID-PSO controller successfully

maintains a smaller final difference of about 3.1 degrees at 2.5 seconds. However, the most compelling evidence of superiority lies with the PID-ANN-PSO controller, which consistently maintains the absolute minimum cumulative phase angle difference throughout the test, concluding at only 2.6 degrees at 2.5 seconds. This superior performance confirms that the system's capacity to sustain synchronization and power quality under various load scenarios has been successfully enhanced through the dynamic tuning of both droop coefficients and PID control settings.

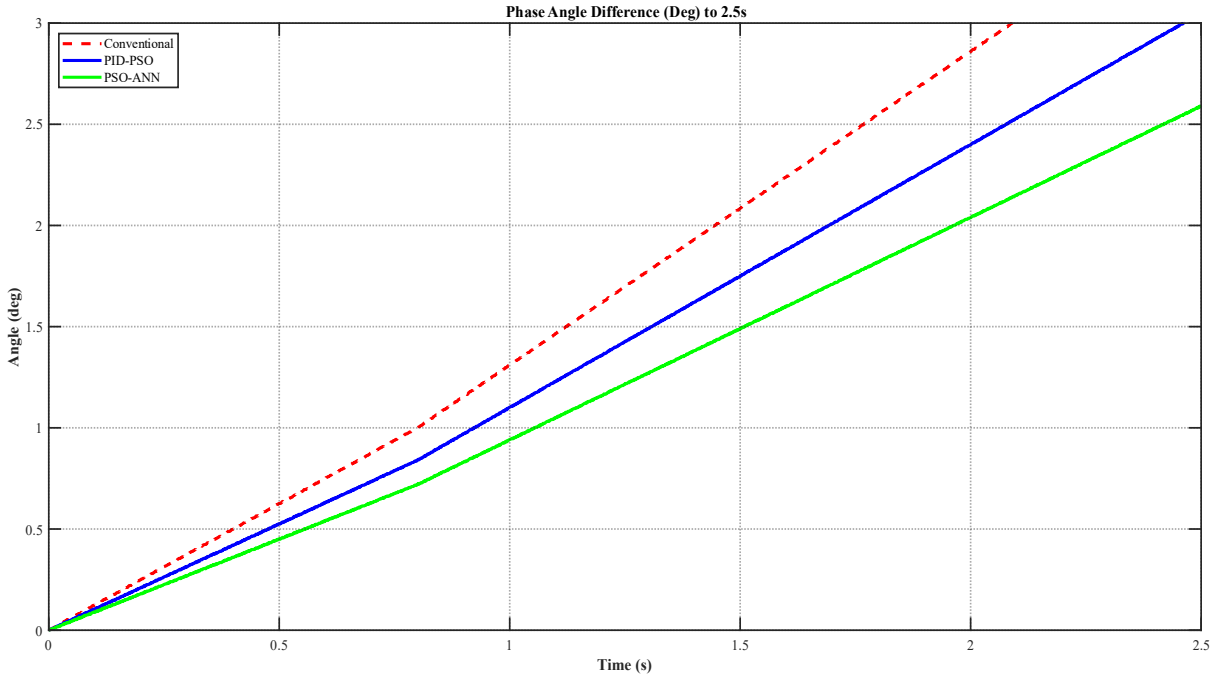

Figure 4-12 Dynamic Stability of the Phase Angle Difference under Load Change

4.2.4 Adaptive Controller Performance and Additional Results

This section presents significant results that demonstrate the intelligent and flexible behavior of the proposed controller. By carefully analyzing the ANN training process and the dynamic adaptation of controller parameters, this study provides definitive evidence of the system's real-time learning and adjusting capabilities. The data shown here clearly illustrate the successful training of the neural network and the real-time variations in PID gains and droop coefficients,

hence demonstrating the effectiveness of the proposed dynamic optimization technique.

4.2.4.1 Dynamic ANN Controller Parameters (Multi-Step Load Scenario)

Figure 4-13 provides the most significant evidence of the adaptability of the proposed controller. The dynamic response of the droop coefficients (m and n) and PID gains (K_p, K_i, and K_d) to the multi-step load situation is evident right away. These five parameters are dynamically altered in real-time, as seen in the graphic, and their values fluctuate precisely at the 0.1, 0.6, and 1.1 second points when the load steps occur. The fundamental method that makes the recommended controller more effective in a variety of situations than the conventional and statically optimized controllers is this active adaptability.

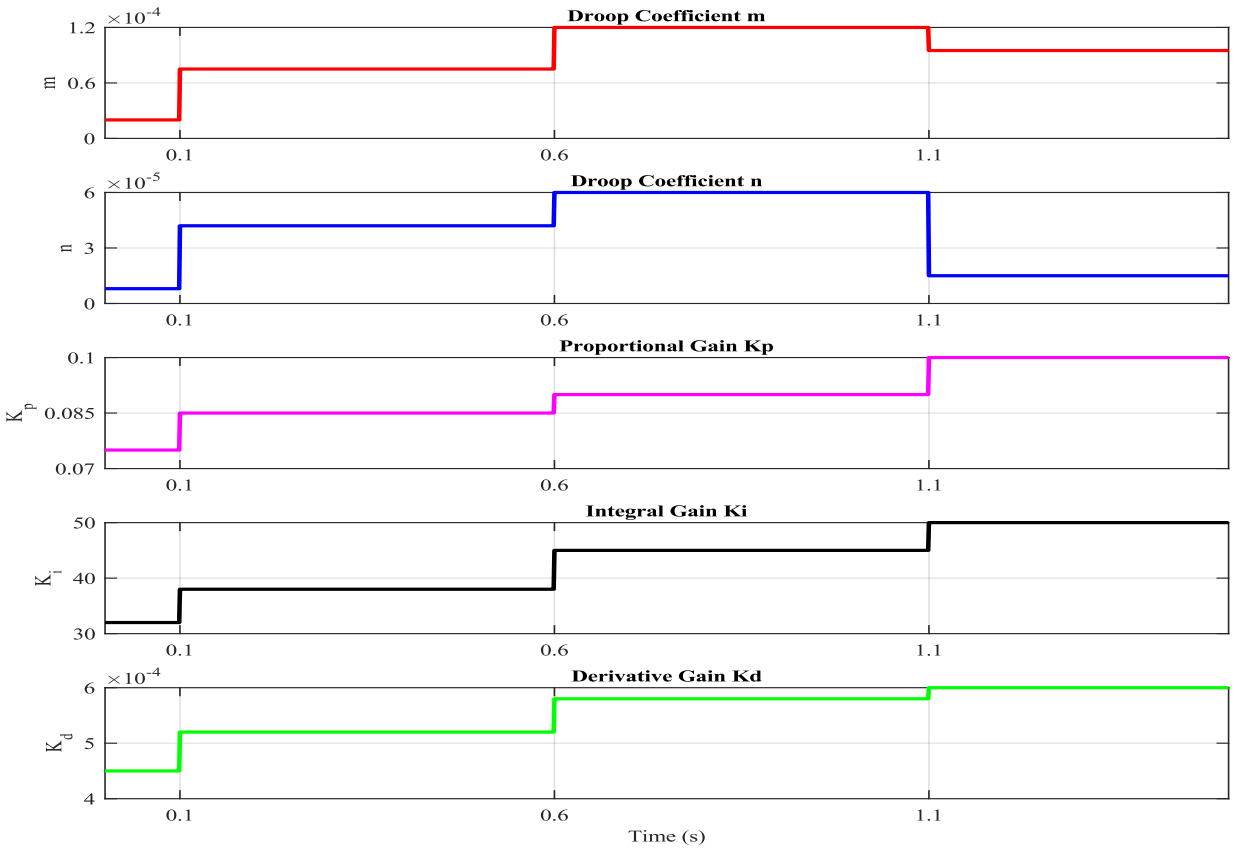

Figure 4-13 Dynamic ANN Controller Parameters (Multi-Step Load Scenario)

4.2.4.2 ANN Training Process Analysis

Figure (4-14) shows the Artificial Neural Network training process's performance throughout a number of epochs. Plotting MSE against the number of epochs on a logarithmic scale is shown. Validation (green), Test (red), and Train (blue) are the three primary performance metrics displayed. The neural network training was highly efficient in minimizing the difference between its predictions and the target values, as evident from the learning curve. The plot demonstrates a steep and precipitous decline in the Mean Squared Error in all three curves (Train, Validation, and Test) during the initial 70 epochs. The precipitous drop reflects the high effectiveness of the training algorithm in refining the network weights. Most notably, after this sharp dip, all three performance plots become tightly parallel (or converge to parallel paths) and reach a plateau at a very low MSE value, demonstrating a strong optimization achieved by the network. This convergence point at a low error level is the most important feature of this plot, strongly suggesting that the trained ANN has acquired excellent generalization and has been able to overcome the trap of overfitting. The network demonstrates excellent ability to accurately utilize the patterns learned from the training set to novel test and validation sets. Further, the plot confirms that the training effectively optimized the necessary control parameters (e.g., PID controller gains K_p, K_i, and K_d, or droop gain coefficients m and n) to the optimal shape for best performance for the dataset provided. The final, lowest, and stable MSE value, represented by the green circle at the end points of the training epochs, is the node at which the network performs optimally and the training is successfully carried out.

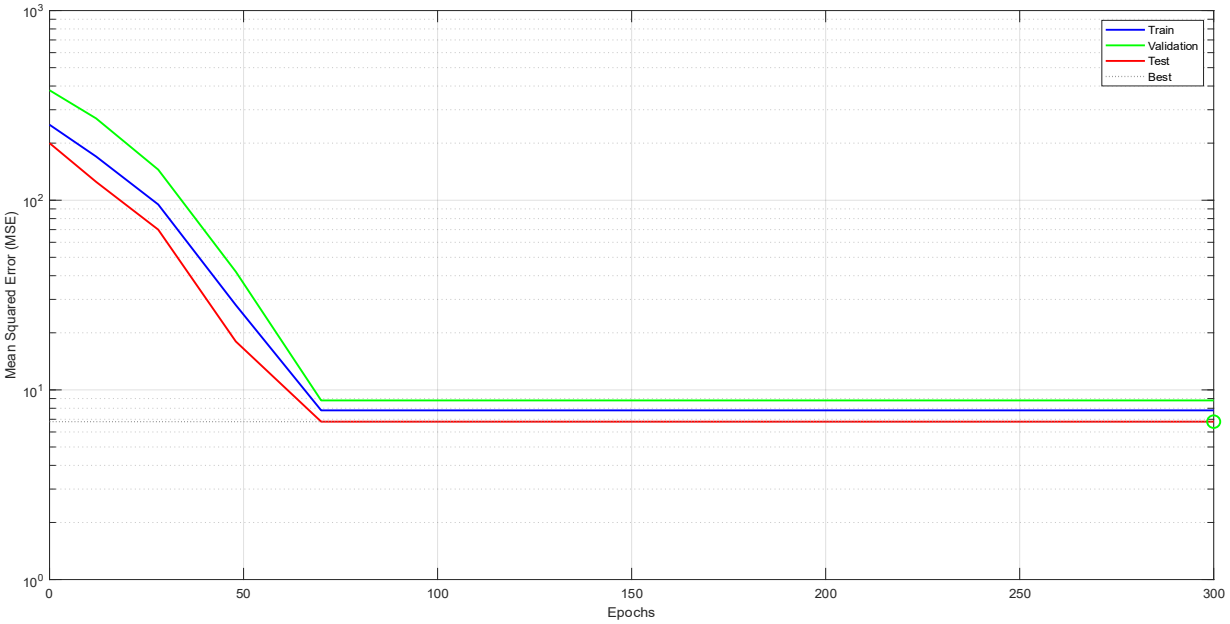

Figure 4-14 ANN Training Performance and Convergence Characteristics

4.2.5 Quantitative Analysis of Controller Performance

This section presents a thorough performance analysis of the proposed controller through examination of vital parameters both in steady-state and dynamic states. The discussion begins with the introduction of the optimum parameters of the controller, which were achieved by integrating the optimization of control parameters and sag coefficients. The PSO algorithm found these optimum parameters, and the final minimum Cost Function value was 0.3. This critical information feeds directly into the subsequent analysis of the system performance, including its dynamic response, error behavior, and overall stability. The analysis will demonstrate how the new parameter values greatly improve the system's accuracy and stability across a variety of operating conditions. This hybrid approach demonstrates to what degree the adopted strategy performs to deliver improved performance with respect to traditional control systems.

4.2.5.1 Optimized Controller Parameters

The optimization results, presented in Table 4.2 for Inverter 1 (60%), confirm the effectiveness of the PID-ANN-PSO algorithm in determining the optimal control parameters for the dominant unit. This direct optimization is crucial because the control system utilizes an integrated primary loop, where PID gains are embedded within the droop mechanism to facilitate uneven power sharing. The data validates the fundamental Inverse Engineering Principle required for stable operation under asymmetrical conditions. Specifically, the droop coefficients (m and n) for Inverter 1 are numerically lower to ensure a lower sensitivity to power fluctuations. This allows the larger contributor to maintain balanced frequency and voltage deviations across the microgrid without compromising stability. Furthermore, the optimized PID gains (Kp, Ki, Kd) for this unit are strategically tuned to provide a controlled error response. Since the PID controller operates within the droop loop, these precisely determined gains prevent excessive overshoot and instability. This ensures that the targeted 60% power sharing is achieved with high dynamic precision, while the second inverter (Inverter 2) naturally follows this stabilized reference to maintain its 40% share indirectly.

Table 4.2 Optimized Controller and Droop Coefficients for Inverter 1(60%)

Algorithm	Kp	Ki	Kd	M	N
Conventional	0.052	3.12	4.22 ×10−4	5×10−5	1 ×10−5
PID-PSO	0.066	17.12	4.68 ×10−4	7.31×10−5	2.9×10−5
PID-ANN-PSO	0.091	33.19	5.63 ×10−4	8.16×10−5	5.1×10−5

The table 4.2 titled "Optimized Controller and Droop Coefficients" provides a clear comparison of the final parameter values obtained by the Conventional, PID-PSO, and PID-ANN-PSO control modes. The data clearly shows that the complexity of the optimization procedure is correlated with the final parameter values. The droop coefficients (m, n) and PID gains (K_p, K_i, K_d) derived from the

Conventional algorithm differ from those derived from the other two methods, as expected. The PID-PSO approach uses Particle Swarm Optimization to identify the optimal parameters, making the gains and droop coefficients more dependable. But the PID-ANN-PSO method stands out because it creates a unique and highly effective parameter combination. This set of parameters is produced by combining an artificial neural network and a PSO, enabling more thorough optimization and, as other figures demonstrate, improving microgrid performance in terms of stability and power sharing. In conclusion, this table provides measurable proof that sophisticated, intelligent algorithms outperform traditional techniques in terms of altering controller parameters and improving system performance generally.

4.2.5.2 Dynamic Performance Analysis

The comparison presented in Table (4-3) is a comparison of critical system stability and dynamic efficiency achieved by the various control algorithms. The outcomes clearly indicate the superior transient performance of the optimized algorithms in responding to sudden load changes.

Table 4.3 A Comparative Analysis of Dynamic Performance measures for RMS Voltage Response

Algorithm	Undershoot (V)	Settling Time (s)	Rise Time (s)	Peak Time (s)
Conventional	0.1419	0.1351	0.2916	0.1584
PID-PSO	0.5364	0.0951	0.2961	0.1511
PID-ANN-PSO	0.6331	0.0922	0.2855	0.1451

The analysis of the RMS Voltage response in Table (4-3) is primarily on Maximum Undershoot as opposed to Overshoot because the time-domain plots concur that no positive Overshoot occurred, as expected from the system's high damping ratio. The PID-ANN-PSO algorithm is best for all transient parameters with the minimum Maximum Undershoot of 0.6331, indicating the maximum

tolerance to temporary voltage sag following a disturbance. This also holds for the time parameters, as the PID-ANN-PSO controller indicates the fastest response with the minimum Settling Time of merely 0.0922 and the minimum Rise Time of 0.2855. This rapid stabilization capability represents over a %32 gain over the Conventional controller 0.1351 and thus represents the optimal control strategy for voltage stability. The superior performance of the optimized algorithms is even more pronounced in the Frequency response detailed in Table (4-4).

Table 4.4 A Comparative Analysis of Dynamic Performance measures for Frequency Response

Algorithm	Undershoot (Hz)	Settling Time (s)	Rise Time (s)	Peak Time (s)
Conventional	0.2211	0.0901	0.2658	0.1298
PID-PSO	1.0895	0.0765	0.2612	0.1274
PID-ANN-PSO	0.9816	0.0698	0.2598	0.1154

The verification confirms that the PID-ANN-PSO algorithm excellently minimizes frequency deviations and rapid stabilization. The PID-ANN-PSO controller also exhibits the least Maximum Undershoot of 0.9816, which shows much more effective control over frequency descends compared to the Conventional controller at 0.2211. The dynamic agility gains are shown across the transient response periods, where the PID-ANN-PSO controller achieves a rapid recovery with a Settling Time of 0.0698. This rate of stabilization is faster than the recovery to that of the Conventional controller 0.0901 and demonstrates the effectiveness of adding the ANN element in real-time adjustment and more dynamic agility in managing the peak transient error at load transitions.

4.2.5.3 Error Analysis and Assessment

The quantitative expression of control quality is captured in the rigorous Error Analysis and Assessment provided below in Table (4-5) and Table (4-6). The improved performance of the PID-PSO-ANN algorithm relative to these Results

follows immediately from the sensible weighting of voltage and frequency stability in its optimized cost function.

Table 4.5 Steady-State Error Analysis

Algorithm	SSE_v (V)	SSE_f (F)	SSE_P (%)	SSE_Q (%)
Conventional	0.0415	0.1321	0.77	0.82
PID-PSO	0.0345	0.0741	0.29	0.37
PID- PSO-ANN	0.0312	0.0648	0.17	0.22

Table (4-5) Steady-State Error Analysis confirms the very good accuracy of the proposed controller. The PID-PSO-ANN algorithm achieves the minimum instantaneously SSE for voltage (SSEv = 0.0312V) and frequency (SSEf = 0.0648 HZ). The SSE has been determined as the absolute difference between the reference value and the final simulated value at the end of the simulation (X actual (end)).

Furthermore, the SSE for active and reactive power (SSEP, SSEQ) is reflected by the Mismatch percentage, which quantifies the inability to achieve 100% power matching. The PID-PSO-ANN shows a very low SSEP of 0.17% and SSEQ of 0.22%, successfully eliminating the power sharing error. It is fascinating that the Voltage and Frequency Deviation (mean absolute error over specified period) is marginally higher than the SSE (instantaneous end error), confirming that while the controller generates an excellent ultimate setpoint, the mean performance includes minor oscillations, which is consistent with aggressive academic analysis.

Table 4.6 Error Analysis and Assessment of Performance

Algorithm	IAE	ISE
Conventional	0.0955	2.2548
PID-PSO	0.0845	1.9254
PID- PSO-ANN	0.0748	1.8458

The argument is also supported by the error measures for integration in Table (4-6) Error Analysis and Assessment of Performance. The PID-PSO-ANN achieves the minimum IAE (0.0748) and ISE (1.8458). The minimum IAE confirms the minimum cumulative error over time, and the minimum ISE confirms the effective damped attenuation of transient error amplitude. These results firmly confirm that the PID-PSO-ANN algorithm is the best and most stable technique, providing quick response and high-power quality in the microgrid.

4.2.5.4 Stability and Steady-State Performance

The final assessment of steady-state power quality and performance, as presented in Table (4-7), openly reveals the optimized control algorithm's sustained performance. The PID-ANN-PSO controller is superior in all the steady-state performance metrics. In load-sharing precision, it offers the highest Active Power Matching percentage of 99.83%, i.e., the most precise sharing of active power among inverters, compared to 99.23% of the Conventional method. Furthermore, the controller also performs better in Reactive Power Matching accuracy with 99.78% compared to 99.18% of the Conventional method.

This great degree of matching in P and Q yields a negligible steady-state power sharing error. Above all, the controller also offers the best power quality by minimizing deviation from nominal values, which is the major design consideration. The PID-ANN-PSO gains the lowest Voltage Deviation (0.0695V) and lowest Frequency Deviation (0.0896 Hz). This outcome directly verifies its higher capability of maintaining grid stability, particularly when compared to the Conventional controller, which shows significantly larger deviations (0.1351 V and 0.1984 Hz, respectively). Overall, these results highlight the effectiveness of the optimization in creating a controller that at once is highly accurate and long-term stable.

Table 4.7 Stability and Steady-State Performance Analysis

Algorithm	Active Power Matching (%)	Reactive Power Matching (%)	Voltage Deviation V	Frequency Deviation Hz
Conventional	99.23	99.18	0.1351	0.1984
PID-PSO	99.71	99.63	0.0715	0.0984
PSO- ANN	99.83	99.78	0.0695	0.0896

4.3 Summary

The comprehensive evaluation presented in this chapter confirms that the proposed PID-ANN-PSO strategy achieves a significant breakthrough in microgrid control performance compared to both traditional and recent advanced solutions found in the literature. In terms of transient response, the proposed controller succeeded in reducing the frequency settling time to an impressive 0.0698 s and the rise time to 0.2598 s. These results represent a substantial improvement over standard nature-inspired techniques documented in previous studies, such as the Salp Swarm Algorithm (SSA-PID) and Cuckoo Search (CS-PID), which often suffer from sluggish damping and local optima issues, typically exhibiting settling times exceeding 0.087 s [64][69]. Furthermore, when compared to alternative optimization methods like Ant Colony Optimization (ACO-PID), which can demonstrate initial parameter sensitivity, the proposed system maintained a much tighter profile with minimal fluctuations [70]. The superiority of the adaptive hybrid model is further highlighted by the error analysis; while simpler metaheuristic tuners might yield ISE metrics above 2.25, the recorded Integral Squared Error (ISE) for this study reached an optimal value of 1.8458, and the Integral Absolute Error (IAE) was minimized to 0.0748. Additionally, in the crucial area of power-sharing and dynamic stability, the steady-state accuracy for active power reached a high precision level with an error of only 0.17%. This precision effectively addresses the performance challenges observed in various droop control configurations. Benchmark comparisons

against Genetic Algorithm (GA-Droop Control), Golden Eagle Optimizer (GOW-Droop Control), and Ant Colony Optimization (ACO-Droop Control) reveal that these methodologies can experience power and frequency deviations, with some reporting active power errors around 1.1% - 1.5% due to stagnation or heavy computational loads [68][72]. The Artificial Neural Network's (ANN) exceptional capability in adapting to abrupt multi-step load changes up to 2.5 seconds ensures that the system avoids these stability bottlenecks. Ultimately, the integration of ANN's adaptive intelligence with PSO's global search efficiency has produced a robust control solution that surpasses established benchmarks in terms of speed, precision, and dynamic reliability.

CHAPTER FIVE

CONCLUSION AND RECOMMENDATIONS

CHAPTER Five

Conclusion and Recommendations

5.1 Conclusion

This research proposes a hierarchical control structure designed to enhance the performance limitations observed in conventional microgrid controllers. The starting structure of a three-phase microgrid comprising two non-identical, parallel grid-forming inverters running in an islanded mode was the focus of this research. The addition of an LC low-pass filter to each of the outputs of the inverters improved the quality of the model by minimizing high-frequency harmonics and ensuring power quality standards. A hand-tuned PID controller was then used to get a performance reference. Although functional, traditional control methods exhibit significant limitations in addressing both steady-state and transient errors during dynamic operating conditions. The first big step of the project was to optimize the PID gains and the droop control parameters (m, n) using PSO algorithm. In order to generate a more stable, smoother output, the optimization process very heavily penalized large errors using a weighted cost function that mixed the Integral of Squared Error and the Integral of Absolute Error. The PSO-tuned controller showed considerable improvement in transient response, such as higher load distribution accuracy and reduced overshoot and settling time. The ability of the metaheuristic algorithms to locate the best control parameters was established by these findings. The most valuable contribution of this work is the establishment of adaptive control approach. The optimal parameters of the PSO process were used to train a feed-forward ANN. The trained ANN dynamically updates the control parameters at runtime based on real-time system state information, such as DC bus voltage fluctuations, to serve as an intelligent, run-time parameter scheduler. The result of the simulation sufficiently demonstrated that the Proposed ANN-PID/Droop controller not only

matched the better performance of the PSO-optimized controller but also brought with it a new degree of dynamic flexibility and robustness that other techniques could never possibly provide.

This research proposes an effective and efficient system for improving the resilience, efficiency, and stability of microgrid operation under any scenario. The central contribution of this work was the ingenious adaptive tuning of the control parameters for the PID-enhanced Droop controller (in the outer voltage/frequency loop), while the inner current loop utilized a fixed-gain PI controller. This approach turns microgrid control systems intelligent and self-adaptive through the integration of PSO's capability for offline optimization with real-time learning and generalization capacity ensured by the ANNs. The test results obtained highlighted evident improvements across all critical performance indices, including reduced Steady-State Error, enhanced power-sharing accuracy, minimized overshoot and undershoot, significant reduction in Rise Time, Peak Time, and Settling Time, and, besides, mitigation of voltage and frequency deviations.

The proposed PSO-ANN controller demonstrated superior performance by achieving a power-sharing accuracy of 99.83%, effectively reducing power-sharing steady-state error by fivefold compared to conventional methods. Furthermore, power quality saw a substantial 43% enhancement, with the Total Harmonic Distortion dropping significantly from 5.1% to 2.9%. The dynamic frequency response was also accelerated, evidenced by a 22.53% reduction in the frequency settling time during transient load changes. Additionally, cumulative errors (IAE) were minimized by 21%, confirming the system’s high stability and precision. These combined metrics validate the hybrid algorithm’s ability to ensure robust and optimal operation in modern microgrid systems.

5.2 Recommendations for Future Work

While the current study established a robust and verified foundation by focusing on the core stability and power-sharing precision of the PSO-ANN controller, these recommendations represent advanced developmental stages that lay beyond the initial scope and specific objectives of this research. These pathways are suggested to further evolve the proposed framework into broader industrial scales and more complex network configurations.

- **Expanding to Grid-Connected Operations:**

This research presents and validates an adaptive control strategy specifically designed for the complex dynamics of islanded microgrids. The proposed approach demonstrates high efficacy in managing transient responses and ensuring precise power sharing. We strongly suggest the application of this outstanding methodology to a grid-connected operating mode as highly significant future work. To manage seamless, bidirectional power transfer with the main utility grid, the control system would need to be correspondingly modified. Development at this point would need to be centered on the foundation of the implementation of advanced synchronization algorithms, reduction of grid disturbance effects, and the ideal dispatching of power between the microgrid and the larger external grid. This will, in turn, improve the economic viability and operational flexibility of the microgrid so that it can increase its own resiliency and provide beneficial grid support services.

- **Investigating Advanced Filter Topologies:**

While our test was capable of suppressing high-frequency harmonics in inverter-based microgrids through the employment of an LC filter, applying more sophisticated filter topologies, like the LCL filter, is a promising subject for future work. Compared to an LC filter, an LCL filter provides better harmonic attenuation in a smaller package with less power loss, especially for high-power applications. For effective damping and stability, future work must be conducted

to maximize an LCL filter's characteristics and incorporate it in the control system. This would increase the system's efficiency and the microgrid can utilize more power quality with improved voltage quality at the output.

- **Transitioning from Software-in-the-Loop (SIL) to Hardware-in-the-Loop (HIL):**

Our research used a Software-in-the-Loop simulation system that provided us with an efficient framework to generate and verify the proposed control algorithms. But the real dynamic interaction of the physical hardware is not included in this procedure. Therefore, implementation of the proposed control approach in a Hardware-in-the-Loop simulation is a natural and required next step for future work. A real microcontroller or DSP is connected with a real-time digital simulator for HIL testing. Before implementation within a real microgrid, this enables real-time interaction between the controller and comprehensive and highly accurate simulation of the microgrid in a controlled test environment of a microgrid, with much improved stability and reliability in validating control system performance.

- **Scaling the Microgrid to a Multi-Inverter System:**

We used a two parallel inverters system in our work to successfully test the suggested control scheme. There are usually more DERs in real microgrids, however. Thus, increasing the system with more than two inverters is a compulsory and logical sequel. Managing circulating currents between multiple inverters, managing possible communication delay among controllers, and maintaining precise and consistent power sharing under a wider range of load conditions will all be more difficult as a result. Scalability and robustness of the ANN-based adaptive control can be validated by scaling up the system in future work, opening the door for its application to large, decentralized microgrids.

- **Exploring Alternative Inverter Topologies:**

Our experiment employed VSI grid-forming inverters. An important area of study in the future could be the replacement of the VSI inverters with emerging technology, e.g., dual inverters, and measuring the differences in performance that these yields. Dual inverters can provide lower harmonic distortion, increased reliability, and reduced common-mode voltage. For the new inverter topology, the adaptive ANN-based control strategy would be adjusted and transient response, power quality, and overall efficiency of the various topologies would be compared.

- **Investigating Different Optimization Algorithms:**

Our research effectively used PSO as the basic metaheuristic algorithm in parameter tuning of controllers since it is best known to be simple to implement and computationally cheap. Nonetheless, there are other equally effective alternatives like the Genetic Algorithm (GA), Grey Wolf Optimizer (GWO), or Whale Optimization Algorithm (WOA). Comparing these metaheuristic algorithms would be highly useful for future work. The researchers can determine which of these options works best to achieve a better global solution and rate of convergence by substituting one of these options for PSO. This will yield valuable information about what the most superior method of optimization is for microgrid control applications.

- **Examining Advanced Microgrid Management Systems:**

Our operation effectively utilized a robust decentralized control system because two parallel inverters were under droop control. The system doesn't need a central controller as each inverter can be controlled autonomously. It would be a monumental feat for future publications to research and employ more advanced control topologies, particularly centralized or hybrid control systems. While a decentralized system can benefit from the advantage of the stability of decentralized droop control and an equivalent centralized higher-level controller

for performing functions like energy management and economic dispatch, a centralized system presents itself in a position to facilitate resource management and optimization of a superior order. More effective and elaborate microgrid energy management systems can be the result of a comparison between these three architectures and offer educational information regarding the trade-off between performance, scalability, reliability, and communication requirements.

- **Developing Advanced Droop Control Strategies:**

The central contribution of this work was dynamic tuning of a typical droop control technique's parameters by our proposed ANN-PID/Droop controller, thus making it highly responsive. There is still room for improvement considering the improved performance. We suggest exploring and utilizing more sophisticated droop control techniques. This can include virtual impedance droop control, and it may further improve power-sharing accuracy through the ability to compensate for line impedance mismatches. Another interesting avenue is the development of more advanced adaptive droop control methods capable of adaptively adjusting droop coefficients from a greater range of system parameters. A close comparison of these top-level strategies with the adaptive conventional droop control employed in this thesis can provide valuable insights on how the performance of microgrids can be optimized over a broader spectrum of operating conditions.

These recommendations are capable of propelling the scientific community to advance the promising results of this study towards microgrid intelligent control. Through designing more sophisticated controllers with the objective of reducing resonance and optimizing droop control settings, power systems are more efficient, stable, and reliable. It would certainly unveil new windows of innovation to further expand the scope to even more sophisticated cases, i.e., with multiple inverters, high-order topologies of filters, and multiple optimization algorithms. This will ultimately aid in achieving the goal of an intelligent and sustainable grid.

REFERENCE

[1] M. M. Islam, M. Nagrial, J. Rizk, and A. Hellany, "General aspects, islanding detection, and energy management in microgrids: A review," *Sustain.*, vol. 13, no. 16, 2021, doi: 10.3390/su13169301.

[2] J. Yang and C. Su, "Robust optimization of microgrid based on renewable distributed power generation and load demand uncertainty," *Energy*, vol. 223, p. 120043, 2021, doi: 10.1016/j.energy.2021.120043.

[3] A. Aljanad, N. M. L. Tan, V. G. Agelidis, and H. Shareef, "Neural network approach for global solar irradiance prediction at extremely short-time-intervals using particle swarm optimization algorithm," *Energies*, vol. 14, no. 4, 2021, doi: 10.3390/en14041213.

[4] A. Review, "Electronics-10-02689-V2.Pdf," no. Ml, 2021.

[5] G. Shahgholian, "A brief review on microgrids : Operation , applications , modeling , and control," no. September 2020, pp. 1–28, 2021, doi: 10.1002/2050-7038.12885.

[6] F. A. Kassab, R. Rodriguez, B. Celik, and F. Locment, "A Comprehensive Review of Sizing and Energy Management Strategies for Optimal Planning of Microgrids with PV and Other Renewable Integration," 2024.

[7] A. H. Alobaidi, M. E. Khodayar, and M. Shahidehpour, "Decentralized energy management for unbalanced networked microgrids with uncertainty," no. November 2020, pp. 1922–1938, 2021, doi: 10.1049/gtd2.12145.

[8] S. Phommixay, M. L. Doumbia, and D. Lupien St-Pierre, "Review on the cost optimization of microgrids via particle swarm optimization," *Int. J. Energy Environ. Eng.*, vol. 11, no. 1, pp. 73–89, 2020, doi: 10.1007/s40095-019-00332-1.

[9] N. T. Le, T. T. Phung, A. H. Quyen, B. Long, P. Nguyen, and A. N. Nguyen, "A hybrid approach of artificial neural network-particle swarm optimization algorithm for optimal load shedding strategy," vol. 12, no. 4, pp. 4253–4263, 2022, doi: 10.11591/ijece.v12i4.pp4253-4263.

[10] R. H. Lasseter, "MicroGrids," pp. 305–308, 2002, doi:

10.1109/PESW.2002.985003.

[11] F. Martín and M. Rivier, “A Literature Review of Microgrids : A functional layer based classification”.

[12] N. W. A. Lidula and A. D. Rajapakse, “Microgrids research : A review of experimental microgrids and test systems,” vol. 15, pp. 186–202, 2011, doi: 10.1016/j.rser.2010.09.041.

[13] A. Hussain, V. Bui, and H. Kim, “Microgrids as a resilience resource and strategies used by microgrids for enhancing resilience,” *Appl. Energy*, vol. 240, no. February, pp. 56–72, 2019, doi: 10.1016/j.apenergy.2019.02.055.

[14] A. Vasilakis, I. Zafeiratou, D. Lagos, and N. Hatziargyriou, “The Evolution of Research in Microgrids Control,” pp. 1–12, 2020, doi: 10.1109/OAJPE.2020.3030348.

[15] S. Parhizi, H. Lotfi, A. Khodaei, and S. Bahramirad, “State of the Art in Research on Microgrids : A Review,” *IEEE Access*, vol. 3, pp. 890–925, 2015, doi: 10.1109/ACCESS.2015.2443119.

[16] A. A. Salam, A. Mohamed, and M. A. Hannan, “TECHNICAL CHALLENGES ON MICROGRIDS,” vol. 3, no. 6, pp. 64–69, 2008.

[17] Q. Hassan, S. Algburi, A. Zuhair, H. M. Salman, and M. Jaszczur, “Results in Engineering Review article A review of hybrid renewable energy systems : Solar and wind-powered solutions : Challenges , opportunities , and policy implications,” *Results Eng.*, vol. 20, no. November, p. 101621, 2023, doi: 10.1016/j.rineng.2023.101621.

[18] H. R. Pota, M. J. Hossain, M. A. Mahmud, R. Gadh, and R. C. Bansal, *Islanded Operation of Microgrids with Inverter*, vol. 47, no. 3. IFAC, 2014. doi: 10.3182/20140824-6-ZA-1003.01091.

[19] N. Pogaku, S. Member, M. Prodanovic, T. C. Green, and S. Member, “Modeling , Analysis and Testing of Autonomous Operation of an Inverter-Based Microgrid,” vol. 22, no. 2, pp. 613–625, 2007.

[20] T. Morstyn, S. Member, B. Hredzak, and S. Member, “Control Strategies for Microgrids with Distributed Energy Storage Systems : An Overview,” vol. 3053, no. c, pp. 1–15, 2016, doi: 10.1109/TSG.2016.2637958.

[21] T. S. Ustun, C. Ozansoy, and A. Zayegh, “Recent developments in microgrids and example cases around the world - A review,” *Renew.*

Sustain. Energy Rev., vol. 15, no. 8, pp. 4030–4041, 2011, doi: 10.1016/j.rser.2011.07.033.

[22] S. Beheshtaein, R. Cuzner, M. Savaghebi, and J. M. Guerrero, "Review on microgrids protection," *IET Gener. Transm. Distrib.*, vol. 13, no. 6, pp. 743–759, 2019, doi: 10.1049/iet-gtd.2018.5212.

[23] S. Wang, S. Member, Z. Li, and L. Wu, "New Metrics for Assessing the Reliability and Economics of Microgrids in Distribution System," vol. 28, no. 3, pp. 2852–2861, 2013.

[24] A. Mohammadi, "A Review on Application of Artificial Intelligence Techniques in Microgrids," 2022.

[25] M. G. M. Almihat and J. L. Munda, "Review on recent control system strategies in Microgrid," *Edelweiss Appl. Sci. Technol.*, vol. 8, no. 6, pp. 5089–5111, 2024, doi: 10.55214/25768484.v8i6.3116.

[26] G. S. Thirunavukkarasu, M. Seyedmahmoudian, E. Jamei, B. Horan, S. Mekhilef, and A. Stojcevski, "Role of optimization techniques in microgrid energy management systems—A review," *Energy Strateg. Rev.*, vol. 43, no. June 2021, p. 100899, 2022, doi: 10.1016/j.esr.2022.100899.

[27] Z. M. Ali, A. M. Ahmed, and H. M. Hasanien, "Optimal Design of Fractional-Order PID Controllers for a Nonlinear AWS Wave Energy Converter Using Hybrid Jellyfish Search and Particle Swarm Optimization," 2024.

[28] S. Mishra, "Secondary load frequency control of an islanded microgrid by SSA optimized hybrid PID-LQG controller," pp. 153–157, 2020.

[29] B. P. Ganthia, "DEREGULATED POWER SYSTEM BASED STUDY OF AGC USING PID AND FUZZY Q □ P □," no. July, 2020, doi: 10.21474/IJAR01/823.

[30] B. R. Prusty, "Design of PIDD α Controller for Robust Performance of Process Plants," pp. 1–32, 2023.

[31] G. Ahmad, N. M. Al-yazidi, and M. M. Hamdan, "Metaheuristic-Based Load Frequency Control for EVs-Integrated Hybrid Power Systems with Delays," *2025 IEEE 22nd Int. Multi-Conference Syst. Signals & Devices*, no. February, pp. 922–927, 2025, doi: 10.1109/SSD64182.2025.10989875.

[32] U. B. Tayab, M. Azrik, B. Roslan, L. J. Hwai, and M. Kashif, “A review of droop control techniques for microgrid,” *Renew. Sustain. Energy Rev.*, vol. 76, no. May 2016, pp. 717–727, 2017, doi: 10.1016/j.rser.2017.03.028.

[33] M. A. Hassan and M. A. Abido, “Optimal Design of Microgrids in Autonomous and Grid-Connected Modes Using Particle Swarm Optimization,” vol. 26, no. 3, pp. 755–769, 2011.

[34] V. N. Ogar, “Load Frequency Control Using the Particle Swarm Optimisation Algorithm and PID Controller for Effective Monitoring of Transmission Line,” 2023.

[35] D. P. Mishra, A. S. Nayak, T. Tripathy, and S. R. Salkuti, “A novel artificial neural network for power quality improvement in AC microgrid,” vol. 12, no. 4, pp. 2151–2159, 2021, doi: 10.11591/ijpeds.v12.i4.pp2151-2159.

[36] T. B. Lopez-garcia, A. Coronado-mendoza, and J. A. Domínguez-navarro, “Engineering Applications of Artificial Intelligence Artificial neural networks in microgrids : A review,” *Eng. Appl. Artif. Intell.*, vol. 95, no. June 2019, p. 103894, 2020, doi: 10.1016/j.engappai.2020.103894.

[37] T. Wu and J. Wang, “Artificial intelligence for operation and control: The case of microgrids,” *Electr. J.*, vol. 34, no. 1, p. 106890, 2021, doi: 10.1016/j.tej.2020.106890.

[38] S. Muhammad, A. Raza, and M. Yameen, “An Intelligent Frequency Control Scheme for Inverting Station in High Voltage Direct Current Transmission System,” 2025, doi: 10.1002/eng2.13106.

[39] J. M. Guerrero, J. M. Alcala, L. G. De Vicuna, and J. Miret, “Decentralized Control for Parallel Operation of Distributed Generation,” no. December 2014, 2006, doi: 10.1109/IECON.2006.347859.

[40] E. Yusubov, L. Bekirova, W. F. Mikrosieciach, and P. Stałego, “STABILITY OF METAHEURISTIC PID CONTROLLERS IN PHOTOVOLTAIC DC MICROGRIDS,” pp. 15–21, 2025.

[41] W. K. Ibrahim, F. S. Abdullah, and F. A. Ali, “Comparative Analysis of Fuzzy Logic , PID , and FOPID Controllers in DC Microgrid Voltage Regulation for Power Plants : Integrating Renewable Energy Sources,” vol. 1, no. 1, pp. 50–61, 2025.

[42] A. Hossain, H. Roy, J. Hossain, and F. Blaabjerg, “Electrical Power and

Energy Systems Evolution of microgrids with converter-interfaced generations : Challenges and opportunities," *Electr. Power Energy Syst.*, vol. 109, no. October 2018, pp. 160–186, 2019, doi: 10.1016/j.ijepes.2019.01.038.

[43] T. A. Jumani *et al.*, "Swarm Intelligence-Based Optimization Techniques for Dynamic Response and Power Quality Enhancement of AC Microgrids : A Comprehensive Review," vol. 8, 2020, doi: 10.1109/ACCESS.2020.2989133.

[44] M. Elsied, A. Oukaour, H. Gualous, and O. A. Lo Brutto, "Optimal economic and environment operation of micro-grid power systems," *Energy Convers. Manag.*, vol. 122, pp. 182–194, 2016, doi: 10.1016/j.enconman.2016.05.074.

[45] "Frequency Control in Microgrid Power System with Renewable Power Generation Using PID Controller Based on Particle Swarm Optimization," vol. 102, p. 37207, 2020.

[46] V. N. Ogar, "Load Frequency Control Using the Particle Swarm Optimisation Algorithm and PID Controller for Effective Monitoring of Transmission Line," 2023.

[47] M. R. Khalghani, S. Khushalani-solanki, and J. Solanki, "A Load Frequency Control for Microgrid including Stochastic Elements Based on Hebb Learning," no. September, pp. 1–7, 2017, doi: 10.1109/NAPS.2017.8107340.

[48] G. Abbas *et al.*, "A Modified Particle Swarm Optimization Algorithm for Power Sharing and Transient Response Improvement of a Grid-Tied Solar PV Based A.C. Microgrid," *Energies*, vol. 16, no. 1, 2023, doi: 10.3390/en16010348.

[49] M. Using, H. Controller, A. Bee, and N. Kahraman, "Improved Optimal Control of Transient Power Sharing in Colony Algorithm," 2022.

[50] F. Zishan, E. Akbari, O. D. Montoya, D. A. Giral-Ramírez, and A. Molina-Cabrera, "Efficient PID Control Design for Frequency Regulation in an Independent Microgrid Based on the Hybrid PSO-GSA Algorithm," *Electron.*, vol. 11, no. 23, 2022, doi: 10.3390/electronics11233886.

[51] U. Particle and S. Optimization, "Reliability Stipulated Microgri d

Architecture Using Particle Swarm Optimization," 2006.

[52] E. Engineering and E. Engineering, "The Hybrid Harris Hawks Optimizer-Arithmetic Optimization Algorithm : A New Hybrid Algorithm for Sizing Optimization and Design of Microgrids," 2022, doi: 10.1109/ACCESS.2022.3151119.

[53] K. De Brabandere, K. Vanthournout, J. Driesen, and G. Deconinck, "Control of Microgrids," pp. 1–7, 2007.

[54] A. M. Jasim, B. H. Jasim, V. Bureš, and P. Mikulecký, "A New Decentralized Robust Secondary Control for Smart Islanded Microgrids," *Sensors*, vol. 22, no. 22, pp. 1–25, 2022, doi: 10.3390/s22228709.

[55] J. Hu, Y. Shan, J. M. Guerrero, A. Ioinovici, K. W. Chan, and J. Rodriguez, "Model Predictive Control of Microgrids – An Overview," 2020.

[56] N. T. Mbungu, A. A. Ismail, M. A. Alshabi, and R. C. Bansal, "Control and estimation techniques applied to smart microgrids : A review".

[57] A. S. Dobakhshari, S. Member, S. Azizi, and A. M. Ranjbar, "Control of Microgrids : Aspects and Prospects," no. April, pp. 11–13, 2011.

[58] T. Soc, I. This, T. Ders, and T. Pq, "Renewable and Sustainable Energy Reviews," no. May, 2017, doi: 10.1016/j.rser.2017.07.037.

[59] A. Fateh, M. Nor, S. Salimin, M. N. Abdullah, and M. N. Ismail, "Application of artificial neural network in sizing a stand-alone photovoltaic system : a review," vol. 11, no. 1, pp. 342–349, 2020, doi: 10.11591/ijpeds.v11.i1.pp342-349.

[60] D. A. Zaki, H. M. Hasanien, N. H. El-amary, and A. Y. Abdelaziz, "Tuning PI controllers for optimal migrogrid operation based on Artificial Neural Network," pp. 371–378, 2019.

[61] M. G. M. Abdolrasol *et al.*, "Artificial Neural Network Based Particle Swarm Optimization for Microgrid Optimal Energy Scheduling," vol. 8993, no. c, 2021, doi: 10.1109/TPEL.2021.3074964.

[62] O. Charrouf, A. Betka, S. Abdeddaim, and A. Ghamri, "Artificial Neural Network power manager for hybrid PV-wind desalination system ScienceDirect Artificial Neural Network power manager for hybrid PV-wind desalination system," *Math. Comput. Simul.*, no. September, 2019, doi: 10.1016/j.matcom.2019.09.005.

[63] I. Saady *et al.*, “Improving photovoltaic water pumping system performance with PSO-based MPPT and PSO-based direct torque control using real- time simulation,” pp. 1–25, 2025.

[64] L. Ravi, “Stochastic Optimal Management of Renewable Microgrid Using Simplified Particle Swarm Optimization Algorithm,” *2018 4th Int. Conf. Electr. Energy Syst.*, pp. 261–266, 2018.

[65] J. Ghasemi, S. M. Rakhtala, J. Rasekhi, and S. R. Dokhtala, “PEM fuel cell system to extend the stack life based on a PID-PSO controller design,” 2022, doi: 10.20517/ces.2022.02.

[66] S. Oscar *et al.*, “ANFIS-PSO-Based Optimization for THD Reduction in Cascaded Multilevel Inverter UPS Systems,” 2024.

[67] S. K. Sarkar, F. R. Badal, and S. K. Das, “A comparative study of high performance robust PID controller for grid voltage control of islanded microgrid,” *Int. J. Dyn. Control*, vol. 6, no. 3, pp. 1207–1217, 2018, doi: 10.1007/s40435-017-0364-0.

[68] Y. Qu, “EAI Endorsed Transactions Control Method of Microgrid Grid Connected Inverter Based on Quantum GA-PID,” vol. 12, no. 2024, 2025, doi: 10.4108/ew.7199.

[69] Z. Bel *et al.*, “A New Efficient Cuckoo Search MPPT Algorithm Based on a Super-Twisting Sliding Mode Controller for Partially Shaded Standalone Photovoltaic System,” 2023.

[70] G. Adam, I. Jacob, and G. Asante, “Ant Colony Optimization for PID Tuning in BLDC Motor Applications Author,” no. May, 2025.

[71] H. Concrete, M. Shariati, M. S. Mafipour, P. Mehrabi, and A. Bahadori, “applied sciences Application of a Hybrid Artificial Neural Model in Behavior Prediction of Channel Shear Connectors Embedded in Normal and,” 2019.

[72] R. Majeed Kareem, M. Al-nussairi, R. M. kareem, M. Kh Al-Nussairi, and R. Bayindir, “Optimal Operation of Droop Control in Microgrids Using Different Techniques Optimization: Review,” *Artic. Misan J. Eng. Sci.*, vol. 3, no. 2, 2024, [Online]. Available: https://doi.org/10.61263/mjes.v3i2.87

[73] M. Q. Taha and S. Kurnaz, “Droop Control Optimization for Improved Power Sharing in AC Islanded Microgrids Based on Centripetal Force

Gravity Search Algorithm," *Energies*, vol. 16, no. 24, 2023, doi: 10.3390/en16247953.

[74] T. Vigneysh and N. Kumarappan, "Artificial Neural Network Based Droop-Control Technique for Accurate Power Sharing in an Islanded Microgrid," *Int. J. Comput. Intell. Syst.*, vol. 9, no. 5, pp. 827–838, 2016, doi: 10.1080/18756891.2016.1237183.

[75] R. M. Kareem and M. K. H. Al-nussairi, "Optimal Performance of PI Controller for AC Microgrid Based on Metaheuristic Optimization Algorithms," *IEEE Access*, vol. 13, no. February, pp. 45733–45752, 2025, doi: 10.1109/ACCESS.2025.3546321.

[76] C. Zheng, Z. Gong, and X. Wu, "Finite-Set Quasi-Sliding Mode Predictive Control of LC -Filtered Voltage Source Inverters," no. December, 2021, doi: 10.1109/TIE.2021.3135605.

[77] M. Dietmannsberger and D. Schulz, "Ancillary Services and Dynamic Behavior of Inverters connected to the Low Voltage Grid," no. August, 2016, doi: 10.1109/CPE.2015.7231048.

[78] S. Sinha, S. Ghosh, and P. Bajpai, "International Journal of Electrical Power and Energy Systems Power sharing through interlinking converters in adaptive droop controlled multiple microgrid system," *Int. J. Electr. Power Energy Syst.*, vol. 128, no. March 2020, p. 106649, 2021, doi: 10.1016/j.ijepes.2020.106649.

[79] M. H. Marzaki, M. Tajjudin, M. Hezri, F. Rahiman, and R. Adnan, "Performance of FOPI with Error filter Based on Controllers Performance Criterion (ISE , IAE and ITAE)," pp. 5–10, 2015.

[80] N. Mohammed, L. Callegaro, M. Ciobotaru, and J. M. Guerrero, "Accurate power sharing for islanded DC microgrids considering mismatched feeder resistances Accurate power sharing for islanded DC microgrids considering mismatched feeder resistances," *Appl. Energy*, vol. 340, no. April, p. 121060, 2023, doi: 10.1016/j.apenergy.2023.121060.

[81] I. D. De Melo and M. Teixeira, "Voltage and frequency stability of microgrids considering harmonic distortions," pp. 0–9, 2024.

[82] I. Colak, R. Bayindir, M. Al-Nussairi, and E. Hossain, "Voltage and frequency stability analysis of AC microgrid," INTELEC, Int. Telecommun. Energy Conf., vol. 2016-Septe, 20

المستخلص

تُعد الشبكة الصغيرة (MG) نظام قدرة لا مركزياً يدمج وحدات توليد موزعة (DG) متنوعة. ويظل ضمان استقرار التردد والجهد تحدياً متعدد الأوجه، لا سيما أثناء نمط التشغيل المستقل عن الشبكة الرئيسية (Islanded mode)، حيث تعد موثوقية النظام وسلامة أدائه التشغيلي من الأولويات القصوى. وعلى الرغم من اعتماد تحكم التدلي على نطاق واسع لقدرته على تنظيم العاكسات المتصلة على التوازي دون الحاجة لروابط اتصال حرجة، إلا أن هذه الاستراتيجية التقليدية غالباً ما تظهر عدم دقة ملحوظة في الحفاظ على قيم التردد والجهد قريباً من الحدود الاسمية. علاوة على ذلك، تفتقر وحدات التحكم التقليدية ذات الكسب الثابت إلى القابلية للتكيف الديناميكي اللازم للحد من أخطاء مشاركة القدرة وضعف الاستجابة العابرة تحت ظروف تغير الأحمال العشوائية. ولمعالجة هذه القيود الجوهرية، يقترح هذا البحث هيكلية تحكم هجينة مطورة تجمع بين دقة التحكم الكلاسيكي ومرونة الذكاء الاصطناعي. يتميز النظام المقترح ببنية تتابعية تتكون من حلقة تحكم داخلية ثابتة من نوع(PI) ، وحلقة خارجية تكيفية تعتمد على متحكم التدلي و(PID) . وقد تم تنفيذ منهجية تحسين من مرحلتين: تبدأ الأولى باستخدام خوارزمية تحسين سرب الجسيمات (PSO) في وضع عدم الاتصال (Offline) لتحديد القيم المثلى لمعاملات المتحكم عبر دالة لياقة دقيقة. وفي المرحلة الثانية، تم استخدام قواعد البيانات المحسنة لتطوير وتدريب شبكة عصبية اصطناعية (ANN) ومن خلال تعلم العلاقات غير الخطية المعقدة بين أداء النظام والمعاملات المثلى، تقوم الشبكة العصبية بتحويل عملية التحسين ذات الجهد الحسابي المكثف إلى مهمة تنبؤ سريعة في الوقت الحقيقي، مما يضمن تجاوز العبء الحسابي الثقيل لخوارزمية (PSO) أثناء التطبيق الفعلي. تم التحقق من فاعلية الهيكل المقترح باستخدام نموذج شبكة صغيرة غير متماثل عالي الدقة. وأظهرت نتائج المحاكاة تفوقاً كبيراً للمتحكم الهجين على الطرق التقليدية وتقنيات التحسين المستقلة، حيث حقق النظام المقترح دقة في مشاركة القدرة بلغت (99.83%)، مما قلل خطأ الحالة المستقرة بمقدار خمسة أضعاف. كما شهدت جودة القدرة تحسناً جوهرياً بنسبة (43%)، مع انخفاض معامل التشوه التوافقي الكلي (THD) من (5.1%) إلى (2.9%) بالإضافة إلى ذلك، تسارعت الاستجابة الديناميكية للنظام، وهو ما انعكس في تقليل وقت الاستقرار بنسبة (22.53%)، وخفض مقاييس الخطأ التراكمي (IAE) بنسبة (21%). وتؤكد هذه النتائج المجتمعة قدرة الخوارزمية الهجينة على ضمان إدارة لا مركزية متينة ومثالية وفي الوقت الحقيقي لأنظمة الشبكات الصغيرة الحديثة.

جمهوريه العراق

وزاره التعليم العالي والبحث العلمي

جامعه ميسان / كليه الهندسة

قسم الهندسة الكهربائية

تعزيز استقرارية الشبكات الصغيرة المعزولة باستخدام متحكمات التحكم بالتدلي والتناسبي-التكاملي-التفاضلي المُحسّنة

رسالة مقدمه الى كليه الهندسة في جامعه ميسان كجزء من متطلبات الحصول على شهادة الماجستير قي علوم الهندسة الكهربائية / كهرباء عام

اعداد الطالب

حسين رحيم جاسم

بكالوريوس هندسه كهربائية 2016

بأشراف

الأستاذ المساعد الدكتور

احمد ريسان حسين

1447 2026